LOCALIZED ELECTROPORATION OF AVIAN EMBRYOS REVEALS A ROLE FOR INTEGRIN AND RHOA DURING THE EMIGRATION OF CRANIAL NEURAL CREST

by

ROSS L. ATKINS
B.Sc., University of Victoria, 1999

A Thesis Submitted in Partial Fulfillment of the
Requirements for the Degree of

DOCTOR OF PHILOSOPHY

in the Department of Biology

LOCALIZED ELECTROPORATION OF AVIAN EMBRYOS REVEALS A ROLE FOR INTEGRIN AND RHOA DURING THE EMIGRATION OF CRANIAL NEURAL CREST

by

ROSS L. ATKINS
B.Sc., University of Victoria, 1999

Supervisory Committee

Supervisor

Dr. Robert D. Burke, (Departments of Biology & Biochemistry/Microbiology)

Departmental Member

Dr. Patrick von Aderkas, (Department of Biology)

Departmental Member

Dr. Louise Page, (Department of Biology)

Outside Member

Dr. Caren Helbing, (Department of Biochemistry/Microbiology)

Supervisory Committee

Supervisor
Dr. Robert D. Burke, (Departments of Biology & Biochemistry/Microbiology)

Departmental Member
Dr. Patrick von Aderkas, (Department of Biology)

Departmental Member
Dr. Louise Page, (Department of Biology)

Outside Member
Dr. Caren Helbing, (Department of Biochemistry/Microbiology)

ABSTRACT

Neural crest cells go through an epithelial-mesenchymal transition (EMT) before they migrate. β1 integrins are necessary during these phases of neural crest development, but it is unclear if integrins are required for both EMT and neural crest migration. Chimeric integrin β1 subunit and mutant Rho GTPases are used in this study to assess function during neural crest emigration. Cultures of chick embryonic cells, transfected with these constructs, are used to confirm the effects and expression in conjunction with a green fluorescent protein (GFP) reporter. In control experiments targeting the neural ectoderm of the hindbrain by localized electroporation, GFP-expressing cells release from the neural tube, migrate along neural crest pathways and express the HNK-1 neural crest marker. Immunolabeling of Sox9 and Slug neural crest markers shortly after electroporation confirms transfection of prospective neural crest cells. Electroporation with a chimeric hemagglutinin-β1 integrin subunit inhibits release of transfected cells from the neural tube. Embryos electroporated with constitutively active RhoA have a few transfected cells outside the neural tube that express N-cadherin, but they fail to migrate to the branchial arch. Electroporation with constitutively active Rac1 results in

numerous cells near the neural tube, none of which express N-cadherin. Embryos electroporated with Cdc42 mutants are not distinguishable from control embryos expressing GFP alone. In embryos co-electroporated with chimeric integrin and dominant negative RhoA together, co-transfected cells migrate along neural crest pathways. The conclusion is that integrin signaling, transduced through RhoA, is necessary for the EMT of cranial neural crest. Key to this investigation of neural crest emigration is the methodology of localized electroporation. This technique introduces transgenes to targeted patches of cells in the embryo. Localized electroporation employs a double-barreled suction electrode to deliver plasmid and produce an electric field. Parameters for localized electroporation are optimized for transfecting a range of cells in the chick embryo, and expansion of the technique to mammals is demonstrated. Localized electroporation has improved reliability and higher efficiency than existing *in vivo* transfection techniques.

TABLE OF CONTENTS

LIST OF FIGURES

LIST OF ABBREVIATIONS

A	ampere
aON	antisense oligonucleotides
APC	adenomatous polyposis coli
Balb/c	Bagg albino mouse strain c
BMP	bone morphogenic protein
BPAG 1	bullous pemphigoid antigen 1
CHEMS	cholesteryl hemisuccinate
CMV IE	cytomegalovirus immediate early [promoter]
CSK	C-terminal Src kinase
DC	direct current
DOPE	dioleoylphosphatidylethanolamine
DOSG	dioleoylsuccinylglycerol
DOTAP	1,2-dioleoyloxypropl-3-N,N,N-trimethylammonium chloride
EGF	epidermal growth factor
EMT	epithelial-mesenchymal transition
FAK	focal adhesion kinase
F	farad
FGF	fibroblast growth factor
GAP	GTPase-activating protein
GEF	guanosine nucleotide exchange factor
GFP	green fluorescent protein
Grb2	growth-factor-receptor-bound protein 2
HA	hemagglutinin
HGF	hepatocyte growth factor
HJV	hemagglutinating virus of Japan [a.k.a. Sendai virus]
Hz	hertz
ILK	integrin-linked kinase
J	joule

LEF	lymphocyte enhancement factor
MAPK	mitogen-activated protein kinase
MCS	multiple cloning site
MDCK	Madin-Darby canine kidney [epithelial cell line]
MLCK	myosin light chain kinase
MMP	matrix metalloproteinase
Ω	ohm
OCT	optimal cutting temperature [embedding compound]
PBS	phosphate buffered saline
PIP_2	phosphatidyl-inositol-4,5-bisphosphate
pps	pulses per second
PTP1B	protein tyrosine phosphatase 1B
RNAi	RNA interference
s.e.m.	standard error of the mean
S180	murine sarcoma [cell line]
SF	scatter factor
SH	Src homology
TGFβ	transforming growth factor β
V	volt

pCMS-eGFP co-expression vectors (in chronologic order):

pCMS	empty control vector expressing only GFP
HA	control vector expressing hemagglutinin and GFP
HAβ1ΔE	chimeric hemagglutinin-β1 integrin construct
Gβ1ΔE	chimeric GFP-β1 integrin construct
CACdc42	constitutively active Cdc42 GTPase construct
CARac1	constitutively active Rac1 GTPase construct
CARhoA	constitutively active RhoA GTPase construct
DNCdc42	dominant negative Cdc42 GTPase construct
DNRac1	dominant negative Rac1 GTPase construct
DNRhoA	dominant negative RhoA GTPase construct

ACKNOWLEDGEMENTS

Thank you Robert Burke for always supporting me and never shying debate. Additional thanks go to Robert and members of my supervisory committee for deftly guiding my program and always making time to meet with me. Thank you Diana Wang for technical advice on nearly everything, especially the art of lighting antibodies. Also thank you Diana for assistance with primary cultures and for performing the immunofluorescence with primordial germ cells and mouse serum. Thank you Norma Lake, Dorothy Paul, Elisa Becker, and David Stuss for helpful comments and discussion throughout the years. Thank you Brian Antonsen, Patrick Kerfoot, and Heather Down for technical guidance and equipment. Thank you Allan Gibson and Caren Helbing for generous gifts of antibodies. Thank you Eugene Marcantonio, Mungo Marsden, and Alan Hall for kind gifts of constructs. Thank you Dan Mellot for sub-cloning the cyan/yellow fluorescent proteins, Rac1, and Cdc42 constructs. Acknowledgements to the Developmental Studies Hybridoma Bank (DSHB, University of Iowa) for providing antibodies and the UMR cDNA Resource Center (www.cdna.org) for providing RhoA. I am further grateful for financial support from the Heart and Stroke Foundation and its donors, BC Medical Health Services, and the University of Victoria. Additional gratitude goes to the Canadian Institutes of Health Research for funding my supervisor and key pieces of equipment. Most of all, thanks to my family for letting me burn their clutch while trying to get traction. Without them I would have surely blown my engine.

In Memory of

Claudius P., Jef R., & Carroll S.

CHAPTER 1 - Investigating Neural Crest Emigration in Embryos

The phenotype of a cell is a result of its transcriptional and translational machinery acting under the influence of internal and external cues. Dramatic shifts in phenotype occur when multipotent cells become restricted during embryogenesis. What are the origin and nature of signals initiating this type of change? How does a cell integrate various signals and how is its response regulated? The epithelial-mesenchymal transition (EMT) is a modulation of cell phenotype that provokes these questions. This process describes how a cell, organized within an epithelial layer, leaves its neighbors and migrates into a new microenvironment. In vertebrate embryos EMT occurs in a wide range of developmental processes including gastrulation, emigration of neural crest cells, and formation of cardiac valves (Shook & Keller, 2003). The neural crest is a diverse population of cells that, before the development of molecular markers, was defined and identified by an EMT event. This chapter will describe neural crest cells and their emigration as a model system for investigating the mechanisms of EMT in a whole organism. It will then focus on the mechanisms of EMT, and its regulation. I will discuss approaches for investigating EMT and the challenges of studying EMT in a whole organism.

Neural Crest Cells Arise from Neural Folds

Neural crest cells are multipotent cells that are formed from the neural folds along the embryonic axis in craniates. They are an induced population, resulting from interactions between the borders of the neural plate and the prospective epidermis (Selleck & Bronner-Fraser, 1996, 2000). Upon emergence, neural crest cells migrate some of the

longest distances in the developing embryo (Bronner-Fraser, 1993). Neural crest derivatives form most of the peripheral nervous system, most pigment cells, the adrenal medulla, thymus, parts of the heart, and much of the cartilage and bone of the head (reviewed by Erickson, 1986; Weston, 1991; Noden, 1986; Hall & Horstadius, 1988; Bronner-Fraser, 1994; Le Douarin & Kalcheim, 1999). Although the number of cells involved varies, neural crest migration pathways have been largely conserved among the fish, amphibians, birds, and mammals. The diversity of destinations and resulting structures inform contemporary debate concerning neural crest cells as a fourth germ layer (Hall, 2000). This debate has historic precedent. When Platt (1893) used the term "mesectoderm" to describe neural crest cells as mesenchymal cells of ectodermal origin, it sparked a controversial reinterpretation of von Baer's (1828) germ layer theory (for a partial English translation see Richards, 1992).

Before neurulation, the prospective neural epithelium has well-developed tight junctions and gap junctions. These gradually disappear during formation of the neural tube; the junctional complexes in the lips of the neural folds become fragmented (Revel & Brown, 1975). Following their induction, neural crest cells release from the neural epithelium. This is correlated with the loss of the cell adhesion molecules N-cadherin and cadherin-6B. The importance of this loss of cell adhesion is demonstrated in experiments in which overexpression of these proteins prevents delamination (Nakagawa & Takeichi, 1998). Neural crest cells acquire a multipolar form before moving through extracellular matrix (ECM), which is rich in fibronectin, laminin, and collagen. Invasion patterns of neural crest from neural tube grafts, in comparison to similar preparations with an invasive melanoma line, demonstrate that emigrating neural crest cells do not penetrate a contiguous basal lamina (Erickson, 1987). At the time of midbrain

emigration, however, the basal lamina covering the neural tube is incomplete. At axial levels caudal to the midbrain, immunolabeling of collagen IV, laminin and fibronectin show that the basal lamina is locally disrupted (Martins-Green & Erickson, 1987). Openings in the basal lamina are correlated with neural crest emigration, and lamina reconstitution occurs once emigration is complete (Erickson *et al*., 1992). It is unknown whether crest cells themselves are responsible, or if it is an effect of the surrounding tissue.

Neural crest emigration begins at the level of the midbrain and then in the forebrain. Neural crest emigration also continues in a rostrocaudal gradient through the hindbrain and down the trunk. In the forebrain and midbrain, emigration begins before the closure of the neural tube, before the ectoderm has sealed over the neural tube. At the level of the hindbrain, neural crest cells emigrate from the dorsal surface of the neural tube after fusion of the neural folds is completed (Le Douarin, 1982). In the avian embryo, the majority of cephalic emigration covers a period of 8 to 9 hours—from the early part of stage 9, through the end of stage 11 (for a standard set of avian developmental stages see Hamburger & Hamilton, 1951). Timelapse microscopy of hindbrain neural crest cells measures their speed at approximately 150 μm/h, and shows they generally complete migration in under 12 h (Kulsea & Fraser, 2000).

Lineage tracing using radiolabels and quail/chick grafts have revealed the pathways and distribution of migrating neural crest cells (Weston, 1963; Le Douarin, 1982). Neural crest cells emigrate from the midbrain as a uniform sheet of cells and move laterally away from the neural tube, but elsewhere along the embryonic axis, there is a segmental pattern. At the level of the hindbrain, streams of neural crest adjacent to even-

numbered rhombomeres are separated by regions lacking neural crest (Sechrist *et al.*, 1993; Graham & Lumsden, 1996). At the onset of neural crest migration in the trunk, cells move ventrally between the somites and the neural tube (Weston, 1963). Subsequently, neural crest cells move only through the rostral half of each somite. Approximately 24 h later, crest cells also exploit a lateral pathway by moving over the somites and underneath the ectoderm.

The populations of neural crest cells emigrating from different axial levels have different developmental fates. This variation is explained by intrinsic differences in their potentials, or extrinsic cues in the environment they encounter. Transplantation experiments show that cranial and trunk neural crest share the ability to produce melanocytes, glia, sensory and autonomic nerves (Noden, 1975; Le Douarin & Teillet, 1974). Only cranial neural crest cells, however, have the ability to produce cartilage and bone (Nakamura & Ayer-Le Lievre, 1982). Single-cell lineage tracing and clonal analyses *in vitro* reveal that most pre-migratory and migrating crest cells are multipotent (Bronner-Fraser & Fraser, 1988; Fraser & Bronner-Fraser, 1991; Le Douarin & Dupin, 1993). The mechanisms responsible for generating distinct streams of crest from even-numbered rhombomeres are under investigation. Transfection of recombinant bone morphogenic protein 4 (BMP4) into cultures of neural crest cells derived from odd-numbered rhombomeres activates the apoptotic pathway suggesting that neural crest precursors in the third and fifth rhombomere are pre-specified to undergo apoptosis (Graham *et al.*, 1993, 1996). Other grafting experiments point to the importance of the microenvironment adjacent to the neural tube in patterning these neural crest streams (Farlie *et al.*, 1999). It seems that a combination of environmental cues and fate specification are important in the emigration and differentiation of neural crest cells.

Mechanisms of Epithelial-Mesenchymal Transition

Before discussing the regulation of EMT, I will briefly review the phenotypes of epithelial and mesenchymal tissue. Epithelial cells form sheets on top of extracellular matrix. These cells are closely linked to each other by cell adhesion molecules and junctional complexes (Farquhar & Palade, 1965). They have desmosomes along their lateral surfaces, which are associated with intermediate filaments composed of cytokeratin. Near their apical surfaces, there are adherens junctions linked to the actin cytoskeleton. One side of an epithelium attaches to the basal lamina through focal adhesions and hemidesmosomes. Matrix components in the basal lamina generally include collagen type IV, certain types of laminin, and entactin. Attachment to these proteins is primarily mediated through the integrin family of receptors (Garratt & Humphries, 1995). The apical-basal polarity of a typical epithelial cell can be further characterized by differences in lipid and protein composition in the plasmalemma (Simons & Fuller, 1985).

Mesenchymal cell morphology is typically elongate. A mesenchyme cell attaches to more matrix proteins than those typical of the basal lamina,. These include fibronectin, and collagens type I, II, III, and V (Geiger *et al*., 1995). Moreover, the adhesion may be mediated by different integrins than those expressed by epithelium. Intermediate filaments in mesenchymal cells are usually composed of vimentin (Jackson *et al*., 1981). Mesenchymal cells exhibit less polarity in the distribution of certain cytoplasmic components such as mitochondria (Stern & MacKenzie, 1983). Mesenchymal cells often secrete enzymes (Stern, 1984) or glycosaminoglycans that aid their invasiveness. Mesenchymal cells downregulate cell-cell adhesion molecules, and make only transient contacts with neighbors, while migrating through ECM.

Cadherins are components of intercellular junctions that must be regulated during EMT. These transmembrane proteins dimerize in the plasmalemma and adhere to adjacent cells by homophilic binding. When the dimers cluster together, a zipper-like oligomer is formed between the cells (Shapiro *et al.*, 1995). Cadherins contain a cytoplasmic domain that binds β-catenin. Along with other proteins, β-catenin links cadherins to the actin cytoskeleton. Desmosomes are a junction connecting the cytokeratin cytoskeleton between cells. They contain the cadherins, desmocollin and desmogleins. These form homodimer transmembrane receptors. In desmosomes, plakoglobin binds to the cytoplasmic tail of cadherins (Hülsken *et al.*, 1994). As this binding is similar to β-catenin binding in adherens junctions, β-catenin can partially compensate for the lack of plakoglobin during the early stages of development in null mice (Bierkamp *et al.*, 1999). Another protein—plakophilin—also associates with the cytoplasmic tail of cadherins. In desmosomes, any of these proteins are linked to the cytoskeleton by desmoplakin.

Integrins mediate attachment to the extracellular matrix and are involved in cell motility. They are transmembrane proteins that form heterodimers, and can be found in hemidesmosomes and focal adhesions. The particular pairing of an α subunit with a β subunit determines the ligand specificity of the integrin receptor. For example, the α6β1 integrin binds laminin, whereas the α5β1 recognizes fibronectin. In vertebrates, at least 24 αβ complexes have been identified, resulting from combination of 9 β subunits and 18 α subunits (Hynes, 2002). In hemidesmosomes, the cytoplasmic tail of the β4 integrin subunit is associated with plectin (Wiche *et al.*, 1984). Plectin, along with bullous pemphigoid antigen 1 (BPAG 1), forms a plaque that mediates attachment to the intracellular cytokeratin matrix (Stanley *et al.*, 1988). In focal adhesions, the cytoplasmic

tail of the β subunit can bind directly to talin. Talin is a major structural protein that binds actin and vinculin, as well as focal adhesion kinase (FAK). Vinculin can bind to actin directly, and indirectly, through tensin. The β subunit also associates with α-actinin in focal adhesions. α-Actinin can cross-link actin filaments as well as bind vinculin (Vuori, 1998). In addition to their mechanical function, integrin complexes are sites of signal transduction during cell proliferation, apoptosis, and differentiation.

Matrix attachment is required to generate tensile force for motility after cells release from the basal lamina during EMT. This suggests that the coordination of integrin function may be more complex than cadherins. Dissecting integrin regulation may be easiest in situations where cells attach to different ECM proteins before and after EMT. Another notable point about these receptor proteins is that they are not restricted to junctional complexes. Cadherins and integrins may have a less localized distribution. One hypothesis is that individual interactions occur first with the cytoskeleton, and then, large complexes form to strengthen a more permanent junction (Chrzanowska-Wodnicka & Burridge, 1996). The number of protein associations in junctional complexes is substantial. The cytosolic activity or concentration of each protein can be important for junctional stability or function. Moreover, each point of protein interaction is a potential site for regulation. The details of such regulation can be categorized in four general mechanisms: transcriptional regulation, post-translational regulation, maintenance, and degradation.

Transcriptional Regulation

Transcriptional regulation is perhaps the most straightforward mechanism involved in the transition to a mesenchymal phenotype. Epithelial cells typically contain cytokeratin

intermediate filaments and a good example of transcription regulation is the synthesis of vinculin intermediate filaments after EMT (Boyer *et al*., 1989). There is also a growing amount of indirect evidence that levels of adhesion protein expression could regulate EMT. Anti-cadherin antibodies dissociate Madin-Darby Canine Kidney (MDCK) epithelial cells and produce mesenchymal morphology with the loss of epithelial polarity (Behrens *et al*., 1985). Transfection with cadherin cDNA prevents invasiveness in mesenchymal cultures (Frixen *et al*., 1991) and promotes cell-cell contact. Cell sorting assays demonstrate a quantitative relationship between the amount of cadherin expressed and strength of adhesion (Steinberg & Takeichi, 1994). Findings such as these have tempted speculation that cadherins could be master regulators for EMT (Hay, 1995), although a direct role of their transcriptional regulation remains to be demonstrated. What is clear is that mechanisms that affect expression of cell adhesion receptors have an effect on EMT.

There are a few families of transcription factors correlated with the induction of EMT. A major one is the Slug/Snail family of zinc-finger proteins. In the chicken embryo, Slug mRNA is expressed in the primitive streak and neural folds (Nieto *et al*., 1994). These areas correspond to sites of prominent EMT. The injection of Slug antisense oligonucleotides into those areas interferes with EMT (Nieto *et al*., 1994). Overexpression of Snail family members in the same areas, likewise, results in increased numbers of cells undergoing EMT (del Barrio & Nieto, 2002). There is also evidence linking the Slug/Snail family to receptors of the EMT signal in the MDCK *in vitro* model of EMT. The expression of dominant negative Ras prevents scattering in MDCK cells. Exogenous Slug will restore the scattering behavior in MDCK cells expressing dominant negative Ras (Boyer *et al*., 1997). Slug/Snail can affect phenotype through a number of

possible mechanisms. Perhaps most importantly, Snail has been found to bind several E-boxes located on the cadherin promoter, which represses expression of the cadherin gene (Batlle *et al.*, 2000). This type of transcriptional regulation could be responsible for EMT. Slug expression *in vitro* decreases the amount of desmoplakin and desmoglein in desmosomes and results in cell spreading. Furthermore, Snail is correlated with increased matrix metalloproteinase (MMP) and vimentin expression (Yokoyama *et al.*, 2003), proteins that are characteristic of mesenchymal phenotypes. The Slug/Snail family cannot, however, be responsible for all the changes during EMT. Induction of EMT by Slug overexpression requires epidermal growth factor (EGF) in NBT-II rat bladder carcinoma cells (Savagner *et al.*, 1997). Moreover, Slug overexpression triggers only desmosome dissociation, and does not promote migration in NBT-II cells (Savagner *et al.*, 1997). It is reasonable that other transcription factors are involved.

Brachyury is a T-box transcription factor that is activated by receptor tyrosine kinases (Smith, 1997). Murine embryos null for Brachyury show decreased ingression during gastrulation leading to a buildup of cells in the primitive streak (Wilson *et al.*, 1995), and cells migrate slowly when cultured on ECM (Hashimoto *et al.*, 1987). Overexpression of Brachyury causes premature migration of cells away from the primitive streak (Wilson & Beddington, 1997). The gene targets of Brachyury during EMT are not yet known, however, they may account for effects that are not associated with Slug/Snail.

Another candidate for transcriptional regulation is the β-catenin/LEF pathway. This pathway is affected by Wnt signals that are involved in many developmental events. The receptor for Wnt, Frizzled, leads to activation of Dishevelled, which inhibits GSK 3β, which in turn, stabilizes β-catenin (Behrens, 1999). A subsequent accumulation of β-

catenin occurs first in the cytoplasm, then in the nucleus where it displaces Groucho to interact with the lymphocyte enhancement factor (LEF) transcription factor. LEF binds to the HMG box of a target gene but has no activity on its own. Addition of β-catenin to the complex converts LEF from a transcriptional inhibitor to a transcriptional activator (Molenaar *et al.*, 1996). In DLD-1 tumor cells, viral overexpression of LEF triggers EMT that is more rapid than those induced by Wnt signaling (Kim *et al.*, 2002). The target genes of this pathway currently include fibronectin (Gradl *et al.*, 1999) and MMP (Brabletz *et al.*, 1999), showing potential redundancy with some Slug/Snail targets. There is also evidence in *Xenopus* that, since the Slug promoter contains a functional LEF binding site, Slug is activated by Wnt signals (Vallin *et al.*, 2001). In conclusion, transcription control is potentially a mechanism that regulates EMT. The β-catenin/LEF pathway and other signaling cascades likely connect the induction of EMT to gene transcription. Future studies should make direct connections between components of the pathways that are currently correlations.

Post-translational Regulation

The post-translation regulation of proteins involved in EMT can produce effects that are similar to transcriptional regulation. Experiments that generate corollary evidence can often be explained by multiple mechanisms. As discussed above, Snail has the ability to repress cadherin expression, and anti-cadherin antibodies cause dissociation of MDCK cells. This is not, however, direct evidence for a developmental inhibition of cadherin expression. The same effect could result from the loss of cadherin function, completely independent of changes in protein level. Indeed, no alterations in the levels of cadherins are detected during certain periods of rapid cell adhesion modulation in *Xenopus* (Brieher

& Gumbiner, 1994). Post-translational mechanisms are hypothesized as regulating EMT in these types of examples.

The structure of adherens junctions allows great potential for regulation. β-catenin, a component of adherens junctions, is also common to the Wnt pathway of gene expression. Since Wnt can control the amount of β-catenin in the cytoplasm, Wnt also has the potential to regulate adherens junctions in situations when the amount of β-catenin is a limiting factor to assembly. Conversely, disassembly of adherens junctions could increase the amount of cytoplasmic β-catenin, thereby changing the LEF transcriptional co-factor to an activator in a Wnt-independent manner. The association of β-catenin with cadherins is tightly regulated by phosphorylation. Phosphorylation of tyrosine-654 on β-catenin reduces its affinity for the cytoplasmic domain of cadherin (Roura *et al.*, 1999). A catalytically inactive form of the protein tyrosine phosphatase 1B (PTP1B) reduces cell-cell interaction (Balsamo *et al.*, 1998). The detachment is correlated with an increase of non-cadherin-associated β-catenin that is phosphorylated on multiple tyrosine residues (Balsamo *et al.*, 1998). It seems that PTP1B is required for maintaining β-cadherin in an unphosphorylated state, which therefore maintains the cadherin-actin linkage, cell-cell adhesion, and the epithelial phenotype. In contrast to this role, PTP1B also dephosphorylates the Crk adapter protein, which promotes cell migration (Takino *et al.*, 2003). A good definition of PTP1B function during EMT requires further investigation.

Another regulator of adherens junctions is the IQ motif containing GTPase activating protein (IQGAP). This protein binds to cadherin-β-catenin complexes and competes for binding with linkages to the actin cytoskeleton (Kuroda *et al.*, 1998). The presence of

IQGAP can therefore render the adherens junctions nonadhesive. IQGAP1 immunoprecipitates with GTP-bound Rac and Cdc42 (Kuroda et al., 1996), which are GTPases involved in EMT. Microinjection of active GTPases into COS-7 monkey fibroblast cells leads to localization of IQGAP at cell-cell adhesion sites, and dominant negative Rac or Cdc42 prevent this accumulation (Kuroda et al., 1996).

Focal adhesions bind the extracellar matrix through integrin receptors. Burridge's group has proposed a model regulating the assembly of focal adhesions. In this model, integrin bound to extracellular ligand couple to cytoplasmic actin through talin or α-actinin. At this point the integrin are not clustered in the membrane and there is no tension in the actin filaments. Strong cell-matrix adhesion depends on the activation of Rho, which causes elevated phosphatidyl-inositol-4,5-bisphosphate (PIP_2) levels. The interaction of PIP_2 to a hinge region in vinculin causes a conformational change that exposes the binding sites for talin and actin (Gilmore & Burridge, 1996). Vinculin can then enhance the structural connection between integrin and the actin cytoskeleton. Rho also activates Rho kinase, which activates myosin light chain kinase (MLCK), resulting in stress fiber contraction. The final result in this model is receptor aggregation and strengthened cell-substrate adhesion (Chrzanowska-Wodnicka & Burridge, 1996).

Integrin signals influence cell-cell attachment either by enhancement or inhibition. In epithelial culture, the application of integrin function-blocking antibodies causes cell-substrate and cell-cell detachment (Carter *et al.*, 1990). In neural crest cells, however, blocking of β1 integrin function by antibodies or RGD peptides results in N-cadherin clustering and cell aggregation (Monier-Gavelle & Duband, 1997). Other studies in β1-deficient epithelial cells find that β1 integrin expression triggers activation of Rho and

Rac and decreases levels of cadherin associated with the detergent-insoluble cytoskeletal fraction (Gimond *et al.*, 1999). One candidate that may mediate the crosstalk between integrin and cadherin adhesion junctions is integrin-linked kinase (ILK). ILK directly interacts with the cytoplasmic tail of integrin β subunits. Overexpression of active ILK in both intestinal and mammary epithelial cells induces an EMT-like effect with the downregulation of cadherin-mediated cell adhesion (Novak *et al.*, 1998). ILK also inhibits GSK 3β, a protein that phosphorylates β-catenin in the canonical Wnt system (Oloumi *et al.*, 2004). This is a potential link between integrin signals and β-catenin/LEF-mediated gene expression in EMT. The pathway may be involved in discriminating between EMT and mitogenic signals, and warrants further investigation. Another good candidate for integrin-cadherin communication is Fer. Fer is a nonreceptor tyrosine kinase found in adherens junctions. The association of Fer with cadherin can be inhibited by synthetic peptides that mimic the Fer binding domain of cadherins (Arregui *et al.*, 2000). In the presence of these peptides, Fer translocates from adherens junctions to focal adhesions. In chick retinal cells, this is correlated with reduced cell-cell adhesion and increased cell-matrix attachment to laminin. Moreover, cell-matrix attachment is rescued with a second peptide that mimics the Fer-binding domain of integrin (Arregui *et al.*, 2000). These results suggest a coordinated regulation of integrin and cadherin that is not mediated by transcriptional control.

Maintenance Pathways

Many cellular proteins are constantly turning over. The balance between production and removal influences the number of functional molecules, and dynamic structures are often associated with high rates of turnover. The turnover of cell adhesion proteins in focal

adhesions and adherens junctions may play a crucial role during EMT. Cranial neural crest cells selectively internalize integrin during rapid migration on fibronectin and laminin-coated slides (Strachan & Condic, 2004). A significant portion of the biotin-labeled receptors are returned to the cell surface after both 20 and 90 min, as indicated by a 39 and 63% increase in the intensity of fluorescently-conjugated strepavidin. This recycling is blocked by bafilomycin A, which inhibits the transport of vesicles out of the endosome by preventing acidification caused by H^+-ATPase (Strachan & Condic, 2004). These experiments show that integrin recycling can occur at a rapid rate in cranial neural crest cells, and therefore, regulation of integrin recycling may be important during EMT. Adherens junctions turn over at a slower rate. Pulse-chase experiments with [^{35}S]methionine indicate the half-life of cadherins in confluent MDCK cells is 5-10 h (Shore & Nelson, 1991). Given that many developmental EMTs occur on time scales shorter than 5 h, the rapid loss of cell-cell adhesion is not likely the result of cadherin turnover.

The normal turnover of an adhesion protein would result in a net decrease if the rate of protein synthesis was inhibited. Transcriptional regulation has already been discussed, however that is only part of the equation. In combination with transcription, mRNA turnover events directly influence the amount of mRNA available for protein translation. Microarrays generated from total poly A^+ mRNA and de-novo-transcribed poly A^+ mRNA indicate that mRNA stability accounts for up to 50% of the variation in total mRNA concentration (Cheadle et al., 2005). This difference supports the importance of mRNA half-life, however, correlation to protein function in a process like EMT remains to be investigated.

In the case of the cytoskeleton, maintenance refers to macromolecular organization. Several GTPases have well-characterized effects on the organization of the cytoskeleton and cell motility. Generally, Rho organizes actin stress fibers, Rac forms lamellipodia or membrane ruffles, and Cdc42 induces filopodial extension (Mackay & Hall, 1998). Rho also has the potential to modulate focal adhesions through regulating the contraction of actin filaments (Chrzanowska-Wodnicka & Burridge, 1996). These GTPases can be indirectly activated by receptor tyrosine kinases during EMT, so they are likely responsible for many of the cytoskeletal changes associated with EMT. Microtubules are another dynamic component of the cytoskeleton. While they do not appear to directly participate in EMT, microtubules are required for apical-basal polarity in epithelia (Ojakian *et al*., 1997). Immunoprecipitations of the microtubule-associated protein EB1, and intracellular localization of EB1-GFP-fusion proteins show that microtubules can sequester adenomatous polyposis coli (APC) (Askam *et al*., 2000), a protein involved in β-catenin degradation. The disruption of microtubules, therefore, could contribute directly to EMT, by causing both the loss of cell polarity and the loss of intercellular junctions.

Protein Degradation

Mesenchymal cells secrete proteases that digest ECM components, including those of the basal lamina. Chemical and translational inhibition of MMP2 in chick embryos prevents EMT of neural crest cells (Duong & Erickson, 2004). Scp2 mammary cells have an epithelial morphology, but adopt a mesenchymal appearance and become invasive in the mammary fat pads of mice when MMP3 expression is induced (Sternlicht et al., 1999). MMP3 expression may simply be a final requirement for motility, or the action of the

protease may facilitate novel matrix signaling that triggers or induces EMT.

Other examples of protein degradation regulating EMT may involve the active removal of a key molecule from a structural or signal pathway. Inside a cell, this type of regulation is accomplished by the ubiquitin-proteasome system (Aberle *et al*., 1997), and protein-protein interaction is very important throughout the process. The total activity of the proteasome has been investigated during the scatter of MDCK cells (Tsukamoto & Nigam, 1999). When the proteasome is chemically inhibited, disruption of cell-cell junctions is almost completely prevented. This indicates that active protein degradation is important for EMT in MDCK cells. Proteasome inhibition has no effect on focal adhesions or cell motility in MDCK cells, suggesting that proteasome degradation does not regulate cell migration. Cadherins and β-catenin are potential substrates. Tryptophan fluorescence, circular dichroism, and one-dimensional proton NMR measurements indicate that the cytoplasmic domain of cadherin is unstructured when not bound to β-catenin (Huber *et al*., 2001). The association of β-catenin with cadherin protects the cytoplasmic domain from degradation in proteolytic assays (Huber et al., 2001). These experiments demonstrate a possible link between the regulation of cadherins and β-catenin. The loss of β-catenin from adherens junctions could cause the removal of cadherins from the plasmalemma by degradation. The regulation of cadherins and β-catenin is also linked in the endoplasmic reticulum. A series of mutations in a chimeric cadherin-β-catenin molecule show that β-catenin is necessary for cadherin to efficiently exit the endoplasmic reticulum (ER) in MDCK cells (Chen et al., 1999). If there is no free β-catenin in the ER, it is possible, therefore, for cadherin protein to be degraded shortly after translation, even before reaching the cell surface.

In Vitro Approaches and *In Vivo* Challenges

Experimental results are evaluated in the context of the methods used to generate the data. A large portion of EMT research has been performed in cell culture (Valster *et al.*, 2005). This approach allows a scientist to control many aspects of the experiment. The approach has also enabled cell lines to be standardized for reproducible results among investigators. The compromise made for this degree of control is that not all *in vivo* conditions can be recreated in a dish. Immortalized cell lines are not identical to the cells from which they are derived. Furthermore, some lines are derived from cancerous tissues, e.g., NBT-II cells from a rat bladder tumor. Results from these models are valuable and insightful, but they are not wholly representative of normal cells *in vivo*. In epithelial cultures such as MDCK cells, EMT-like scatter behavior is often induced with a single factor. It is clear, however, that EMT is highly regulated process, resulting from multiple inputs, and acting through numerous mechanisms. For these reasons, the emigration of neural crest cells in the avian embryo is an appropriate choice of model for investigating EMT.

The objective of my work is to identify the *in vivo* requirement for β1 integrin function in emigrating cranial neural crest cells and to investigate the relation of integrins to potential components of the signaling pathway. Investigating EMT in a developmental system is accompanied by several technical challenges. In the case of neural crest in the avian embryo, the interplay of multiple cell types must be considered. To make precise conclusions, it is desirable to specifically target the experimental treatment to neural crest cells. If precursors of neural crest cells were targeted, it would be difficult to separate effects on neural crest specification from neural crest emigration. After their formation, neural crest cells interact with other cells and matrix components in the neural epithelium

and along their migration paths. Ideally, mutant neural crest cells would be evaluated in a wild-type background. Furthermore, it is important to consider the brief window of time between the formation of neural crest cells and their emigration. This relatively quick event necessitates a fast acting methodology, and to enable this work I have developed a new method of targeting the expression of transgenes to create genetic mosaic embryos. I hypothesize that β1 integrin function is required for cranial neural crest EMT and that RhoA GTPase is involved with transducing the integrin signal.

CHAPTER 2 - Cranial Neural Crest Cells Require β1 Integrin Signaling through RhoA for Epithelial-Mesenchymal Transition

INTRODUCTION

The epithelial-mesenchymal transition (EMT) is a fundamental modulation of cell phenotype. EMT features the loss of intercellular junctions and the acquisition of migratory ability (Hay, 1995; Boyer *et al*., 2000; Shook & Keller, 2003). A good model of EMT is the neural crest. These cells arise from interactions between the neural ectoderm and prospective epidermis. Neural crest cells go through EMT before they migrate to various destinations in the embryo. One signaling protein implicated during these early phases of neural crest development is the β1 integrin (Bronner-Fraser, 1985a; 1986; 1987; Bronner-Fraser & Lallier, 1988; Kil *et al*., 1996). The integrin family of transmembrane receptors is involved in bidirectional signaling and attachment to the extracellular matrix (Hynes, 2002), however, the precise role of integrins in neural crest development, is incompletely understood. Integrins may be required for both EMT and directed migration, or perhaps required for only one of these phases.

Integrin Signaling and Chimeric Constructs

Integrin signaling is regulated by conformational changes, and also, by the clustering of receptors in the membrane. Distinct roles for these mechanisms are demonstrated by an experiment in Chinese Hamster ovary cells (Hato et al., 1998). A chimeric αIIbβ3 integrin fused to FK506-binding protein can be clustered by application of AP1510, a membrane-permeable ligand. AP1510 is sufficient to generate a 2.8-fold increase in tyrosine phosphorylation of Syk, but does not affect phosphorylation of FAK. The

combined application of fibrinogen (the αIIbβ3 ligand) and AP1510 results in a 3.5-fold increase in FAK phosphorylation. The separate application of fibrinogen leads to phosphorylation of Syk and not FAK. Thus, integrin downstream signaling has a range of requirements: clustering, ligation, or a combination of both.

Functional experiments, crystal structure, NMR, and electron microscopy studies indicate that ligation of integrin causes conformational changes, and similarly that integrin affinity is primed or activated by conformational changes (Shimaoka *et al.*, 2002). Springer and colleagues have described a model regulating integrin signaling through conformational changes. The low affinity integrin conformer is shaped like a jackknife, with the ligand-binding head bent down towards the membrane. High-affinity or ligand-bound integrin adopts an extended conformation that is correlated with rearrangements around a metal ion-dependent adhesion site in the inserted (I) domains of the head in α and β subunits. This conformation allows an acidic residue of the ligand to interact with a metal ion that is positioned by water molecules coordinated by two serines, two aspartic acid residues, and one threonine from the I domain (Takagi & Springer, 2002). The presence of the acidic residue of the ligand moves the metal ion 2.3 Å laterally away from one of the aspartic acids residues, and towards the threonine. The rearrangement of these coordinating residues is coupled to lateral shifts in the loops that form the backbone of the metal ion-dependant adhesion site. These shifts are linked to a movement 10 Å downward of the C-terminal α-helix, which transmits conformational changes throughout the stalk of the integrin by an outward swinging of the β1 hybrid domain (Luo & Springer, 2006). Studies using fluorescent resonance energy transfer demonstrate that straightening of the extracellular stalk is coupled to a large spatial separation of the α and β transmembrane and cytoplasmic domains (Kim et al., 2003).

Separation of the α and β cytoplasmic domains is linked to interaction with other molecules. The head domain of talin, for example, binds to the cytoplasmic domain of the β subunit (Calderwood et al., 1999). The binding region overlaps the area of αβ cytoplasmic interaction, and talin is associated with integrin activation. In this model, extracellular signals from ligand binding can be transduced into the cell, and furthermore, integrin affinity can be regulated by cytoplasmic interactions. Both phenomena are a reflection of a single allosteric mechanism whereby the extended integrin conformer is stabilized from outside or from inside the cell.

Focal adhesion kinase functions as a scaffold, interacting with many proteins, including talin and the cytoplasmic domain of β integrin subunits. Once recruited to integrin signaling complexes, FAK autophosphorylates on Y397, creating a high affinity site for the SH2 domain of Src (Schlaepfer & Hunter, 1996). Binding of Src to FAK precedes phosphorylation of Y576/577 in the kinase domain a FAK, a step that is essential for maximal FAK kinase activity (Hanks et al., 2003). Src can also phosphorylate Y407, Y861, and Y925 on FAK, and these binding sites appear to be used during certain cellular events. For example, phosphorylation of Y861 is necessary for cell migration in Ras-transformed murine fibroblasts and for the TGFβ-induced EMT of murine mammary epithelial cells (Lim et al., 2004; Nakamura et al., 2001). FAK phosphorylation on Y925 acts as a docking site for the Grb2 adapter protein, which leads to activation of the Ras/MAPK cascade (Downward, 1994; Zarich et al., 2006). In addition to phosphorylating FAK, Src phosphorylates a number of tyrosine residues on p130CAS, paxillin, and tensin. FAK also has SH3 domains that bind p130CAS, an adapter protein that binds Crk and Nck—effectors that have pathways in common with Cdc42 and Rac (Vuori, 1998). Autophosphorylated FAK may furthermore activate C-

terminal Src kinase (CSK). CSK can negatively regulate Src by phosphorylating a C-terminal tyrosine on Src, causing a conformational change in Src that inactivates its catalytic domain (Chong et al., 2005). The C-terminal domain of FAK also binds and phosphorylates p190RhoGEF (Zhai et al., 2003), a RhoA-specific guanosine nucleotide exchange factor that enhances RhoA activity (van Horck et al., 2001).

Recruitment of FAK to integrin complexes is clearly important for many signaling pathways, and integrin complexes may form by a few mechanisms. Contraction of the cytoskeleton can facilitate integrin clustering during the assembly of focal adhesions (Chrzanowska-Wodnicka & Burridge, 1996). Binding of more than one integrin to a multivalent ligand can clustering integrins on a smaller scale, and recruit some cytoplasmic proteins such as FAK (Miyamoto et al., 1995). It is also possible that separation of the α and β transmembrane and cytoplasmic domains in the activated conformer may lead to clustering. Experiments with isolated αIIbβ3 transmembrane domains in micelles found a preference for α and β subunits to have homomeric interactions, forming dimers and trimers respectively (Li et al., 2001). The G708N mutation in the transmembrane domain of β3 enhanced the tendency to form homotrimers and induced constitutive phosphorylation of FAK (Li et al., 2003). It appears that clustering might be sufficient to initiate signaling by FAK, although clustering alone may not generate signals that require complex cytoskeletal complexes.

Chimeric integrin constructs have been used to investigate integrin-mediated adhesion and signaling. β1 integrin chimeras containing the extracellular domain of CD4 are reported to inhibit matrix adhesion in human embryonic kidney cells (Lukashev *et al.*, 1994) and murine mammary gland development (Faraldo *et al.*, 1998). Furthermore, the

CD4-integrin chimera inhibits FAK phosphorylation, which is normally induced by the antibody-clustering of endogenous integrins (Lukashev *et al.*, 1994). A β integrin chimera containing a short extracellular hemagglutinin tag causes varying abnormalities in *Caenorhabditis elegans*, including defects in cell migration and organogenesis, depending on the level of transgene expression (Lee *et al.*, 2001). These studies suggest that single-subunit chimeras containing the β cytoplasmic domain inhibit cell adhesion and function as dominant negative inhibitors of some integrin signals, presumably by competing for cytosolic molecules that associate with endogenous integrins. Integrin chimeras that can be clustered have different effects. A β1 chimera containing the extracellular portion of the interleukin-2 receptor can increase phosphorylation of FAK in human fibroblasts when exposed to beads coated with anti-interleukin-2 antibodies (Akiyama *et al.*, 1994). Furthermore, antibody-induced clustering of this chimera is sufficient to generate a 4.7-fold increase in Rac1 GTPase activity (Berrier et al., 2002). These studies suggest that clustering of chimeras containing the cytoplasmic domain of β integrin subunit can initiate inappropriate signaling.

Integrins Expressed by Neural Crest Cells

The entire repertoire of integrins expressed by cranial neural crest cells is not known. It is clear that the β1 family predominates: notably α1β1, α4β1, and α5β1 (Lallier & Bronner-Fraser, 1992; Kil *et al.*, 1996, 1998). Additional αV integrins (Delannet *et al.*, 1994), and other β families (Desban & Duband, 1997; Testaz *et al.*, 1999), are found in cultures of trunk neural crest. In avian embryos, but not mice, *in situ* hybridization and immunolabeling demonstrate brief expression of the αVβ3 integrin in cranial neural crest cells during the early phase of migration (Pietri *et al.*, 2003). This is the only report of a

non-β1 integrin being expressed during this developmental period. Since αV also pairs with β1, and β3 does not appear until after EMT, targeting the β1 subunit is a reasonable approach to assess integrin function during EMT.

Trunk neural crest cells adhere to slides coated with collagen I and IV, whereas cranial neural crest cells do not (Lallier *et al.*, 1992). Trunk neural crest cells require laminin plated with divalent cations for attachment, whereas cranial neural crest cells can bind laminin plated in a cation-absent conformation (Lallier *et al.*, 1992). Application of a β1 integrin function-blocking antibody to cranial and trunk neural crest cell cultures causes rounding and detachment from fibronectin and laminin substrates (Lallier & Bronner-Fraser, 1991). Antiserum to α1 integrin subunit inhibits attachment of trunk neural crest cells to laminin substrates, whereas cranial neural crest cells are unaffected (Lallier *et al.*, 1992). Comparison of α1, α3-through-7, and αV mRNA by Q-PCR with their biotinylated surface protein levels show that differences between cranial and trunk neural crest cells are not due to transcriptional differences of integrins, suggesting a role for post-translational regulation (Strachan & Condic, 2003). These studies demonstrate that neural crest cells possess distinct integrins depending on their axial level and may correlate with differences in migratory ability or the pathways they use.

Neural crest cells may use integrins to adhere and migrate on substrate. Trunk neural crest cells preferentially migrate on fibronectin-coated stripes when simultaneously presented with laminin, collagen, or glass, and move at speeds similar to those observed *in vivo* (Rovasio *et al.*, 1983). These common integrin ligands are present in the extracellular matrix of the embryo (Erickson, 1987). Approaches of grafting murine sarcoma S180 cells into avian neural crest migratory pathways also suggest roles for

integrins (Beauvais *et al.*, 1995). Transfection of α4β1 or α5β1 integrin enhances the motility of S180 cells on fibronectin substrates by more than 3-fold. When grafted into the trunk, parental S180 cells and host neural crest cells migrate first in between the somites and the neural tube. These cells do not normally pass through the somites, until 24 h later in development, however, when the S180 cells are made to overexpress α5β1 integrin, they began to migrate in both pathways simultaneously (Beauvais *et al.*, 1995). These experiments suggest that neural crest cells respond to integrin ligands and that altered integrin expression changes the behavior of cells in the neural crest environment. Thus, integrins potentially regulate the pathways chosen and behavior of neural crest cells.

Perturbation of Integrin Function

The first *in vivo* studies of integrin in neural crest emigration employed an antibody perturbation approach (Bronner-Fraser, 1985a; 1986). Grafting hybridoma cells and injecting anti-integrin antibodies into the path of avian cranial neural crest cells results in reduced neural crest migration. Some neural tube defects, which may be consistent with impaired EMT, are also observed. Neural crest cells of the trunk are affected to a much lesser extent. Perturbation with anti-HNK-1 and anti-laminin-heparan sulfate proteoglycan complex antibodies produce similar defects (Bronner-Fraser, 1987; Bronner-Fraser & Lallier, 1988). Injection of several α integrin antisense oligonucleotides (aON) into the cranial mesenchyme alters cranial neural crest migration, resulting in neural tube defects, cells within the neural tube lumen, and an apparent inhibition of EMT (Kil *et al.*, 1996). In contrast to antibody perturbations, injections of aON against β1 integrin produce no defects (Kil *et al.*, 1996). A similar approach

introducing β1 integrin antisense morpholinos to trunk neural crest found a range of phenotypes (Tucker, 2004). Some embryos had HNK-1 positive cells in the neural epithelium, many had cells in the neural tube lumen, and 5 of 11 embryos had apparently normal migration. Targeted deletion of the β1 integrin subunit in mice causes lethal, placentation-related defects before neural crest formation (Stephens *et al.*, 1995), however, chimeric embryos containing β1 null cells can be generated (Fässler & Meyer, 1995). Many tissues derived from neural crest in these chimeric embryos are found to contain β1 null cells, suggesting that emigration of individual neural crest in mice does not require integrin. In comparison to perturbation experiments, however, it is possible that other β integrin genes compensate for loss of function, or that community effects of neural crest cells compensate for loss of integrins on individual cells. When avian embryos are injected with β1 deficient mouse embryonic stem cells, the characteristic migration of control stem cells is impaired, but the deficient cells are apparently able to follow some neural crest pathways (Beauvais-Jouneau *et al.*, 1999). In conclusion, there are conflicting results as to whether β1 integrins are necessary for avian neural crest migration. The experiments do not show if detachment from the epithelium is affected and they are not able to distinguish effects on migration from effects on EMT.

EMT Signals Originate Outside the Cell

Some of the first demonstrations that EMT could be experimentally induced were done with type I collagen (Greenburg & Hay, 1982). In these experiments, corneal explants are cultured in a three dimensional collagen gel. Cells on the surface of the epithelium not covered by a basal lamina, develop filopodia and become invasive. While this is similar to EMT, the role of collagen is uncertain. It is possible that collagen may be a

secondary requirement of a primary inducing factor, perhaps a serum component present in the culture. Other signals for EMT include epidermal growth factor (EGF), scatter factor/hepatocyte growth factor (SF/HGF) and members of the fibroblast growth factor (FGF) and transforming growth factor β (TGFβ) families (Savagner *et al.*, 1994). NBT-II cells derived from a rat bladder carcinoma, disassemble adherens junctions and downregulate cytokeratin following exposure to FGF (Vallés et al., 1990). The scattering NBT-II cells express vimentin, individualize, and migrate (Boyer *et al.*, 1989). Since matrix components are present in growth factor experiments, but do not induce a complete transition by themselves, it is possible that signals from both soluble factors and matrix components are required during some EMTs. In conclusion, the induction of EMT involves factors outside the epithelial cell, and the signal is transduced at the membrane by receptors.

Kinase Pathways Determine the Specificity of the EMT Signal

In addition to causing EMT, growth factors regulate cell proliferation. The mechanism used by the cell in reacting to this multifunctional signal is incompletely understood. SF/HGF accelerates cell division, disrupts cellular junctions, induces process extension, and increases cell motility in Madin-Darby canine kidney (MDCK) epithelial cell cultures. SF/HGF binding to the c-met receptor induces interaction with growth-factor-receptor-bound protein 2 (Grb2), a SH2-3-2 domain adapter protein (Fixman et al., 1995). When synthetic tripeptide-based antagonists of Grb2 are added to MDCK cells, the application of SF/HGF promotes only mitogenic effects (Atabey *et al.*, 2001). This suggests that interaction of Grb2 with c-met is necessary for EMT. Ras, which is activated by Grb2 through the guanine-nucleotide exchange factor Sos (son of sevenless),

activates mitogen-activated protein kinase (MAPK) pathways. A MAPK cascade is active during SF/HGF and EGF induced scattering (Potempa & Ridley, 1998; Boyer *et al.*, 1997), and furthermore, scattering can be prevented by expression of dominant negative Ras (Boyer *et al.*, 1997). Since a MAPK cascade does not appear to be required for the mitogenic effects of SF/HGF (Day et al., 1999), GTPases are candidates for controlling the specificity of the EMT signal by activating pathways that are distinct from the mitogenic effects of the signal.

GTPase Expression in Cranial Neural Crest

The Rho GTPases are a family of small guanine nucleotide-binding proteins involved in the transduction of extracellular signals (Van Aelst & D'Souza-Schorey, 1997; Hall & Nobes, 2000; Bishop & Hall, 2000). Rho GTPases function as molecular switches, cycling between an inactive GDP-bound state and an active GTP-bound form. Once activated, Rho GTPases are able initiate a downstream response or signal cascade in effector molecules. Intrinsic GTPase activity returns the molecule to an inactive GDP-bound form, although this activity can be regulated by GTPase activating proteins (GAPs) and guanosine nucleotide exchange factors (GEFs). More than 20 GAPs and 30 GEFs have been identified, and many of these associate with more than one GTPase (Lamarche & Hall, 1994; Van Aelst & D'Souza-Schorey, 1997). The diversity in GEFs may be important in restricting the interaction of a GTPase to a subset of effector proteins (Bishop & Hall, 2000). Rho GTPases can be C-terminal prenylated and localize to membranes (Adamson et al., 1992), or, they can exist in an inactive soluble form bound to a guanosine nucleotide dissociation inhibitor (Olofsson, 1999). Activation of Rho induces the formation of stress fibers (Nobes & Hall, 1995, 1999). Activation of Rac and Cdc42 induces polymerization of actin in a meshwork underlying the plasma membrane.

Activation of Rac promotes the formation of membrane lamellipodia, while activating Cdc42 results in membrane filopodia (Luo *et al*., 1996). The abilities of Rho GTPases to affect the actin cytoskeleton is well characterized, however they are also involved in pathways regulating transcription and proliferation.

Signaling from integrins and growth factor receptors is linked with Ras and Rho GTPases (Hotchin & Hall, 1995, 1996). In EMT-like cell scattering models, RhoA is a candidate for regulating cell-cell adhesion by transducing integrin signals. Expression of various forms of β1 integrin subunit in β1-null cell lines triggers activation of RhoA and Rac1 (Gimond *et al*., 1999). Cell-cell adhesion is simultaneously disrupted, as cadherin levels decrease, and cells change to a spindle-shaped fibroblast-like morphology. Rac1 may be involved in the regulation of migratory ability (Small *et al*., 2002), and may even be activated by Rho (Katoh *et al*., 2005). The expression of a chimeric integrin construct, with the ability to mimic endogenous ligand-occupied integrin (Akiyama *et al*., 1994), but not participate in matrix interactions, results in a similar morphological transition, but fails to promote cell migration on fibronectin (Gimond *et al*., 1999). This indicates that integrins act as signaling molecules during the disruption of cell adhesion, and not simply to enhance migratory ability.

The expression pattern of RhoA in chick embryos correlates with EMT. In stage 10 embryos, *RhoA* mRNA is expressed throughout the neural plate and neural folds (Liu & Jessell, 1998). Expression decreases in the ventral portion of the neural tube following fusion of the neural folds, but is maintained in the dorsal neural tube. *RhoA* mRNA is not present in neural crest cells after EMT. *RhoB* mRNA and RhoB protein is expressed in the dorsal neural tube, but in contrast to *RhoA*, is maintained in neural crest cells,

especially in the cranial region, throughout early migration (Liu & Jessell, 1998). The expression pattern of RhoB is correlated with the early stages of neural crest differentiation (Liu & Jessell, 1998; Liem *et al*., 1995). *RhoB* expression is activated by LSox5 misexpression in the avian neural tube following the onset of Slug expression (Perez-Alcala *et al*., 2004). LSox5 is involved in the segregation of neural crest cell lineages—specifically non-neural phenotypes—including glia. Neural tube cells outside the domain of neural crest competence, which are induced to express *RhoB*, remain in the neural tube and maintain epithelial features (Perez-Alcala *et al*., 2004). This makes it unlikely that RhoB mediates the changes of cell shape and adhesion associated with delamination. In the mouse embryo, RhoB is not expressed in pre-migratory neural crest (Henderson *et al*., 2000). RhoB is expressed throughout neural crest migration in mice and for at least one day after migration has ended. This time correlation is more consistent with a role for RhoB in neural crest differentiation rather than delamination. *RhoC* is expressed in the avian neural ectoderm, but at a very low level, and is primarily restricted to the notochord (Liu & Jessell, 1998).

I hypothesize that β1 integrin function is required for cranial neural crest EMT and that RhoA GTPase is involved with transducing the integrin signal. In this study, a new method was used to express a chimeric form of the β1 subunit in a small number of pre-migratory neural crest cells in chick embryos. This approach permits a requirement for integrin signaling during EMT to be identified. Expression of dominant negative and constitutively active forms of GTPases individually permits an evaluation of loss of function and gain of function on EMT and migration of cranial neural crest cells. By expressing the mutant GTPases with chimeric β1 integrin and rescuing EMT, I have identified a potential downstream component of integrin signaling.

MATERIALS AND METHODS

Vector Construction

Unmodified pCMS-eGFP (BD Biosciences Clontech), which contains enhanced green fluorescent protein under control of the SV40 enhancer/promoter, is used as a control (Figure 1A). Additional constructs were created by modification of pCMS-eGFP. The HA control vector co-expresses GFP and the extracellular and transmembrane domains of viral hemagglutinin (Marsden & DeSimone, 2001) under the control of the cytomegalovirus immediate early (CMV IE) promoter (Figure 1B). The HAβ1ΔE construct is comprised of full-length hemagglutinin extracellular and transmembrane domains (ending with residue Q556, accession # J02090) joined to the entire *Xenopus* β1 integrin cytoplasmic tail (comprised of residues K752 through K798, accession # M20180), cloned into pCMS-eGFP (Figure 1C). The rationale for incorporating hemagglutinin and integrin domains is two-fold. Hemagglutinin forms trimers that project from the plasmalemma in a parallel rod-shaped structure (Skehel & Wiley, 2000). On the influenza virus, these trimers normally acquire membrane fusion activity at endosomal pH (Gething et al., 1986). For the chimeric integrin, trimerization is thought to cluster the β1 cytoplasmic domains, and thereby cause inappropriate integrin signaling. Furthermore, antibodies against hemagglutinin epitopes allow for easy identification of chimeric protein. A GFP-tagged β1 integrin lacking the extracellular domain (Gβ1ΔE) has been previously described (Smilenov *et al*., 1999). This construct (E. Marcantonio, Columbia UHS) is also expressed in pCMS-eGFP under the control of the CMV IE promoter (Figure 1D). Control plasmids for co-transfection experiments, pCMS-eCFP (expressing enhanced cyan fluorescent protein) and pCMS-eYFP (expressing enhanced

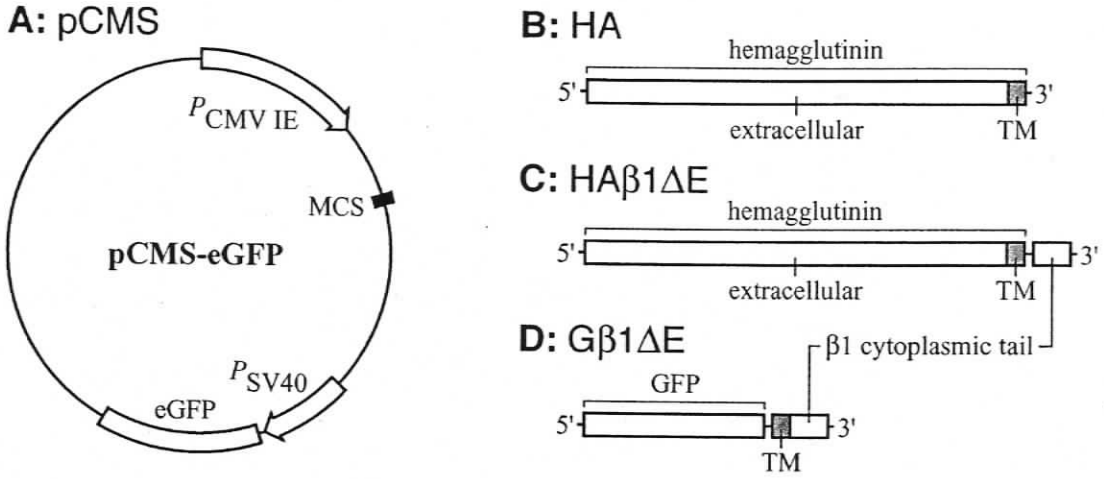

E: GTPases

```
RhoA   ---MAAIRKKLVIVGDGACGKTCLLIVFSKDQFPEVYVPTVFENYVADIEVDGKQVELALWDTAGQED--   65
Rac1   -----MQAIKCVVVGDGAVGKTCLLISYTTNAFPGEYIPTVFDNYSANVMVDGKPVNLGLWDTAGQED--   63
Cdc42  -----MQTIKCVVVGDGAVGKTCLLISYTTNKFPSEYVPTVFDNYAVTVMIGGEPYTLGLFDTAGQED--   63

RhoA   --YDRLRPLSYPDTDVILMCFSIDSPDSLENIPEKWTPEVKHFCPNVPIILVGNKKDLRNDEHTRREL--  131
Rac1   --YDRLRPLSYPQTDVFLICFSLVSPASFENVRAKWYPEVRHHCPNTPIILVGTKLDLRDDKDTIEKL--  129
Cdc42  --YDRLRPLSYPQTDVFLVCFSVVSPSSFENVKEKWVPEITHHCPKTPFLLVGTQIDLRDDPSTIEKL--  129

RhoA   --AKMKQEPVKPEEGRDMANRIGAFGYMECSAKTKDGVREVFEMATRAALQ-ARRGKKK--SGCLVL---  193
Rac1   --KEKKLIPITYPQGLAMAKEIGAVKYLECSALTQRGLKTVFDEAIRAVLCPPPVKKRKRK--CLLL---  192
Cdc42  --AKNKQKPITPETAEKLARDLKAVKYVECSALTQKGLKNVFDEAILAALEPPEP--KKSR-RCVLL---  191
```

Figure 1. Co-expression vector and constructs used in this study. (A) The pCMS control is pCMS-eGFP plasmid with an empty multiple cloning site (MCS). A single transcript for enhanced green fluorescent protein (eGFP) is controlled by the SV40 enhancer/promoter. (B) The HA control construct contains the extracellular and transmembrane (TM) domains of hemagglutinin (HA). (C) The HAβ1ΔE chimera has the β1 integrin subunit extracellular and TM domains changed to those of HA. (D) The Gβ1ΔE chimera contains the TM and cytoplasmic domains of β1 integrin subunit joined to green fluorescent protein (GFP). (E) Alignment of RhoA, Rac1, and Cdc42 GTPases (adapted from Wennerberg & Der, 2004) showing the location of substitution mutations (boxes) used to generate dominant negative and constitutively active forms. Constructs are cloned into the MCS of the pCMS-eGFP expression vector, behind the cytomegalovirus immediate early (CMV IE) promoter. Thus, the plasmids produce two transcripts: one for the construct in the MCS, and one for eGFP.

yellow fluorescent protein), are derivatives of pCMS-eGFP (BD Biosciences Clontech), wherein the fluorescent protein sequence has been replaced with those encoded in peCFP and peYFP (BD Biosciences Clontech). The GTPase constructs are human (Figure 1E; accession # L25080, # M29870, and # M35543 for RhoA, Rac1, and Cdc42 respectively) and have 2× myc tags (MEQKLISEEDLEQKLISEEDL) at to the N-termini. *RhoA* T19N mutation (RHO0A0MND0, UMR cDNA Resource Center), *Rac1* T17N mutation, and *Cdc42* T17N mutation (gifts from A. Hall, University College London) contain an asparagine substitution in the putative Mg^{+2} binding site of the GTPase domain. This causes preferential affinity for GDP over GTP (Stacey *et al.*, 1991), and confers a dominant negative phenotype by sequestering guanine nucleotide-exchange factors from endogenous RhoA (Quilliam *et al.*, 1994). *RhoA* Q63L mutation, *Rac1* Q61L mutation, and *Cdc42* Q61L mutation (gifts from A. Hall) contain a leucine substitution that blocks intrinsic and GAP-stimulated GTPase activity. This creates a constitutively active phenotype by locking the GTPase in the active GTP-bound form (Bos, 1989). The six mutant GTPases were each cloned into pCMS-eGFP expression vector.

Cell Manipulations and Analyses

Embryonic chick fibroblast cultures were established as previously described (Burke *et al.*, 1994). Explants from cardiac outflow tract were dissected into cold phosphate buffered saline (PBS: 0.8% NaCl, 0.02% KCl, 0.144% Na_2HPO_4, 0.024% KH_2PO_4). Tissue was mechanically minced, rinsed twice in PBS, and dissociated with 0.25% trypsin and 0.5% collagenase (Sigma) at 37 °C for 10 min. Cells were washed twice in PBS containing 10% fetal bovine serum (Invitrogen), then inoculated onto human fibronectin-coated 8-well culture slides (Becton Dickinson) in 200 μL of DMEM/F12

containing 5% fetal bovine serum. For comparison of integrin constructs, cultures were plated at 4×10^4 cells/well Cells were rinsed two hours later and FuGENE 6 (Roche) was used to transfect the cells according to manufacturer protocol. At 24 h post-transfection, the cells were fixed in 4% paraformaldehyde in PBS (pH 7.4) for 8 min, then 100% methanol for 2 min, in preparation for immunofluorescent labeling. This procedure destroys GFP fluorescence, so Living Colors A.v. anti-GFP antibody (rabbit polyclonal, BD Biosciences Clontech) was used to detect transfected cells. If a double-label was performed with another rabbit primary antibody, then monoclonal anti-GFP (mouse IgG, Stressgen) was used instead of Living Colors. Cells were labeled with anti-HA antibody (rabbit polyclonal) or anti-chicken vinculin VN 3-24 (mouse IgG, Samuelsson *et al.*, 1993) in PBS containing 0.1% Tween and 5% lamb serum (GIBCO Invitrogen). Goat anti-rabbit or anti-mouse conjugated to Alexa Fluor 488 or 568 (Molecular Probes) were used for secondary antibodies, as appropriate. When indicated, phalloidin (Alexa Fluor 350, Molecular Probes) was added to visualize F-actin. Slides were mounted with *n*-propyl gallate in glycerol (Sigma).

In experiments with mutant GTPases, normal density wells contained 2.2×10^4 cells, while low density conditions contained 1.1×10^4 cells/well. Live cells were visualized at 12 and 24 h using an inverted microscope equipped for epifluorescence (Nikon Diaphot). Images were collected using an IR-10000 CCD camera (DAGE-MTI), set to manual gain, on an LG-3 frame grabber board run by Scion Image 4.0.3 (Scion). Twenty random fields of view were captured per condition per observation period. Living Colors antibody was used exclusively, and anti-HA antibody was obtained from Sigma (mouse IgG). When indicated, cultures were labeled with 9E10 anti-myc antibody (mouse IgG,

ATCC). Cultures processed for histochemistry of actin were fixed in 4% paraformaldehyde in PBS (pH 7.4) for 8 min, then 100% acetone for 2 min. This procedure retains GFP fluorescence. Phalloidin (Alexa Fluor 568, Molecular Probes) was used to visualize F-actin, and Hoechst 33342 (Sigma) was added to stain DNA.

Cell cultures comparing integrin constructs were visualized using a compound microscope equipped for epifluorescence (Zeiss). Images were collected using a DC-330 CCD camera (DAGE-MTI) on a CG-7 frame grabber board run by Scion Image 4.0.3 (Scion). Experiments with mutant GTPases were visualized using a digital microscope equipped for epifluorescence (Leica Model DM6000B). Images were collected using an ORCA-ER CCD camera (Hamamatsu Model C4742-80) controlled by OpenLab 4.0.2 (Improvision). Image color was adjusted and figures were assembled with Photoshop 6.0.1 (Adobe). Morphometric analysis was done with Image-Pro Plus 4.5.0.19 (Media Cybernetics). Aspect was measured by the ratio of the major axis to the minor axis of each cell. Cell roundness was determined by the formula:

$$\frac{4\pi \cdot Area}{Perimeter^2}$$

The number of cellular processes was manually tabulated. Statistical values were calculated using a one-way analysis of variance followed by a Tukey-Kramer post-test (InStat 3.0.5, GraphPad Software). Regression analyses were performed with DeltaGraph 4.0.5 (SPSS), and regression curves were calculated with eighth degree polynomials.

Localized Electroporation of Cranial Neural Crest

The electrode was constructed as previously described (Atkins *et al.*, 2000; US Patent

6977172). In brief, a double-barreled glass capillary tube was pulled and forged with 200 μm openings at the tip. A wire was inserted down each barrel to within 1 mm of the tip. The double-barrel tip was sealed to a single-barrel shaft, to allow for control of suction, and mounted in a micromanipulator. The tungsten wire leads from the electrode were connected through a DPDT switch to the RF module of a Gene Pulser II power supply (BioRad). Refer to appendix I for a detailed guide to electrode construction.

Fertilized White Leghorn eggs (University of Alberta Experimental Farm) were incubated at 38 °C to developmental stage 9 or 11 for neural ectoderm transfections (Hamburger and Hamilton, 1951). Eggs were windowed and the vitelline layer was reflected with a tungsten needle. Plasmid was prepared to a final concentration of 350 ng/μL in chick Ringer's solution (0.72% NaCl, 0.017% $CaCl_2$, 0.037% KCl) with 0.4% fast green FCF (triarylmethane). Plasmid solution was injected into the lumen of the neural tube through the anterior neuropore using a pulled glass capillary tube. The embryo was moistened with a few drops of saline, and the electrode containing only saline was positioned dorsolaterally near the 4th and 6th rhombomere. Settings for electroporation were: 95 V at 100% modulation (DC amplitude of 47.5 V), a frequency of 30 kHz, a pulse duration of 40 ms, a total of 10 pulses with a pulse interval of 200 ms. The program was repeated once after switching barrel polarity.

For control experiments with rhodamine-labeled DNA, embryos were incubated to developmental stage 12, when uniform cranial ectoderm is easily manipulated. Plasmid (pGeneGrip rhodamine/blank vector, Gene Therapy Systems) was diluted to 250 ng/μL in chick Ringer solution. A surface electroporation was performed by front-filling the electrode with plasmid solution and targeting the dorsal midbrain. Electroporation

parameters were as described above, except voltage was raised to 100 V as tolerated by the older developmental stage.

Following transfection, eggs were sealed with adhesive cellophane tape and returned to the incubator for 24 h, unless otherwise noted. Embryos were dissected into PBS and the amnion was removed. Whole embryos were mounted on a depression slide and visualized using a compound microscope equipped for epifluorescence (Zeiss). GFP-expressing cells were counted by focusing through the specimen. Images were collected using the same methods that were used for cell cultures.

Co-transfection of Two Plasmids

Plasmids that express cyan and yellow fluorescent proteins were mixed together in equal parts w/v (1:1), or at 1 part cyan to 10 parts yellow (1:10), or at 1 part cyan to 100 parts yellow (1:100). Combined-plasmid solutions were diluted in chick Ringers to a final concentration of 325 ng/μL. Control experiments with cyan and yellow fluorescent plasmids followed the same methods that were used for rhodamine-labeled DNA. Surface electroporations were performed at the dorsal midbrain of stage 12 embryos and images were collected 24 h post-transfection.

Co-transfections in cell culture were performed at a 1:1 w/v ratio of HAβ1ΔE and the plasmid indicated. The concentration of each plasmid was kept constant, so the total amount of plasmid for co-transfection was twice the amount used for single-plasmid treatments. Co-transfection of neural ectoderm in embryos by localized electroporation was also performed with equal w/v ratios. The final combined concentration of HAβ1ΔE, and the plasmid indicated, was 450 ng/μL in chick Ringers. The electrode

used for these data contained the same tip and wire positions as the electrode used for investigation of integrin function. Twenty-seven of 115 embryos were excluded from analysis (6 died, 9 had no transfection, 4 had scarring from the electroporation, and 8 were mistargeted).

Fixation, Sectioning and Immunolabeling of Mosaic Embryos

Embryos for sectioning were fixed in 100% methanol overnight at 4 °C, transferred to ethanol, and infiltrated with polyester wax (Electron Microscopy Sciences). Sections were cut transversely (8 μm) on a microtome (Spencer Model 820) and attached to gelatin-coated slides. Wax was removed with xylene, and sections were rehydrated with an ethanol dilution series followed by PBS. Living Colors A.v. anti-GFP antibody (rabbit polyclonal, BD Biosciences Clontech) or anti-GFP (mouse IgG, Stressgen) was used to detect transfected cells. Some embryo sections were labeled with Toots anti-HA antibody (rabbit polyclonal), anti-Slug (mouse IgG, DSHB), anti-HNK-1 (mouse IgG, ATCC), anti-Sox9 (rabbit polyclonal, Chemicon), anti-chicken N-cadherin (rat IgG, Zymed), or anti-HA (mouse IgG, Sigma). When indicated, Hoechst 33342 (Sigma) was added to stain DNA. Secondary labeling and imaging of embryo sections were completed with the same methods that were used for cell cultures.

RESULTS AND DISCUSSION

Expression of Integrin Constructs in Culture

Chimeric integrin (Gβ1ΔE or HAβ1ΔE) or control (HA or pCMS) plasmids were transfected into chick primary culture cells to determine their effects. Cells transfected with pCMS plasmid express GFP, and are not immunoreactive to anti-HA antibody. The transfected cells are irregular in outline; most are spindle-shaped and have processes (Figure 2A). Cells transfected with HA plasmid express GFP and are immunoreactive with anti-HA (Figure 2B). Cells transfected with Gβ1ΔE or HAβ1ΔE plasmid and expressing GFP are generally round and lack processes (Figure 2C, D). Cells transfected with HAβ1ΔE plasmid are anti-HA immunoreactive. This preparation confirms that transfected cells, identified with the GFP reporter, contain the HA epitope of the chimeric protein that is encoded as a second transgene in the pCMS-eGFP expression vector. Expression of the HA epitope was also confirmed *in vivo* (Figure 2E).

The degree that the proteins affect cellular morphology *in vitro* was quantified. Mean aspect, roundness, and number of processes for cells expressing pCMS plasmid are not significantly different from cells expressing HA plasmid (Figure 3). Cells expressing Gβ1ΔE have a mean aspect of 1.74 (± 0.04 s.e.m.) and cells expressing HAβ1ΔE have a mean aspect of 1.65 (± 0.05 s.e.m.). The aspect does not differ between these treatments, but does differ significantly from both control preparations ($P < 0.001$). Mean roundness is 0.67 (± 0.01 s.e.m.) for Gβ1ΔE-expressing cells and 0.69 (± 0.01 s.e.m.) for HAβ1ΔE-expressing cells. The mean number of processes is 0.22 (± 0.03 s.e.m.) for Gβ1ΔE-expressing cells and 0.15 (± 0.02 s.e.m.) for HAβ1ΔE-expressing cells. The roundness

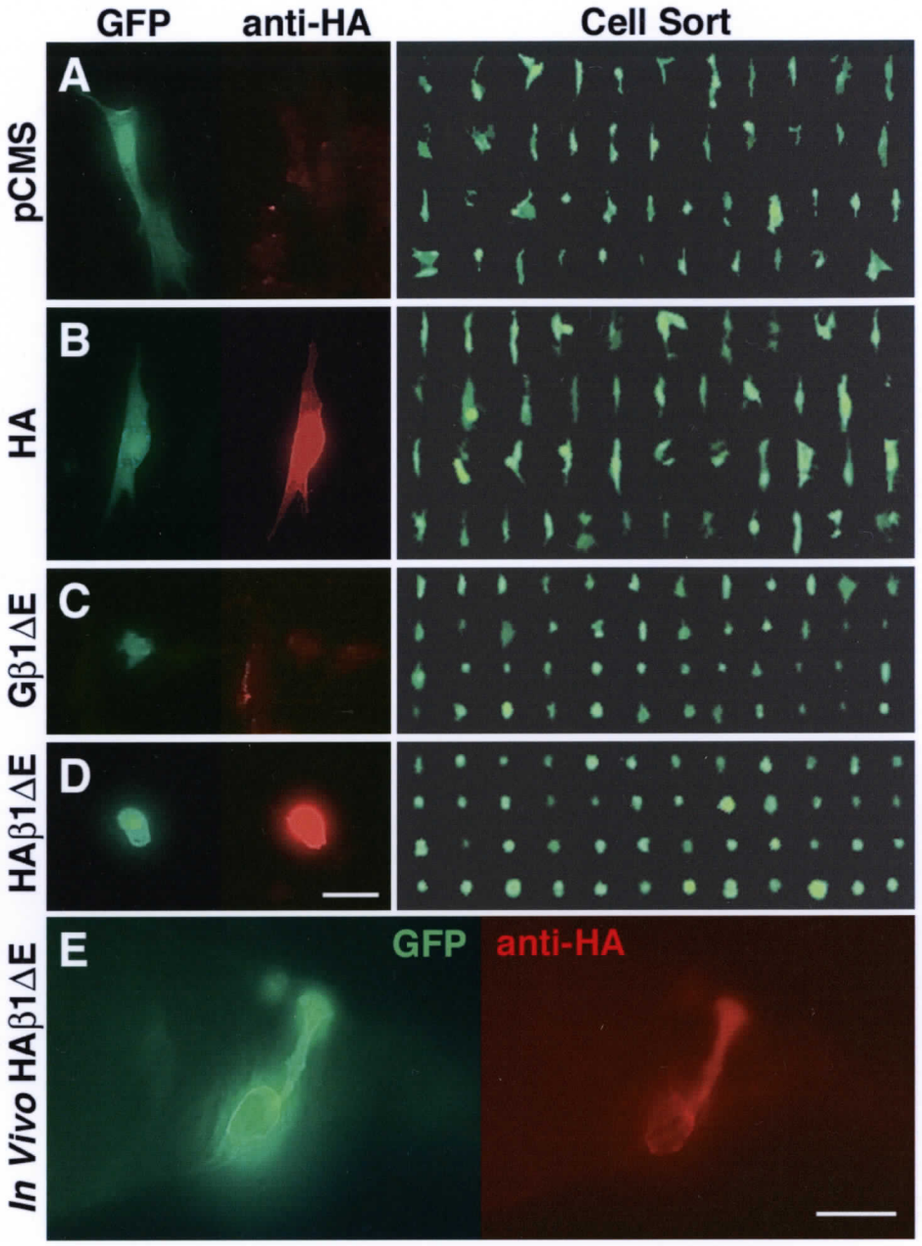

Figure 2. Expression and effect of two chimeric β1 integrin constructs and controls on chick aorta cells in primary culture. (A) Cells transfected with pCMS plasmid have normal morphology and no HA immunoreactivity. (B) Cells transfected with HA plasmid have similar morphology to (A), but are labeled with anti-HA antibody. (C) Cells transfected with Gβ1ΔE plasmid are rounded. (D) Cells transfected with HAβ1ΔE are rounded and HA immunoreactive. The cell sort panel is a representative portion of each culture, sorted in increasing order of roundness, by morphometric computer analysis. (E) A transverse section through the neural tube of a transfected embryo confirms HAβ1ΔE expression *in vivo* with HA immunoreactivity. Bars = 10 μm.

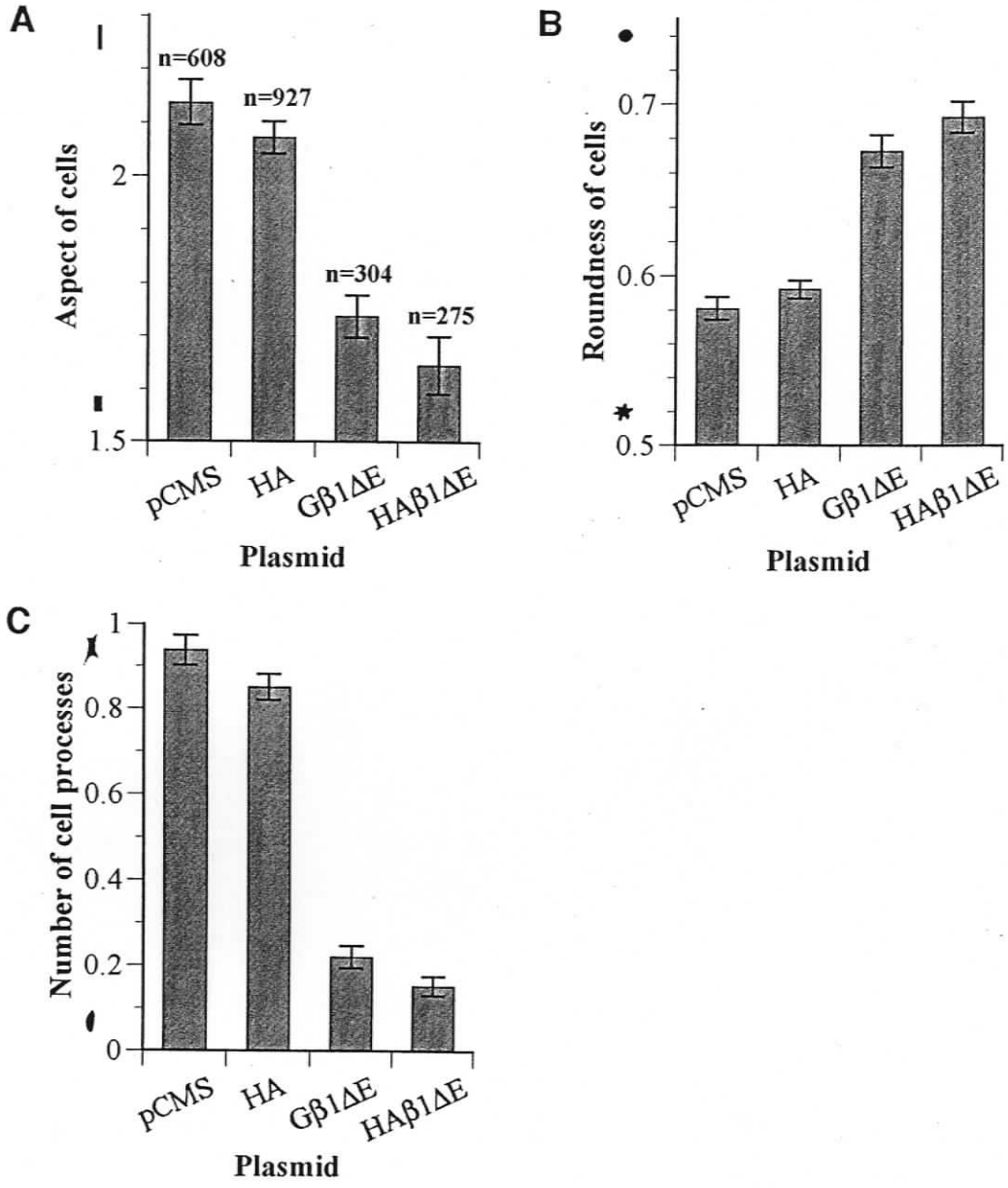

Figure 3. Morphometric analyses of the changes in the shape of primary culture cells resulting from chimeric β1 integrins. (A) Aspect is the ratio of the major axis to the minor axis of each cell. (B) Roundness is calculated from the area and perimeter of a cell, and is defined so that a perfect circle has a roundness of 1. (C) The number of processes is the mean for the population. In all analyses, there is no significant difference between pCMS and HA control plasmids, or Gβ1ΔE and HAβ1ΔE chimeric integrins. There is a significant difference between the control and chimeric plasmids. Bars, s.e.m.

and number of processes do not differ between these treatments, but do differ significantly from both control preparations ($P < 0.0001$). These changes in cell morphology are consistent with an inhibition of cell adhesion to the fibronectin-coated plates. This suggests that matrix adhesion is directly inhibited by Gβ1ΔE and HAβ1ΔE, rather than being indirectly affected by transgene toxicity.

Immunohistochemistry was employed to investigate the mechanism of cell-substrate inhibition. Cells expressing HA plasmid have anti-vinculin immunoreactive patches at their perimeter (Figure 4B), cortical actin, and stress fibers (Figure 4C). Cells expressing HAβ1ΔE plasmid have diffuse vinculin immunoreactivity that is not localized near the cell edges (Figure 4F). Cells expressing HAβ1ΔE lack stress fibers and have only diffuse actin staining (Figure 4G). These alterations of focal adhesions, with the disruption of the cytoskeleton, suggest that expression of HAβ1ΔE plasmid interferes with cell-substrate attachment through mechanisms involving integrins.

Localized Electroporation of Cyan and Yellow Reporters

Two plasmids were mixed together to determine the feasibility of co-transfecting cells in the avian embryo by localized electroporation. Co-transfection would allow for the simultaneous expression of multiple transgenes, without requiring them to be encoded on the same vector. Plasmid encoding cyan fluorescent protein (FP) was mixed with plasmid encoding yellow FP in a 1:1 ratio, surface electroporated into stage 12 embryos, and imaged 24 h later (Figure 5A). Embryos have a scattered patch of cells expressing cyan FP, and a nearly identical pattern in the channel of yellow fluorescence. Expression of cyan FP appears slightly lower than yellow FP on average, but this is likely due to variation in quantum yield between the chromophores, or sub-optimal emission filters.

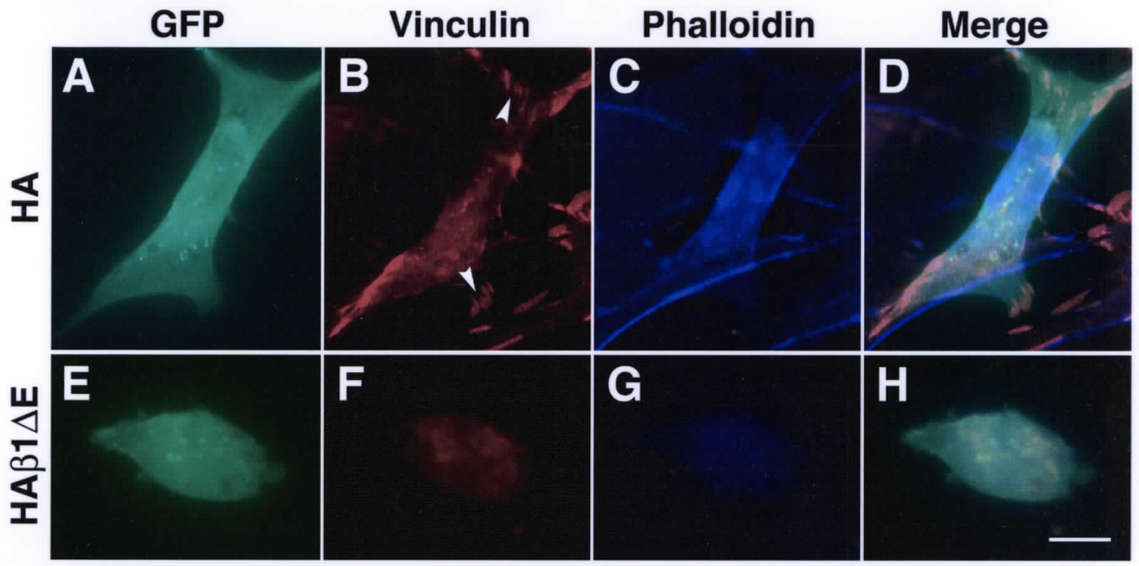

Figure 4. Changes in the *in vitro* organization of focal adhesions (arrowheads) and filamentous actin when integrin function is blocked. The top row shows a cell transfected with HA plasmid, (A) expressing GFP after 24 h, (B) immunolabeled with anti-vinculin, and (C) stained with phalloidin. (E) The cell in the lower row is transfected with the HAβ1ΔE plasmid. (F) Its rounded shape is associated with diffuse vinculin labeling, and (G) the loss of stress fibers. The merged column (D, H) contains overlays of the three images in each row. Bar = 5 μm.

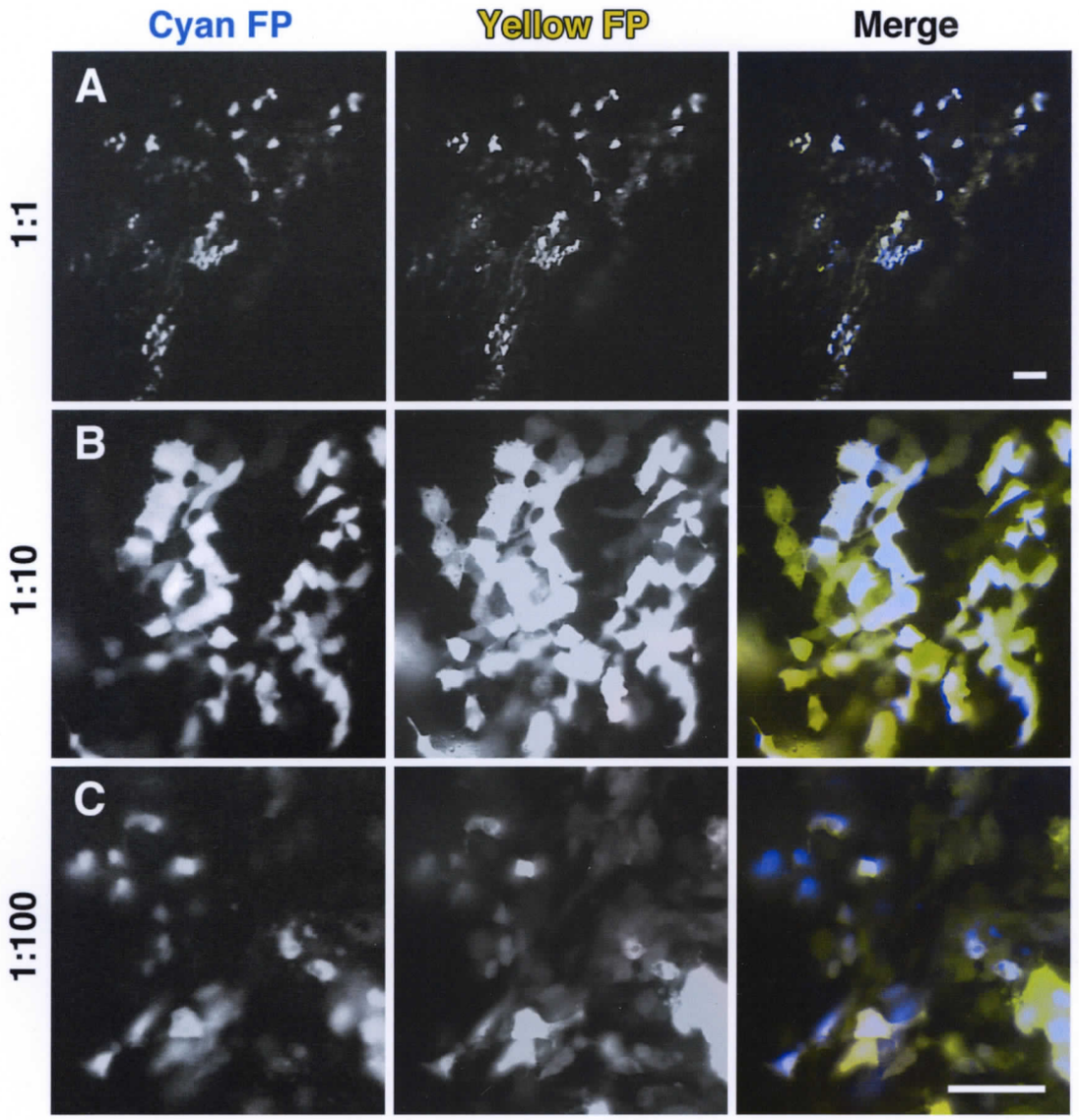

Figure 5. Co-transfection by localized electroporation of epidermal ectoderm in embryos. Plasmids encoding cyan fluorescent protein (FP) and yellow FP were mixed together in various ratios. Cyan and yellow channels were imaged 24 h post-transfection. The third column shows an overlay of both channels. (A) A 1:1 ratio of cyan and yellow plasmids results in nearly identical expression of each plasmid in all transfected cells. Yellow FP is slightly brighter. (B) A 1:10 cyan to yellow ratio also produces a similar expression pattern. Fluorescence resulting from the cyan plasmid is very weak in cells that weakly fluoresce yellow. (C) At a 1:100 ratio, cyan fluorescence is frequently dimmer than yellow fluorescence. Cells expressing yellow FP also contain cyan fluorescence, although it is difficult to detect in weakly transfected cells. Bars = 20 μm.

Cyan and yellow FP plasmids mixed at a 1:10 ratio, produce a transfection pattern similar to the 1:1 ratio (Figure 5B). Cells that highly express yellow FP, also fluoresce brightly in the cyan channel. Cells apparently transfected at a lower efficiency, fluoresce dimly in both channels. At a 1:100 ratio, cyan fluorescence in some cells is considerably weaker than yellow fluorescence (Figure 5C). No yellow FP-expressing cells, however, are observed that do not contain visible cyan FP at least under long exposures. Electroporations of cyan or yellow FP plasmids alone have no fluorescent crossover detectable in the other channel (data not shown). This experiment demonstrates that even at very skewed ratios, both plasmids are taken up by all transfected cells. The confidence in the co-transfection technique, therefore, would be extremely high when plasmids are mixed in equal ratios.

Expression of GTPase Constructs in Culture

Mutant GTPases and empty pCMS vector were transfected into chick primary cultures to confirm that the constructs are functional in avian cells. Cultures transfected with plasmids encoding dominant negative (DN) or constitutively active (CA) RhoA, Rac1, or Cdc42 plasmid (Figure 6A - F). All cells identified as transfected by the presence of GFP fluorescence also express the exogenous transgene. GFP fluorescence co-localizes with cytoplasm, while myc-labeling shows more detail near the edges of cells (Figure 6A, C) and creates a distinct perimeter in rounded cells (Figure 6B, F). Cells transfected with empty pCMS show no myc immunoreactivity (data not shown).

Mutant GTPases were co-transfected into chick primary cultures with HAβ1ΔE plasmid to confirm the transgenes express together. Immunolabeling myc and HA epitopes were separately performed in duplicate culture preparations. This compromise

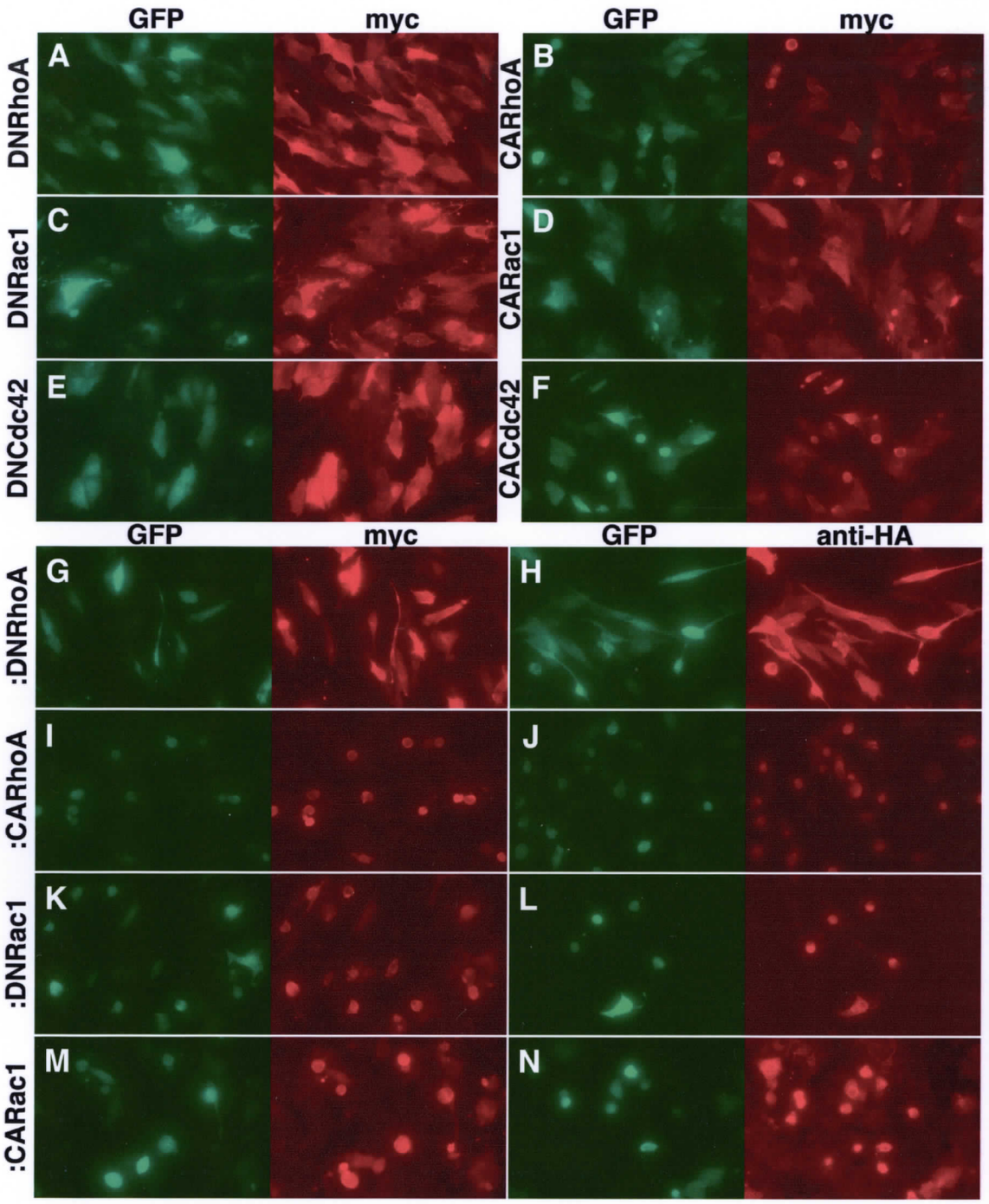

Figure 6. Expression and effects of mutant GTPases in culture. (A-F) Cells were transfected with plasmid encoding dominant negative (DN) or constitutively active (CA) RhoA, Rac1, or Cdc42 and fixed 24 h post-transfection. Each image pair shows GFP-positive cells and a second fluorescent channel of myc immunoreactivity. (G-N) Cells co-transfected with plasmid encoding a chimeric β1 integrin subunit and a plasmid encoding a mutant GTPase are labeled by anti-myc and anti-hemagglutinin (HA) antibodies in separate preparations. Bar = 50 μm.

was necessary because GFP must be visualized with one fluorophore, and a triple label was not feasible. Cultures co-transfected with HAβ1ΔE plasmid and DNRhoA, CARhoA, DNRac1, or CARac1 plasmid, contain cells expressing GFP that are also immunoreactive to anti-myc antibody (Figure 6G, I , K, M). Duplicate preparations contain GFP-expressing cells that are immunoreactive to anti-HA antibody (Figure 6H, J, L, N). Since all GFP-positive cells contain myc-label, and all GFP-positive cells contain HA-label, it is likely that GFP-positive cells contain both labels. Since two plasmids can be reliably electroporated *in vivo*, it is expected that co-expression of both transgenes will occur in the embryo.

The effects of mutant GTPase plasmids, and co-transfection of plasmids, on cellular morphology *in vitro* were quantified in a large number of cells (Figure 7). The aspect of cells appears static between observation periods, and is not related to plating density (Figure 8). The HAβ1ΔE co-transfections are nearly identical within plasmid groups ($P < 0.0001$). Preparations transfected with pCMS, transfected with DNRhoA, and co-transfections of HAβ1ΔE:DNRhoA have more elongated aspects than other preparations ($P < 0.001$). The elongation in these HAβ1ΔE:DNRhoA preparations is quite prominent in some cells (Figure 6G, H). It appears the effect of HAβ1ΔE alone may be rescued by co-transfection of DNRhoA.

The mean roundness of cells was quantified in culture (Figure 9). Preparations co-transfected with HAβ1ΔE and CARhoA have a higher roundness than preparations of HAβ1ΔE alone ($P < 0.001$), which have higher roundness than control preparations expressing pCMS plasmid ($P < 0.05$). To determine if mean roundness increases in all cells, the distribution of roundness was plotted for control, chimeric integrin, and the

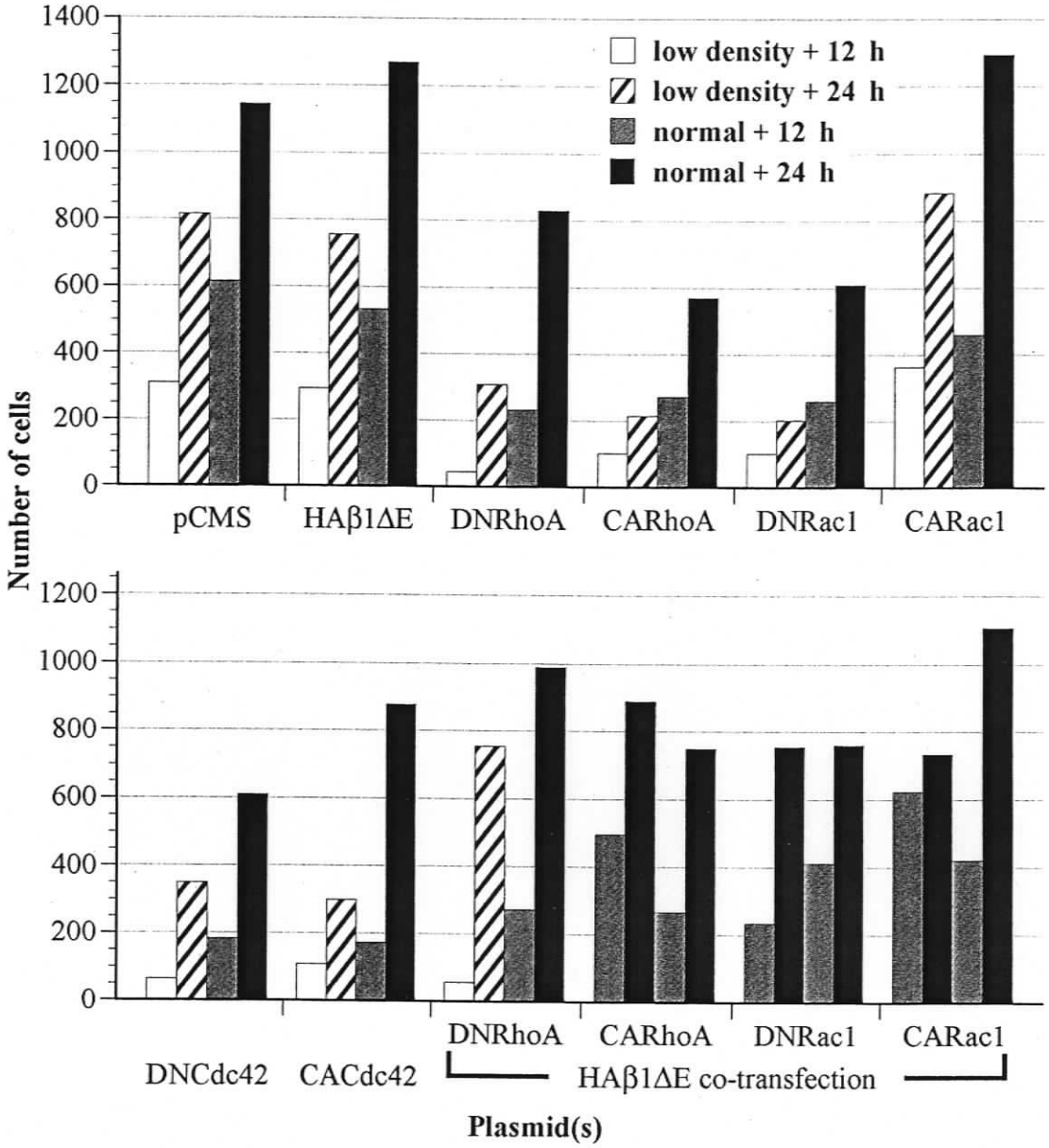

Figure 7. N-sizes for the in vitro quantifications. The GFP-positive cells above the threshold level of background fluorescence were analysed in each culture condition at 12 and 24 h post-transfection. For most conditions, there is a 2 to 5-fold increase in the number of GFP-cells detected between the imaging periods. Sample counts do not indicate that any plasmid or condition impairs cell survival.

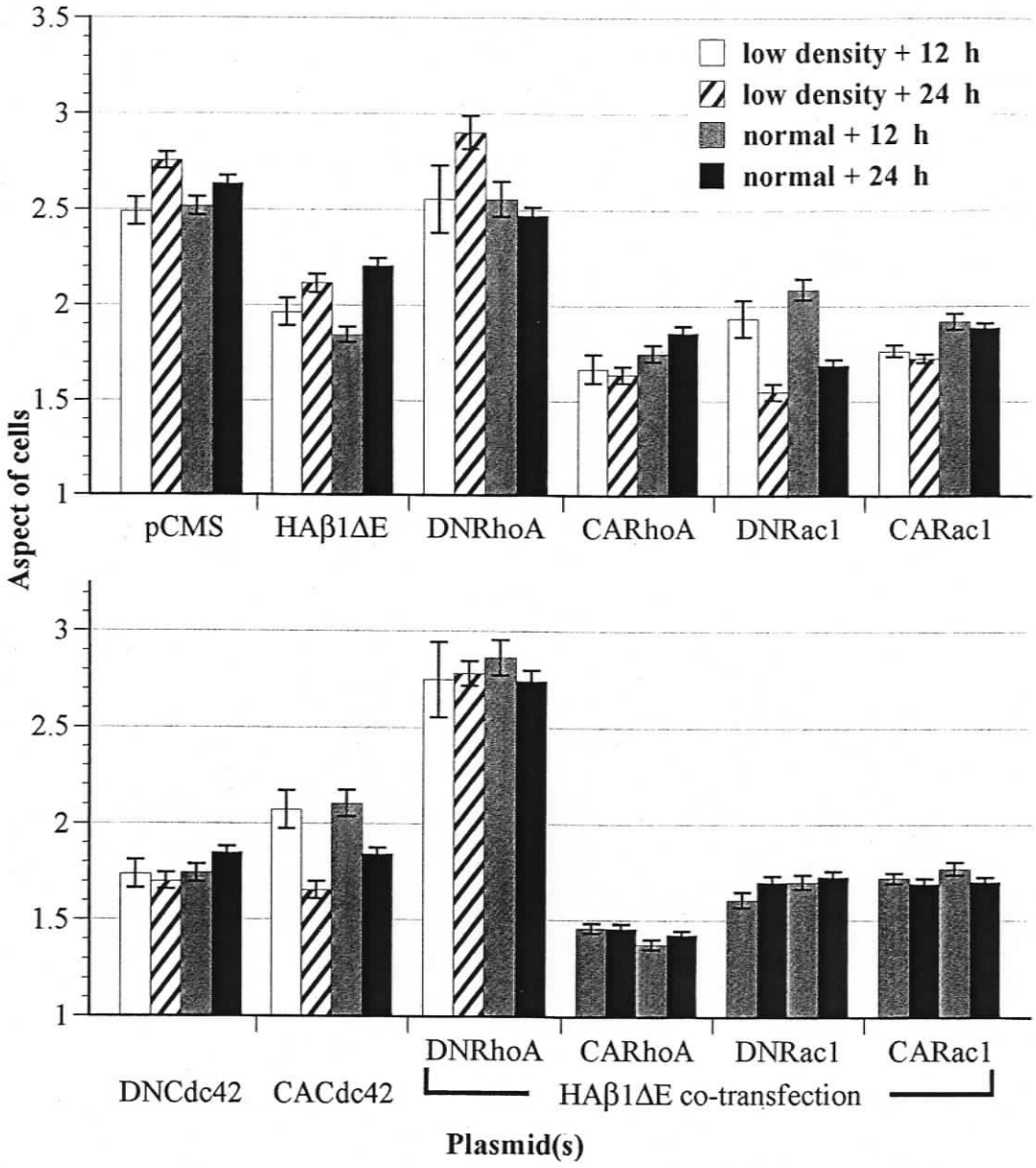

Figure 8. Morphometric analysis of cell aspect in culture resulting from mutant GTPases. Cells were subcultured at low or normal density and transfected with pCMS-eGFP plasmid (pCMS), pCMS encoding chimeric β1 integrin (HAβ1ΔE), or pCMS encoding a dominant negative (DN) or constitutively active (CA) form of RhoA, Rac1, or Cdc42. Co-transfections were also performed with a 1:1 mix of pCMS-eGFP encoding HAβ1ΔE and a DN or CA form of RhoA or Rac1. Live cells were imaged at 12 and 24 h. Aspect is the ratio of the major axis to the minor axis of each cell. Co-transfection of DNRhoA with HAβ1ΔE elongates cells as least as much as pCMS control. Bars, s.e.m.

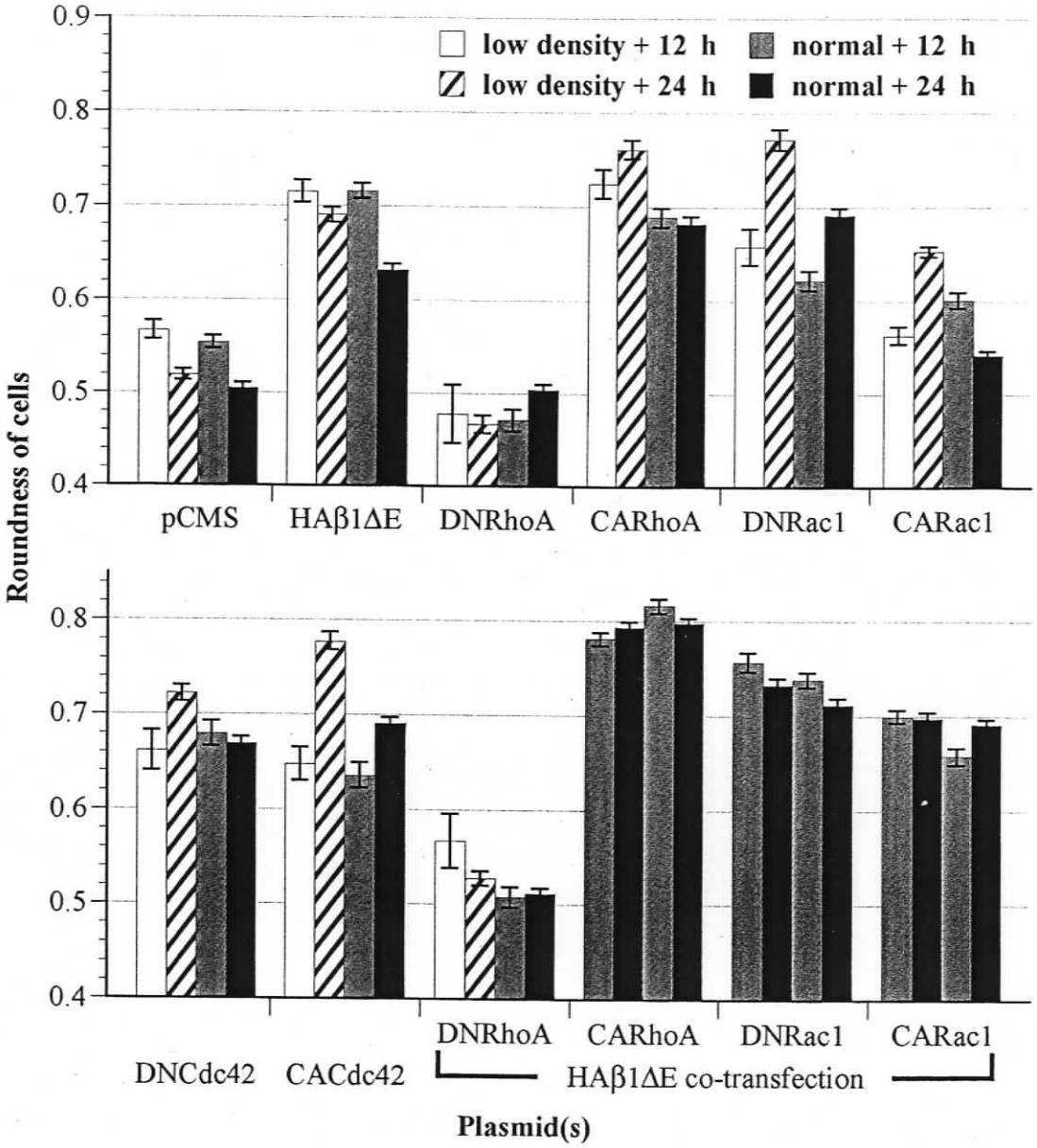

Figure 9. Morphometric analysis of cell rounding in culture resulting from mutant GTPases. Cells were subcultured at low or normal density and transfected with pCMS-eGFP plasmid (pCMS), pCMS encoding chimeric β1 integrin (HAβ1ΔE), or pCMS encoding a dominant negative (DN) or constitutively active (CA) form of RhoA, Rac1, or Cdc42. Co-transfections were also performed with a 1:1 mix of pCMS-eGFP encoding HAβ1ΔE and a DN or CA form of RhoA or Rac1. Live cells were imaged at 12 and 24 h. Roundness is calculated from the area and perimeter of a cell, and is defined so that a perfect circle has a roundness of 1. Co-transfection of DNRhoA with HAβ1ΔE decreases rounding to a level comparable to pCMS control. Bars, s.e.m.

most round culture (Figure 10). There is an overall shift from less rounded cells to cells measuring more than 0.7 roundness. This discrete variation of cell shape suggests that cells reach some form of threshold before detaching from the culture substrate.

It is possible that this hypothetical threshold is dependent on plasmid copy number. If a significant relationship exists between transfection efficiency and transgene effect, then it must be taken into consideration when evaluating cells of different GFP intensities in the embryo. Cells transfected with control plasmid exhibit a fairly even spectrum of roundness over the range of fluorescence density (Figure 11). There is a small positive correlation that explains 2.02% of the variation ($t = 4.85$). Cells in the culture co-transfected with HAβ1ΔE and CARhoA plasmid show a shift to high roundness over most of the density spectrum (Figure 12), with a correlation explaining 20.1% of the variation ($t = 14.9$).

Cytoskeleton of GTPase-Transfected Cultures

Cells expressing HA plasmid are indistinguishable from pCMS-expressing cells (Figure 13A, B), confirming that the full length HA is innocuous. Many cells expressing HAβ1ΔE plasmid are rounded. These cells have speckled patches of cortical actin and generally lack stress fibers (Figure 13C). At 24 h post-transfection some nuclei are irregularly shaped and appear sub-divided. Apoptosis is likely a consequence of anchorage dependence on the fibronectin-coated slides (Ruoslahti & Reed, 1994), as HAβ1ΔE-expressing cells are not rounded in the embryo (Figure 8C, D).

Cells transfected with dominant negative RhoA have similar actin cytoskeletons to control cells expressing pCMS or HA plasmid (Figure 13D). This is consistent with the

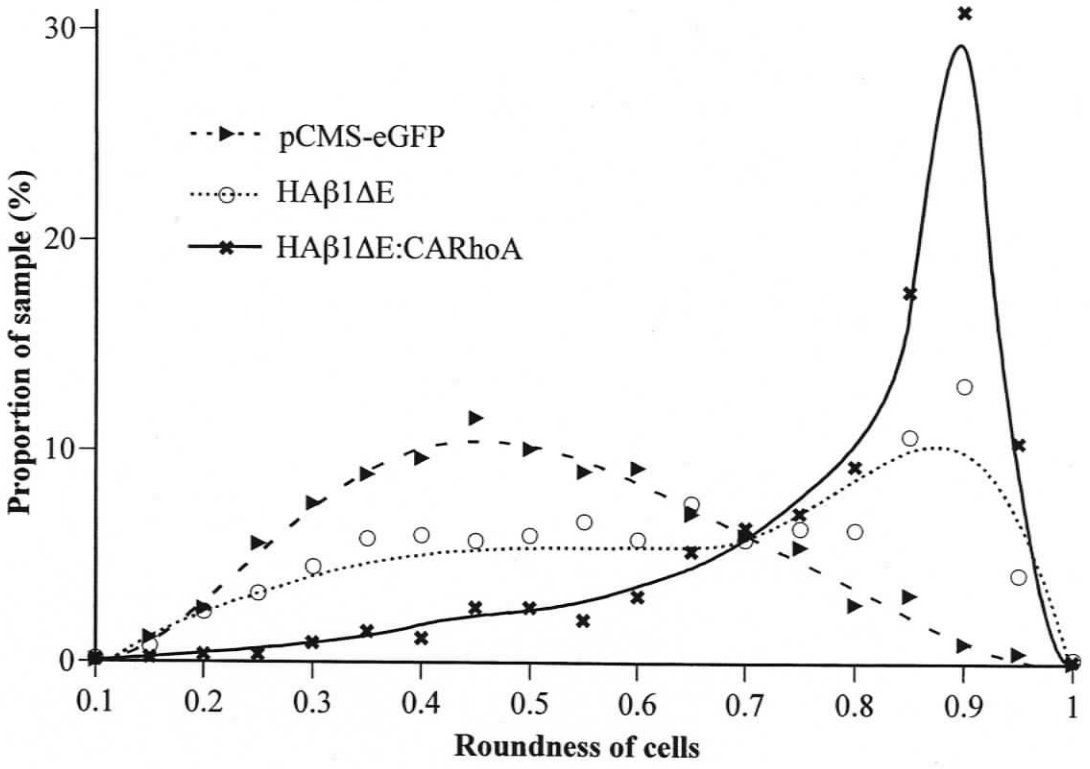

Figure 10. Distribution of roundness in cultures 24 h post-transfection. The dashed line (►) represents cells expressing pCMS-eGFP plasmid (pCMS), the dotted line (✖) represents cells expressing pCMS encoding chimeric β1 integrin subunit (HAβ1ΔE), the solid line (○) represents cells co-transfected with a 1:1 mix of pCMS encoding HAβ1ΔE and constitutively active (CA) RhoA. Cultures transfected with HAβ1ΔE, in comparison to pCMS, show an increase in the number of cells measuring approximately 0.9 roundness This is associated with a decrease in the numbers of cells having a roundness between 0.25 and 0.65. There is a point near 0.7 where the profiles cross. These general trends are seen to a greater degree in the culture co-transfected with HAβ1ΔE and CARhoA plasmid. This suggests the mutant constructs do not make cells more rounded, they make more cells rounded.

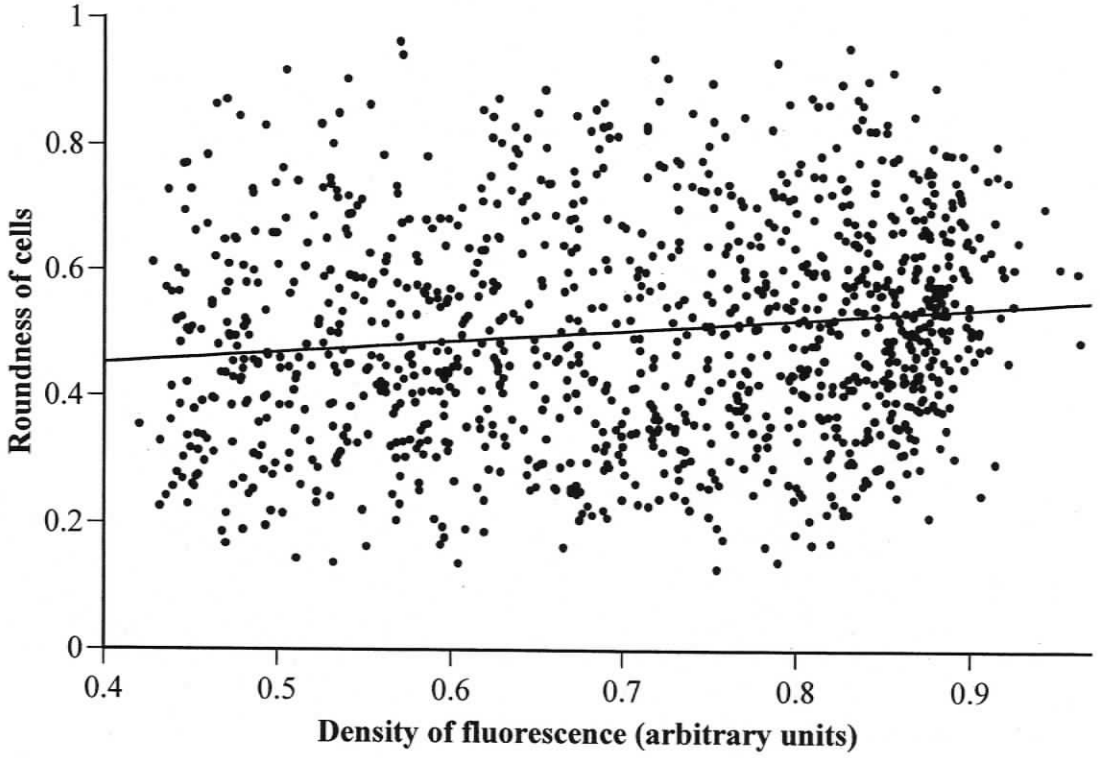

Figure 11. Correlation of cell roundness to the intensity of GFP expression. This is the 24 h post-transfection profile of a culture expressing pCMS-eGFP—a condition with low mean roundness. Linear regression shows a small positive correlation to roundness as the GFP fluorescence becomes brighter (roundness = 0.174·density + 0.382). The R-squared value indicates that 2.02% of the variation in cell roundness is explained by GFP fluorescence.

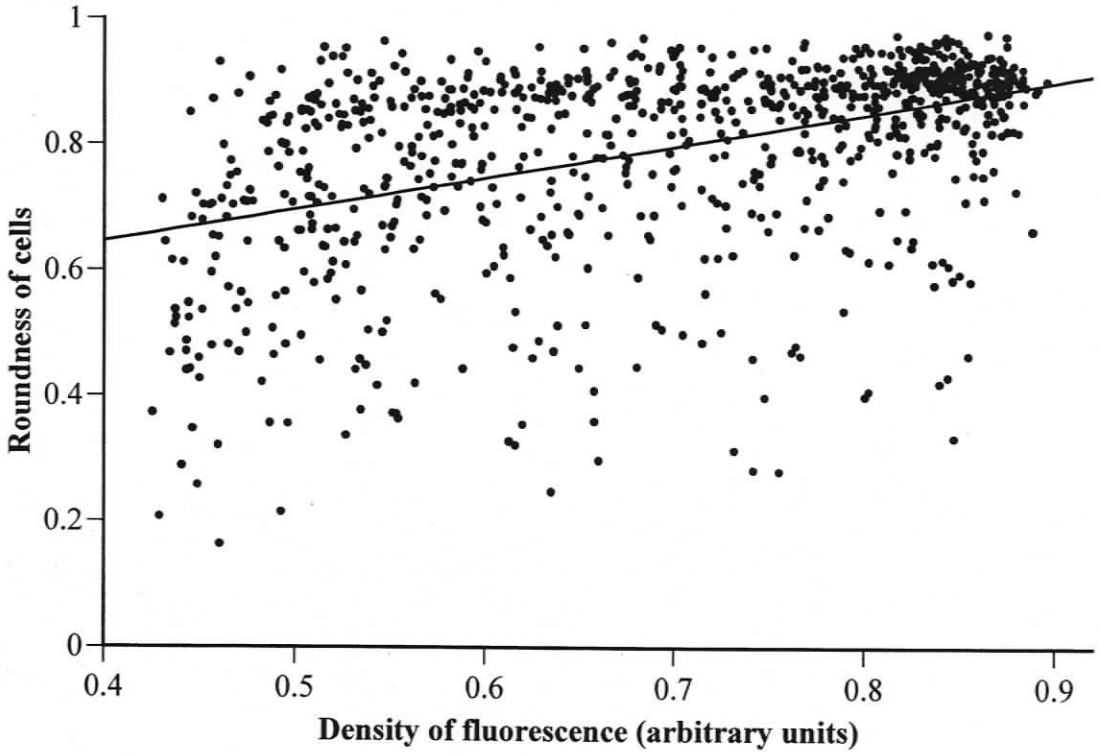

Figure 12. Correlation of cell roundness to the intensity of GFP expression. This is the 24 h profile of a culture co-transfected with a 1:1 mix of pCMS-eGFP plasmid encoding chimeric β1 integrin subunit (HAβ1ΔE) and constitutively active RhoA—a condition with the highest mean roundness. Linear regression shows a positive correlation to roundness as the GFP fluorescence becomes brighter (roundness = 0.504·density + 0.444). The R-squared value indicates that 20.1% of the variation in cell roundness is explained by GFP fluorescence.

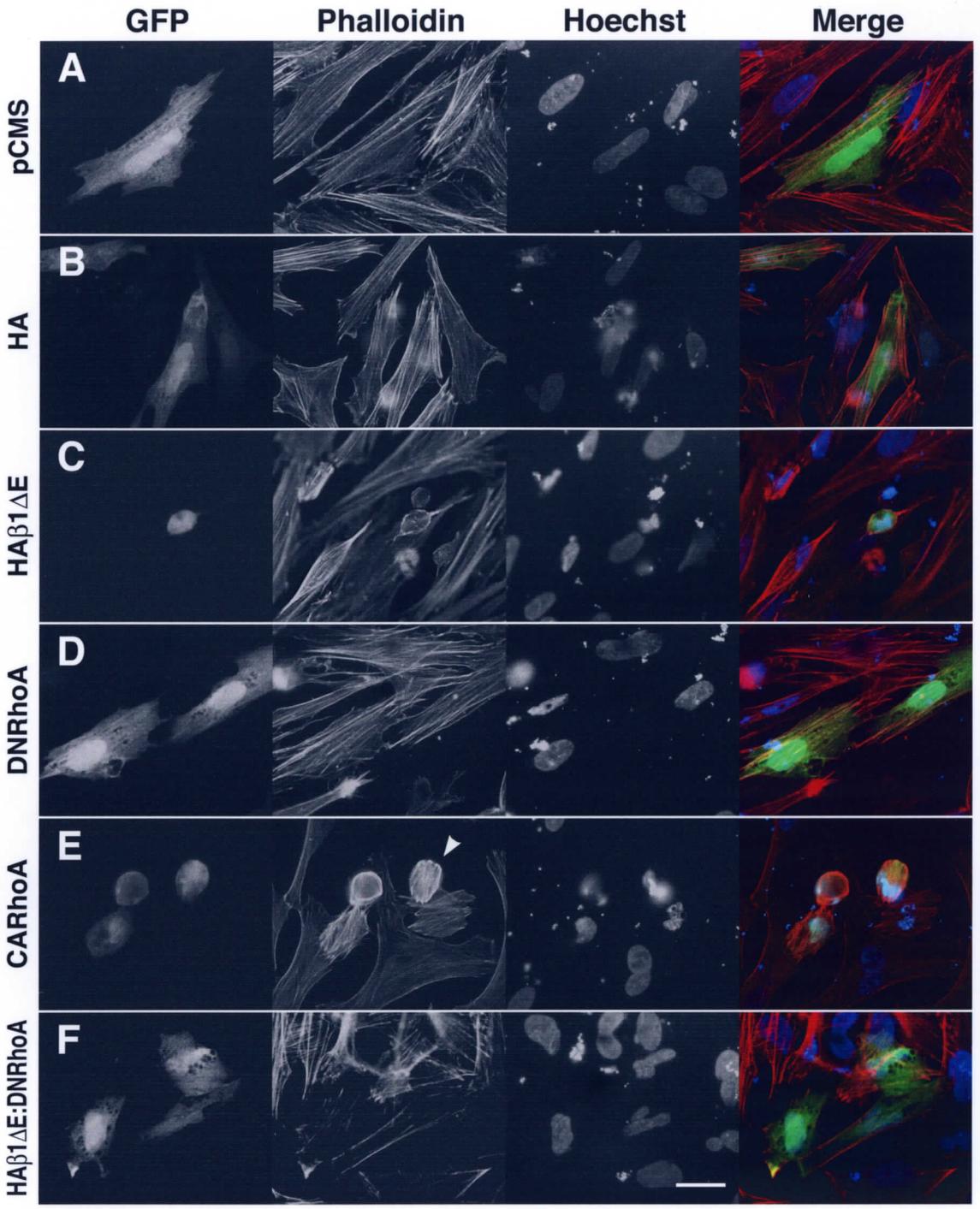

Figure 13 Changes in the actin cytoskeleton 24 hours after transfection with mutant GTPase. Each row shows GFP fluorescence, phalloidin label of actin, Hoechst label of DNA, and a merged overlay of all channels. Cultures were transfected with (A) pCMS-eGFP plasmid (pCMS), or pCMS encoding: (B) hemagglutinin, (C) dominant negative β1 integrin, (D) dominant negative RhoA, or (E) constitutively active RhoA. (F) Cells were co-transfected with plasmids C and D. Bar = 20 μm.

morphometrics of cell aspect and roundness. Most cells transfected with constitutively activate RhoA contain prominent stress fibers (arrowhead, Figure 13E). This is a typical effect of constitutively active Rho protein (Hall, 1998), which confirms the construct has the intended effect in avian cells. The rounding may be caused by prolonged exposure to the mutant, as observed in renal cell culture (Tamma *et al*., 2001). Cells co-transfected with HAβ1ΔE and DNRhoA plasmids contain stress fibers and cortical actin, although the stress fibers are less prominant than in cells transfected with pCMS, HA, or DNRhoA alone (Figure 13F). Dominant negative RhoA seems to prevent the disruption of the cytoskeleton seen in all other HAβ1ΔE transfections and co-transfections. The cells also have smooth oval nuclei. This suggests that nuclear fragmentation in preparations transfected with HAβ1ΔE alone is not a toxic effect.

Transfection of Presumptive Neural Crest Cells

The goal of localized electroporation is to simplify the analysis of mosaic embryos by minimizing the transfection of unintended tissues. The transfection of presumptive neural crest cells in the neural ectoderm, before EMT, was performed by injecting plasmid in saline into the lumen of the neural tube and applying a saline-filled electrode to the surface of the embryo at the level of the hindbrain (Figure 14A, B). Only cells of the neural ectoderm would be transfected because the plasmid is restricted to the neural tube. Cells in the overlying epidermal ectoderm and mesenchyme are exposed to the electric field, but since they are not contacting the plasmid, they are not transfected.

Rhodamine-labeled DNA was used to visualize the electroporation process. This molecule allows for transfected cells to be identified without the time lag of transcription and translation. The transfection pattern, therefore, can be seen before it is distorted by

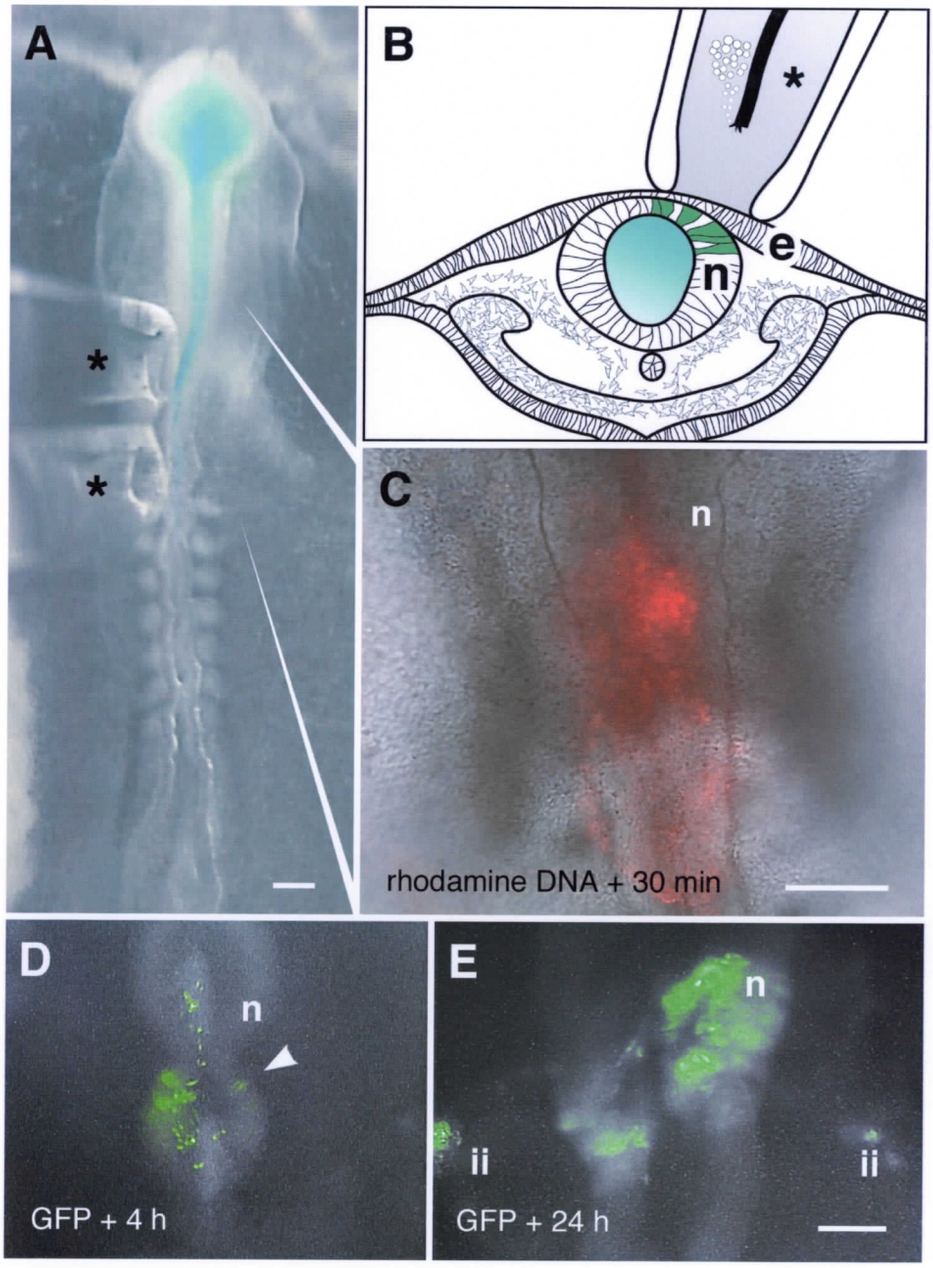

Figure 14. Localized electroporation of chick embryos *in ovo*. (A) Arrangement for targeting hindbrain neural ectoderm. Plasmid-containing saline (dyed blue) has been injected into the neural tube. The electrode barrels (*) are visible emerging from the left. (B) Schematic representation of a neural tube electroporation in transverse section through hindbrain. Cells within the neural ectoderm (n), but not the epidermal ectoderm (e) are transfected (green). (C) Combination fluorescent/light image of a rhodamine-labeled DNA surface electroporation 30 min post-transfection. The lines into (A) indicate the bounds of the field of view. (D) Similar view as (C), of a neural tube electroporation 4 h post-transfection. There are GFP-expressing cells in the dorsal neural ectoderm and lateral walls (arrow). (E) Similar preparation as (D), but 24 h post-transfection. The transfection patch is brighter and GFP-expressing cells are present in the second branchial arches (ii). Bars = 150 μm.

cell movement and embryo growth. Stage 12 embryos (n = 4), observed at 30 min post-transfection, have fluorescent patches at the target areas (Figure 14C). The pattern is in a figure eight and corresponds to the tip of the double-barreled electrode. Thus, barrel diameter determines the number of cells transfected. Rhodamine fluorescence is slightly more intense near the edges of the transfection patch. This indicates a higher transfection efficiency at the rim and is likely related to the shape of the electric field between the barrels. This control experiment is the only preparation where plasmid was loaded inside the electrode (a surface transfection). All other experiments target the neural ectoderm with plasmid in the lumen of the neural tube.

Electroporation of the neural ectoderm can be observed after 4 h using pCMS plasmid. These embryos, electroporated at stage 9, have cells weakly expressing GFP scattered within a shape similar to rhodamine-labeled DNA transfections (Figure 14D). The cells appear to be below the surface, in the dorsal neural tube at the midline. There are often GFP-expressing cells to both sides of the midline, although the right side is always biased during targeting. In most examples, cells in the right lateral wall of the neural tube are also transfected. The occurrence of this phenomenon may be related to the alignment of the barrel rim with the wall of the neural tube. This variation in the transfection pattern of neural ectoderm is likely insignificant as the lateral wall does not generate neural crest cells. At 24 h post-transfection, there is intense GFP fluorescence in the neural tube at the site of transfection (Figure 14E). Cells that weakly expressed GFP at 4 h are now very bright. Transfected cells that were undetected at 4 h, have visible fluorescence. The general shape of the transfection patch remains the same, but cellular movements frequently occur.

Migration Pathways in Control Embryos

Presumptive neural crest cells in the neural ectoderm were targeted shortly after fusion of the hindbrain neural folds. This occurs in early stage 9 embryos, and limits this injection technique. The rationale was to transfect neural crest cells before EMT commenced. The same electrode was used to electroporate all embryos in order to minimize the variation in transfection efficiency associated with slightly different tip shapes and sizes. Fourteen of 58 embryos (24%) were excluded from study (2 died, 4 had no transfection, 3 had scarring from the electroporation, and 5 were mistargeted).

At 24 h post-transfection all embryos have a similar-sized patch of cells expressing GFP in the neural tube within rhombomeres 4 to 6 (Figure 15). Embryos transfected with pCMS plasmid (stage 9: n = 8) or HA plasmid (stage 9: n = 7, stage 11: n = 5), have GFP-positive neural crest cells within the second or third branchial arches (Figure 15A, G). Embryos transfected with pCMS plasmid have a mean of 49.6 (± 4.04 s.e.m.) transfected cells within the neural crest pathway (Figure 16A). Embryos transfected with HA plasmid have a mean of 44.1 (± 6.07 s.e.m.) transfected cells from stage 9, and 30.8 (± 4.42 s.e.m.) transfected cells from stage 11. In preparations with either plasmid there are transfected cells outside the neural tube, within the neural crest pathway. In sections of HA-transfected embryos, there are fluorescent cells within the dorsal neural ectoderm. In addition, there are cells transfected with the HA plasmid dispersed in the mesenchyme lateral to the neural tube and in the branchial arches (Figure 15B). These cells are polygonal or elongate and are most abundant 15-20 μm beneath the ectoderm within the second and third branchial arches (Figure 15C).

Cells expressing GFP in the branchial arch mesenchyme are assumed to be neural

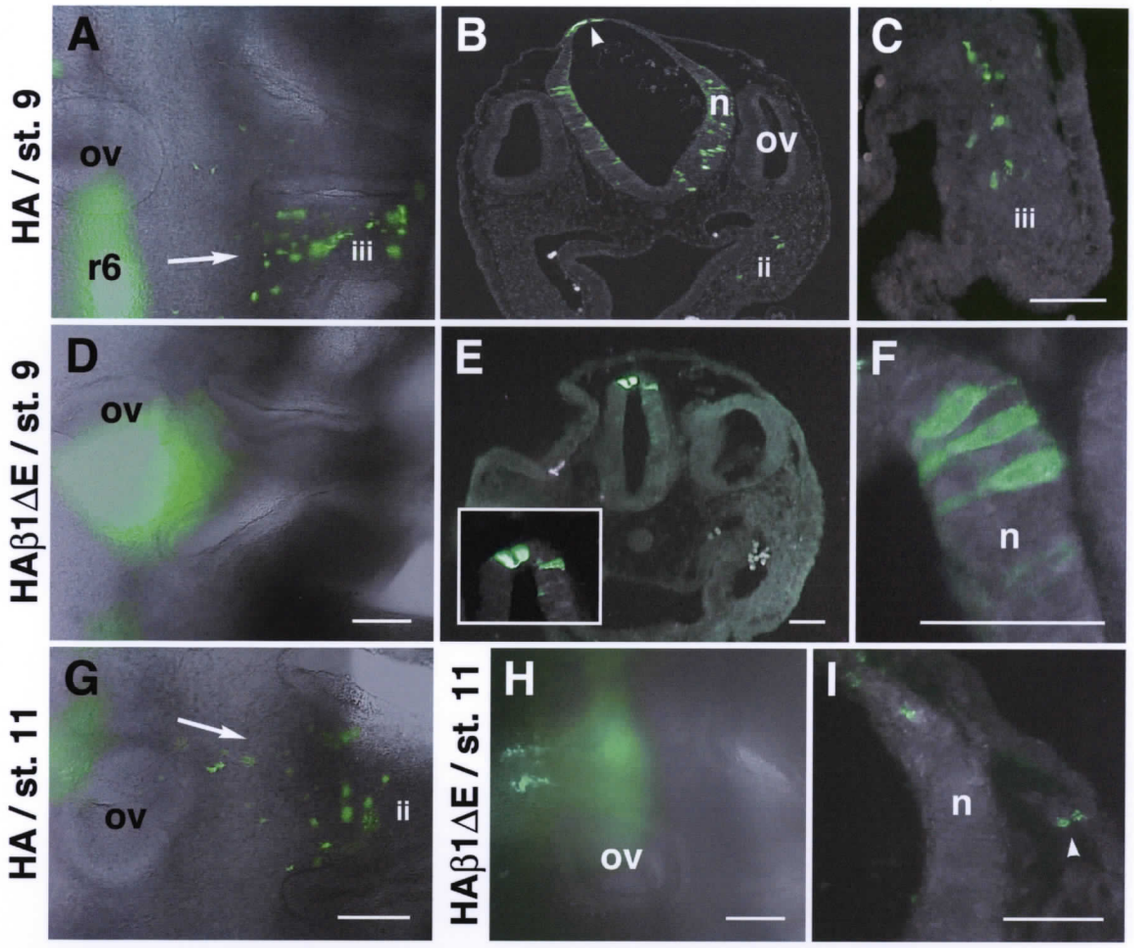

Figure 15. Localized electroporation of hindbrain neural crest cells in the neural ectoderm. The top row shows HA mosaic embryos 24 h after they were transfected at stage 9. (A) Combination fluorescent/light image of a whole mount. Neural crest cells, transfected in the sixth rhombomere (r6), have undergone EMT and have migrated (arrow) to the third branchial arch (iii). ov, otic vesicle. (B) Fluorescent image of a transverse section. Neural crest cells have released from the dorsal neural ectoderm (arrowhead) and migrated to the branchial arch. (C) Transverse section with HA cells in the mesenchyme of the branchial arch. (D) Embryos transfected with HAβ1ΔE plasmid are in the middle row. No GFP-expressing cells are observed outside of the transfection patch. (E) Sections confirm that the GFP-positive cells remain within the neural ectoderm. A magnification of the dorsal neural tube is inset. (F) HAβ1ΔE cells within the neural tube have normal epithelial morphology *in vivo*. (G) The bottom row shows embryos 24 h after they were transfected at stage 11. In control embryos, cells expressing GFP and HA migrate to the branchial arch. (H) Embryos transfected with HAβ1ΔE do not have GFP-expressing cells outside the transfection patch, but there are some cells that appear to have completed EMT. (I) A transverse section shows these cells (arrow) are between the neural ectoderm and the epidermal ectoderm. Note: white cells present in (B, E) are autofluorescent red blood cells. Bars = 25 μm.

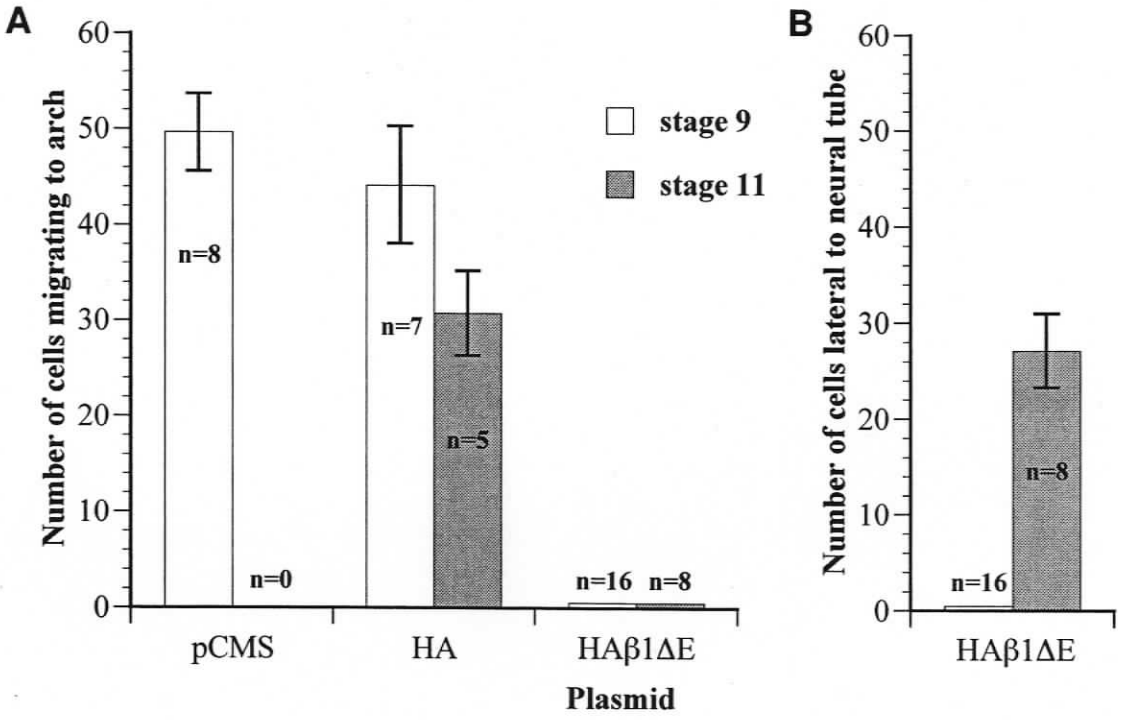

Figure 16. Effects of inappropriate integrin signaling in hindbrain neural crest cells. Neural ectoderm of stage 9 or 11 chick embryos was electroporated with pCMS-eGFP plasmid (pCMS), pCMS encoding hemagglutinin (HA), or pCMS encoding chimeric HA-β1 integrin subunit (HAβ1ΔE). (A) The number of transfected cells migrating toward the branchial arch was counted 24 h post-transfection. The mean is not significantly different between cells expressing pCMS or HA control plasmids at stage 9. Fewer HA-expressing cells migrate to the branchial arch when electroporated at stage 11 ($P < 0.05$). There is a significant inhibition of emigration by the HAβ1ΔE plasmid ($P < 0.0001$). (B) The HAβ1ΔE-transfected embryos, which have no transfected cells outside the transfection patch, are presented again to show the estimated number of transfected cells lateral to the neural tube. Bars, s.e.m.

crest. The pattern is consistent with cells releasing from the neural tube shortly after transfection and migrating along neural crest pathways into non-transfected areas. The majority of cells in the neural ectoderm do not form neural crest; the 45-50 cells that migrate from a transfection patch are a fraction of the total number of cells transfected. The majority of neural crest emigration in the hindbrain occurs through stage 10 (Le Douarin & Kalcheim, 1999), so it is anticipated that fewer migrating cells would result from stage 11 transfections. The number of cells migrating to the branchial arch expressing pCMS or HA control plasmids is not significantly different ($P > 0.05$). This suggests that the full length HA is innocuous—a conclusion that is consistent with cell culture experiments.

Immunolabeling of Control Cells

Immunohistochemistry was used to identify the types of cells transfected with HA plasmid. Slug is a transcription factor expressed in pre-migratory avian neural crest cells and maintained through early migration (Liem *et al.*, 1995). Embryos transfected with HA control plasmid at stage 9 were fixed 5 h later and sectioned. These preparations have GFP-positive cells in the dorsal neural tube (Figure 17A). Some of the GFP-expressing cells have anti-Slug immunoreactive nuclei. This demonstrates that localized electroporation can target neural crest cells within the neural ectoderm before EMT.

The HNK-1 epitope is a well characterized neural crest cell marker (Tucker *et al.*, 1984). It is expressed by most migrating neural crest cells, and by some neural crest cells that have completed migration. Embryos transfected with HA plasmid at stage 9, fixed 24 h later and sectioned, have GFP-positive cells in the mesenchyme of the branchial arch (Figure 17B). This region is a hindbrain neural crest migratory pathway, and

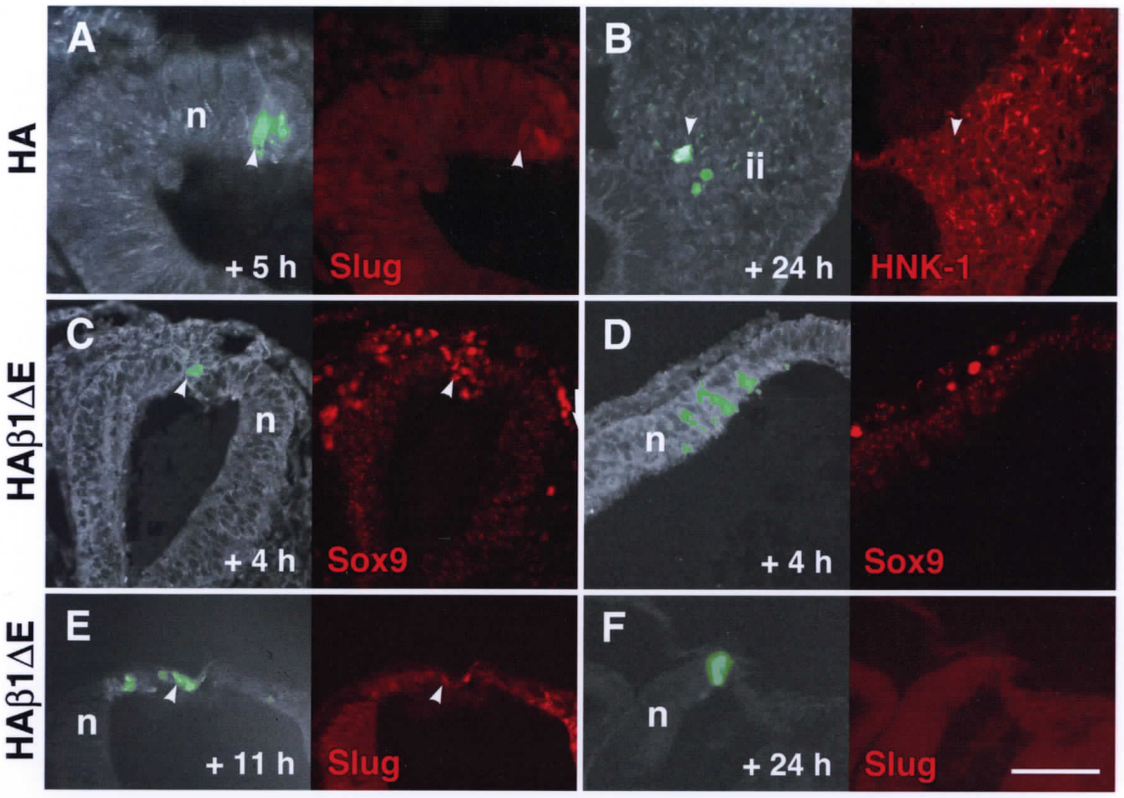

Figure 17. Immunofluorescent evidence for the transfection of neural crest cells. The neural ectoderm of stage 9 embryos was targeted by localized electroporation. Image pairs show the GFP channel and another channel from transverse sections. Arrowheads are placed in the same location within each image pair. (A) At 5 h post-transfection, HA-expressing cells in the neural ectoderm (n) co-localize with anti-Slug. (B) HA-expressing cells have migrated into an HNK-1 positive region in the mesenchyme of the second (ii) branchial arch. (C) A cell transfected with HAβ1ΔE in the midbrain is surrounded by anti-Sox9 immunoreactive cells undergoing EMT. (D) HAβ1ΔE-expressing cells remain in the neural ectoderm of the hindbrain, while anti-Sox9-labeled cells are nearby in the mesenchyme. (E) An HAβ1ΔE-expressing cell in the dorsal neural ectoderm appears to co-localize with anti-Slug label 11 h post-transfection. (F) A cell transfected with HAβ1ΔE is in the dorsal neural ectoderm 24 h post-transfection, but Slug label is not present. Bar = 25 μm.

furthermore, the cells express HNK-1. Taken together, this indicates that this method of localized electroporation can transfect neural crest cells, in the neural tube, that subsequently migrate to the branchial arches.

Chimeric β1 Integrin Prevents Epithelial-Mesenchymal Transition

Presumptive neural crest cells in the neural ectoderm were transfected with HAβ1ΔE plasmid at stage 9. All of these embryos have cells expressing GFP within the neural tube (Figure 15D, H). In none of the embryos transfected at stage 9 (n = 16) are there any GFP-positive cells outside the neural tube or within the branchial arches 24 h later (Figure 16A). In sections, the HAβ1ΔE-expressing cells are within the neural ectoderm where they maintain an epithelial phenotype (Figure 15E, F). It appears that HAβ1ΔE expression blocks EMT in presumptive neural crest cells by interfering with integrin function.

Cells expressing HAβ1ΔE in the neural ectoderm have a pseudostratified morphology (Figure 15F). This observation provides additional evidence that HAβ1ΔE does not produce a general cytotoxic effect. HAβ1ΔE-expressing cells in the embryo are not rounded, as observed in culture. This suggests that epithelial morphology is not dependent on β1 integrin function.

The neural ectoderm was also transfected at stage 11 with HAβ1ΔE plasmid. Cells are undergoing EMT at this stage (Le Douarin & Kalcheim, 1999). None of the embryos transfected at stage 11 (n = 8) have HAβ1ΔE cells in or near the branchial arches 24 h later (Figure 15H). In contrast to the stage 9 transfections, however, all the embryos transfected at stage 11 have cells that appear distinct from the diffuse fluorescence of

deep cells in the neural tube. In section, these HAβ1ΔE cells are lateral to the neural tube, beneath the epidermal ectoderm (Figure 15I). The cells are more difficult to count than those in other preparations, but there are approximately 27.1 (± 3.82 s.e.m.) cells free of the neural ectoderm expressing HAβ1ΔE (Figure 16B). This is comparable to the number of cells expressing HA control plasmid and migrating to the branchial arches in stage 11 embryos. It appears that HAβ1ΔE-expressing cells from stage 11 electroporations undergo EMT, but fail to migrate to the branchial arches.

There is a lag between transfection and the transgene effect. Chimeric integrins do not cause a dominant negative effect when expressed at low levels (LaFlamme *et al.*, 1994; Smilenov *et al.*, 1999), so effects of the chimera are not likely instantaneous. Cells released from the neural tube after stage 11 transfection may result from cells that are in the process of EMT during transfection at stage 11. They release from epithelium and integrin signaling is subsequently affected. The implication is that cells transfected at stage 9 are not yet involved in EMT and the chimeric integrin has enough time to establish itself and affect the integrin signaling involved in EMT. Cells transfected at stage 11 are unlikely to represent a population that employs different mechanisms of EMT than earlier populations of neural crest, as stage 9 transfections would be expected to include all neural crest precursors.

It appears that β1 integrin function is necessary for hindbrain neural crest cells to undergo EMT. The transfection of slightly older embryos produces a variation of the result, which indicates that a failure to release from the neural tube is distinct from a failure to migrate.

Immunolabeling of Chimeric β1 Integrin-Transfected Embryos

Immunohistochemistry was used to identify the types of cells transfected with HAβ1ΔE plasmid. Sox9 is an early marker of prospective avian neural crest cells (Cheung & Briscoe, 2003). An embryo transfected with HAβ1ΔE plasmid at stage 9, fixed 4 h later and sectioned, has GFP-positive cells in the dorsal midbrain (Figure 17C). The GFP-positive cells co-localize with a region containing Sox9-positive cells that are undergoing EMT. There are some cells expressing Sox-9 between the neural and epidermal ectoderm but none of these cells express GFP. This demonstrates that prospective neural crest cells express the HAβ1ΔE plasmid, at least in the midbrain, but no GFP-expressing cells are observed outside the neural ectoderm.

I was not able to identify Sox9-expressing cells among the transfected cells in the hindbrain. HAβ1ΔE-expressing cells are in the hindbrain neural ectoderm, beneath Sox9-positive cells (Figure 17D). I sectioned 8 embryos to determine if HAβ1ΔE-expressing cells co-express Sox9 in the hindbrain.

Embryos transfected with HAβ1ΔE plasmid at stage 9 were also labeled with anti-Slug antibody. Preparations fixed 11 h post-transfection have GFP-expressing cells restricted to the dorsal neural ectoderm (Figure 17E). Some of these cells co-localize with anti-Slug, although the signal is weak at this stage. The co-labeled cells remain within the transfection patch and have normal morphology. Neural crest cells typically migrate at 150 μm/h, and generally reach their destination in less than 12 h (Kulsea & Fraser, 2000), so this should be ample time to observe the displacement of even a slow moving cell. The Slug expression shows that neural crest cells, expressing chimeric integrin β1 subunit, are still present in the neural ectoderm 11 h after transfection.

I sectioned 15 embryos to find anti-Slug labeling in HAβ1ΔE-expressing cells at a time when Slug was no longer present in non-transfected neural crest cells. Embryos transfected at stage 9, fixed 24 h later and sectioned, do not maintain Slug immunoreactivity in any GFP-expressing cells (Figure 17F). It would have been insightful to see Slug or Sox9 expressed in transfected cells at a stage later than normal. It seems, however, that downregulation of Slug and Sox9 expression is not interrupted by interfering with integrin signaling. These data are consistent with indications that neural crest specification is separable from the initiation of EMT. For example, the normal gradient of Noggin in the neural tube can be disrupted by grafting Noggin-secreating cells. These preparations inhibit the release of Slug-expressing cells in the neural tube, while the addition of BMP4 restores EMT (Sela-Donenfield & Kalcheim, 1999). Furthermore, downregulation of N-cadherin and cell outgrowth from pre-EMT neural tube explants is precociously stimulated by the protein kinase inhibitors staurosporine and bisindolymaleimide (Newgreen & Minichiello, 1995).

Dominant Negative RhoA Permits Emigration

At 24 h post-electroporation, embryos transfected with DNRhoA plasmid (n = 11) have a patch of cells expressing GFP within rhombomeres 4 to 6 (Figure 18A). There is a mean of 23.6 (± 3.20 s.e.m.) GFP-positive cells migrating to the second or third branchial arch (Figure 19). These cells are outside the neural tube and within the neural crest migration pathway. The pattern is identical to control embryos transfected with pCMS plasmid, but fewer cells are migrating ($P < 0.001$). This reduction may suggest that dominant negative RhoA is partially suppressing RhoA signals required for EMT. Alternatively, the reduction may be insignificant if the lower *in vitro* lipofection efficiency of DNRhoA

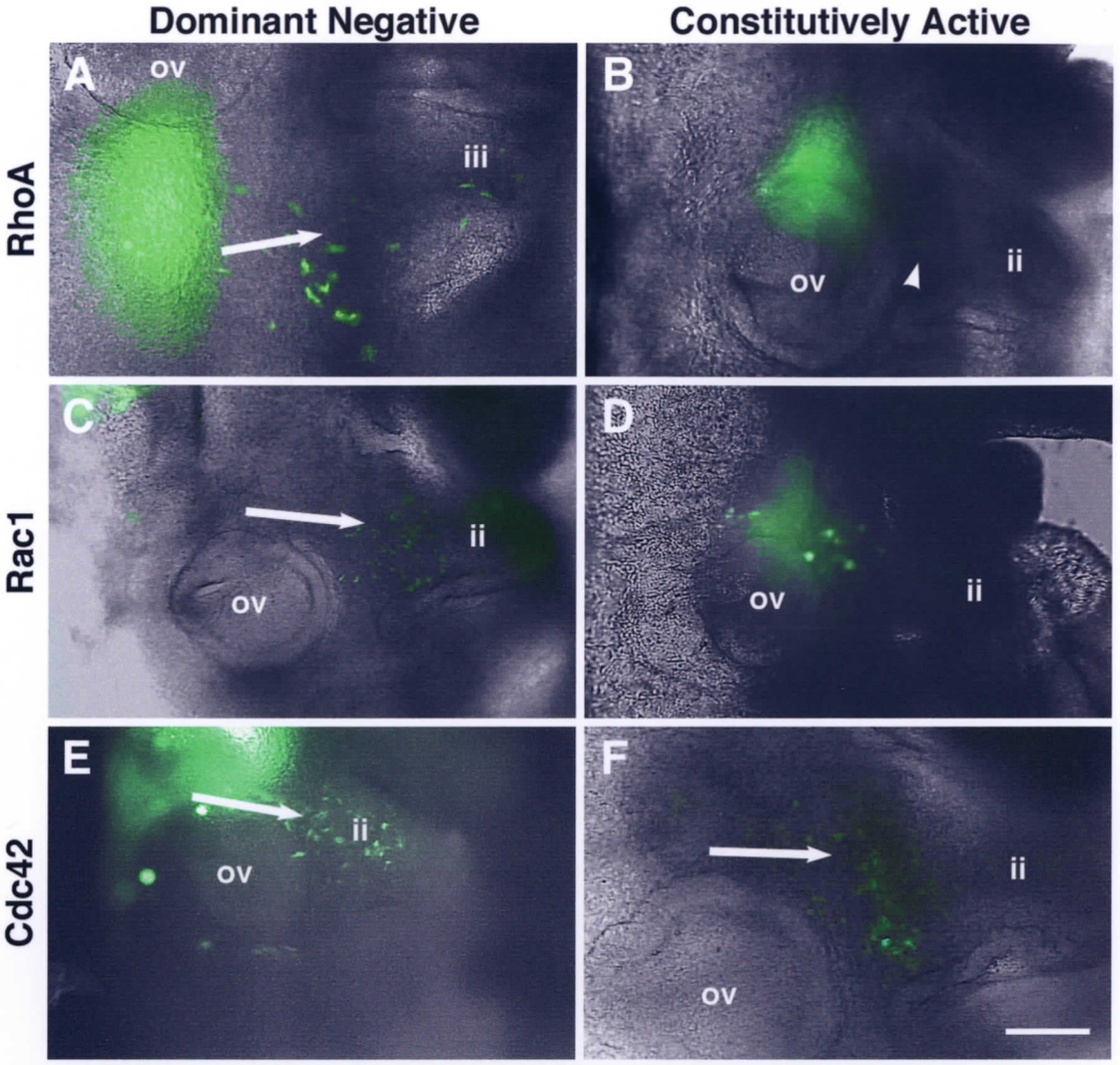

Figure 18. Localized electroporation of hindbrain neural crest cells with dominant negative (DN) and constitutively active (CA) GTPases. Neural ectoderm of the fourth to sixth rhombomeres was targeted in embryos at stage 9 and combination fluorescence/light images were collected 24 hours later. Images show the neural crest migration pathway near the otic vesicle (ov) on the right side of the embryo. The anterior of the embryo is to the top of the images and dorsal is to the left. (A) Neural crest cells, transfected with DN RhoA in the sixth rhombomere, have undergone EMT and migrated (arrow) to the third branchial arch (iii). (B) Most embryos transfected with CA RhoA do not have any GFP-positive cells outside the transfection patch. This embryo has one cell (arrowhead) migrating toward the arch. (C) Cells transfected with DN Rac1 emigrate from the fourth rhombomere and are found in the second branchial arch. (D) Most embryos transfected with CA Rac1 have GFP-positive cells restricted to the transfection patch. (E) Cells transfected with DN Cdc42 emigrate from the fourth rhombomere and are found in the second branchial arch. (F) Similar to (E), but transfection with CA Cdc42. Bar = 25 μm.

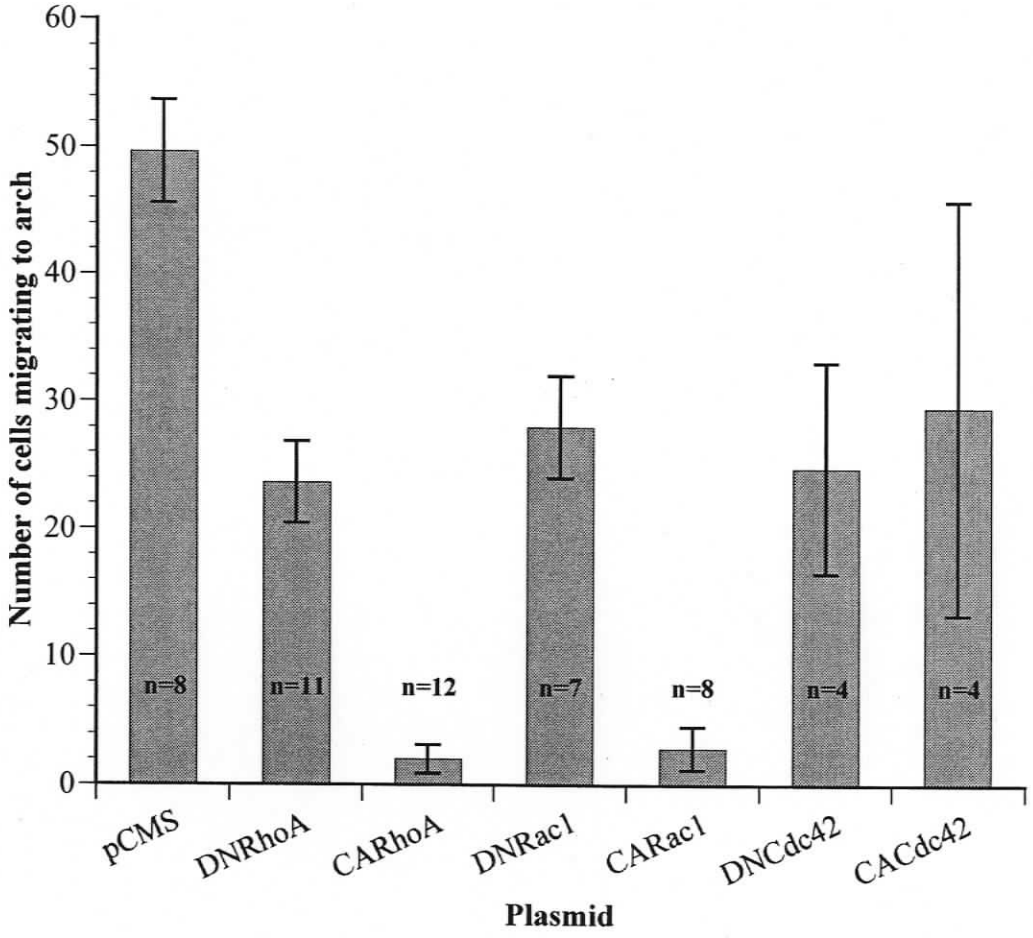

Figure 19. Effect of dominant negative (DN) and constitutively active (CA) GTPases in hindbrain neural crest cells. Neural ectoderm of stage 9 chick embryos was electroporated with pCMS-eGFP plasmid (pCMS) or pCMS encoding DN and CA forms of RhoA, Rac1, or Cdc42. The number of transfected cells that undergo epithelial-mesenchymal transition and migrate toward the arch was counted 24 h post-transfection. There is a significant inhibition of emigration by CARhoA and CARac1 ($P < 0.0001$). Bars, s.e.m.

plasmid (Figure 7) is predictive of the plasmid efficiency during electroporation of embryos. Regardless of the explanation, many transfected cells do emigrate to the branchial arch in embryos transfected with dominant negative RhoA. This suggests that the emigration of cranial neural crest cells does not require activation of RhoA signaling.

Constitutively Active RhoA Inhibits Emigration

Presumptive neural crest cells in the neural ectoderm were transfected with CARhoA plasmid at stage 9. All of these embryos ($n = 12$) have cells expressing GFP within the neural tube. Seven of the embryos have no GFP-positive cells outside the neural ectoderm 24 h later. The 5 remaining embryos have a few GFP-positive cells midway in the migration path leading to the branchial arch (arrowhead, Figure 18B). There is an overall ($n = 12$) mean of 2.00 ($\pm$ 1.10 s.e.m.) transfected cells migrating away from the neural tube (Figure 19). This is a significant reduction in comparison to control preparations with pCMS or DNRhoA plasmid ($P < 0.001$). The migration pattern and mean number of cells is comparable to HAβ1ΔE transfections, which have no transfected cells outside the neural tube ($P > 0.05$). It appears that activation of RhoA prevents EMT in almost all transfected cells.

Embryos with cells expressing CARhoA outside the neural tube were sectioned and immunolabeled for N-cadherin. This cell-cell adhesion molecule is found on epithelial cells, including those in the neural ectoderm. Transverse sections confirm that a few GFP-positive cells are in the mesenchyme. All of these cells observed ($n > 8$) are rounded, and co-localize with intense patches of N-cadherin label (Figure 20A). The release of these few cells without downregulation of N-cadherin suggest that EMT is incomplete. This indicates that activation of RhoA interferes with EMT and migration.

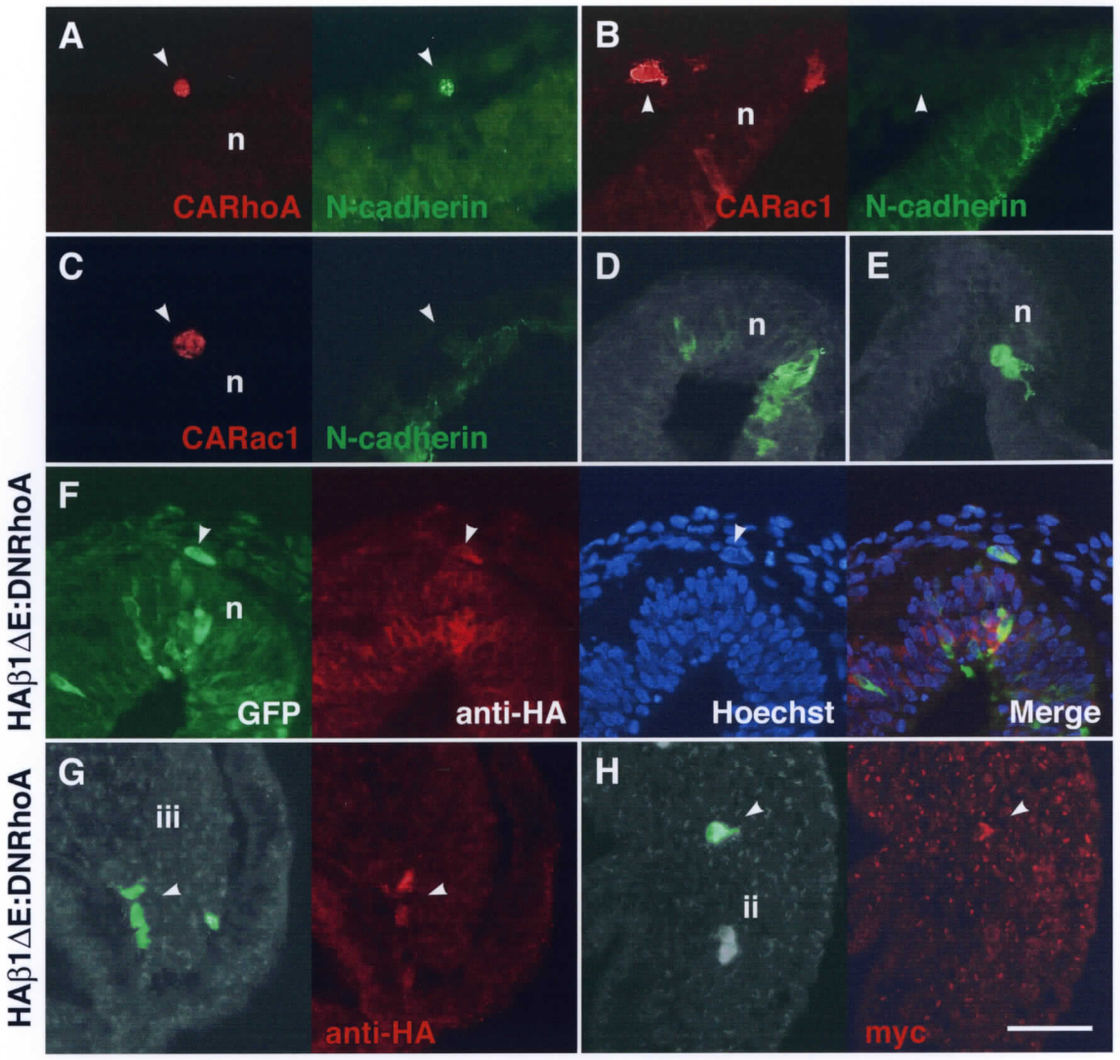

Figure 20. Immunofluorescence labeling of transverse sections from embryos 24 hours post-transfection. (A) A hindbrain cell transfected with constitutively active (CA) RhoA is in the mesenchyme above the neural ectoderm (n) and is rounded. The paired image shows co-localization of N-cadherin. (B) A cell transfected with CARac1 is in the mesenchyme and does not have N-cadherin immunoreactivity (arrow). (C) A rounded CARac1-expressing cell is N-cadherin negative. (D) Cells in the dorsal neural ectoderm of the hindbrain were co-transfected with dominant negative β1 integrin subunit (HAβ1ΔE) and CARhoA. (E) A process is visible on this HAβ1ΔE:CARhoA co-transfected cell in the neural ectoderm. (F) A cell co-transfected with HAβ1ΔE and DNRhoA is outside the dorsal neural ectoderm. It co-localizes with hemagglutinin (HA) label, and contains a round nucleus. (G) Cells co-transfected with HAβ1ΔE and DNRhoA in the neural ectoderm have migrated to the mesenchyme of the third branchial arch (iii) and are labeled with HA antibody. (H) A HAβ1ΔE:DNRhoA co-transfected embryo has a myc-positive cell in the mesenchyme of the second branchial arch. Bars = 25 μm.

Constitutively Active Rac1 Blocks Migration

Presumptive neural crest cells in the neural ectoderm at stage 9 were transfected with plasmids encoding mutant Rac1 GTPases (Figure 18C, D). At 24 h post-electroporation, embryos transfected with DNRac1 plasmid (n = 7) have a mean of 28.0 (± 3.99 s.e.m.) GFP-positive cells migrating to the branchial arch (Figure 19). These cells are outside the neural tube and within the neural crest migration pathway. There are fewer GFP-positive cells relative to pCMS-transfected embryos ($P < 0.05$), but there is no difference in mean migrating GFP-positive cells in HA and DNRhoA-transfected embryos. This demonstrates that cells expressing dominant negative Rac1 can undergo EMT and migrate. The emigration of cranial neural crest cells must not require activation of Rac1 signaling.

Hindbrain neural ectoderm was also transfected with CARac1 plasmid. All of these embryos (n = 8) have many cells that appear distinct from the diffuse fluorescence of deep cells in the neural tube; but, only 3 of these embryos have GFP-positive cells in or near the branchial arches 24 h later (Figure 18D). There is an overall mean of 2.88 (± 1.68 s.e.m.) transfected cells ventrolateral to the neural tube (Figure 19). This is significantly fewer GFP-positive cells migrating than pCMS or HA transfected embryos ($P < 0.001$). It appears that presumptive neural crest cells have released in these embryos, but almost all have failed to migrate.

Transverse sections confirm that CARac1-expressing cells are separate from the neural ectoderm. Most are irregular in shape (n > 20) and none are labeled by anti-N-cadherin antibody (Figure 20B). One rounded cell was observed, and it is also unlabeled by anti-N-cadherin (Figure 20C). Cells expressing CARac1 have a mesenchymal

phenotype unlike cells expressing CARhoA. This suggest that cranial neural crest cells can complete EMT but not migrate when Rac1 is constitutively activated. Regulation of lamellipodia through Rac1 signaling is involved in migration (Small *et al*., 2002), and it appears that cranial neural crest cells cannot effectively migrate with constitutively active Rac1.

Cdc42 is Not Required for EMT or Migration

Presumptive neural crest cells in the neural ectoderm at stage 9 were transfected with plasmids encoding mutant Cdc42 GTPases (Figure 18E, F). At 24 h post-electroporation, embryos transfected with DNCdc42 plasmid (n = 4) have a mean of 24.75 (± 8.24 s.e.m.) GFP-positive cells migrating to the branchial arch (Figure 19). Embryos transfected with CACdc42 plasmid (n = 4) have a mean of 29.50 (± 16.2 s.e.m.) GFP-positive cells migrating to the branchial arch. The migration pattern is similar to normal neural crest migration pathways. Neither the DNCdc42 mean or the CACdc42 mean is significantly different from the number of transfected cells migrating in control embryos ($P > 0.05$). These preparations demonstrate that EMT and migration can proceed in cranial neural crest cells with dominant negative inactivation or constitutive activation of Cdc42 signaling.

RhoA is Required for Integrin Signaling during EMT

Presumptive neural crest cells in the neural ectoderm at stage 9 were electroporated with HAβ1ΔE plasmid mixed together with mutant RhoA or Rac1 plasmid (Figure 21). Embryos co-transfected with HAβ1ΔE and DNRhoA plasmids (n = 14) have a mean of 27.14 (± 2.99 s.e.m.) GFP-positive cells migrating to the branchial arch (Figure 21A; 22).

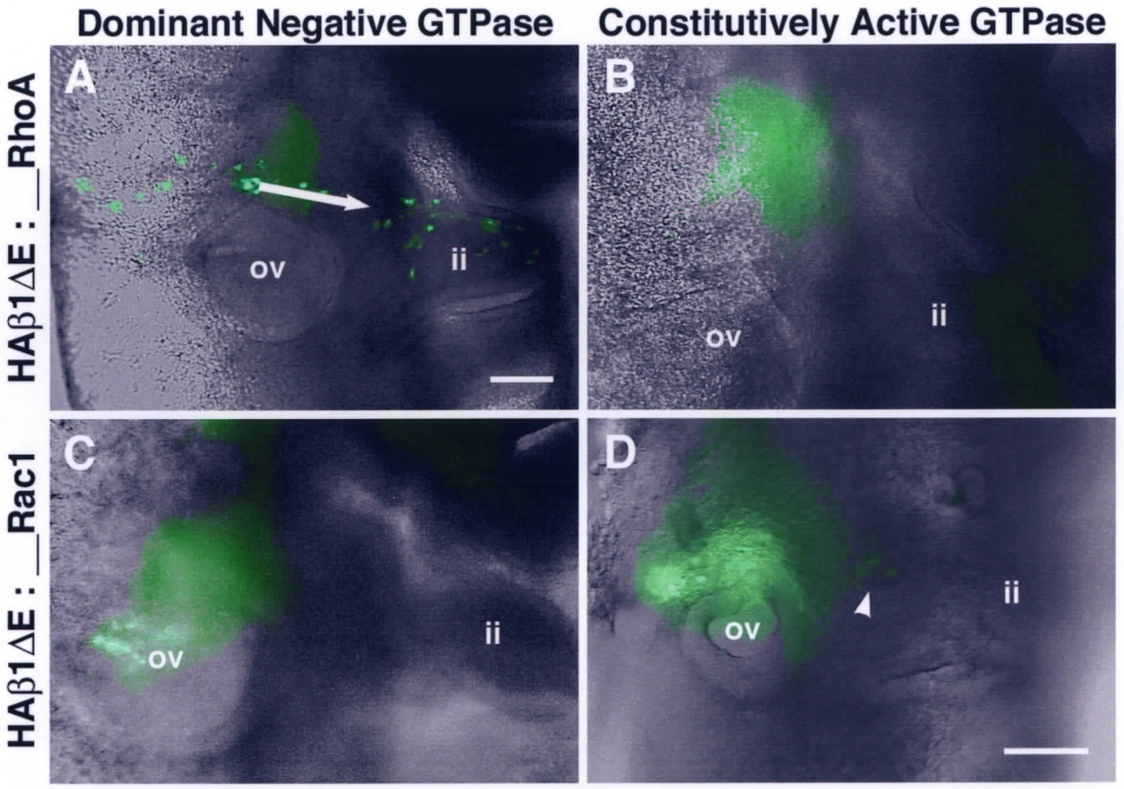

Figure 21. Co-transfection of hindbrain neural crest cells with dominant negative β1 integrin subunit (HAβ1ΔE) and dominant negative (DN) or constitutively active (CA) GTPases. Neural ectoderm of the fourth to sixth rhombomeres was targeted in embryos at stage 9 and combination fluorescence/light images were collected 24 hours later. Images show the neural crest migration pathway near the otic vesicle (ov) on the right side of the embryo. The anterior of the embryo is to the top of the images and dorsal is to the left. (A) Neural crest cells, co-transfected with HAβ1ΔE and DN RhoA in the fourth rhombomere, have undergone EMT and migrated (arrow) to the second branchial arch (ii). (B) In all but one embryo co-transfected with HAβ1ΔE and CA RhoA, GFP-positive cells remain within the transfection patch. (C) Cells co-transfected with HAβ1ΔE and DN Rac1 remain within the transfection patch. (D) Almost all embryos co-transfected with HAβ1ΔE and CA RhoA do not have any GFP-positive cells outside the transfection patch. This embryo has a few cells (arrowhead) migrating toward the arch. Bars = 25 μm.

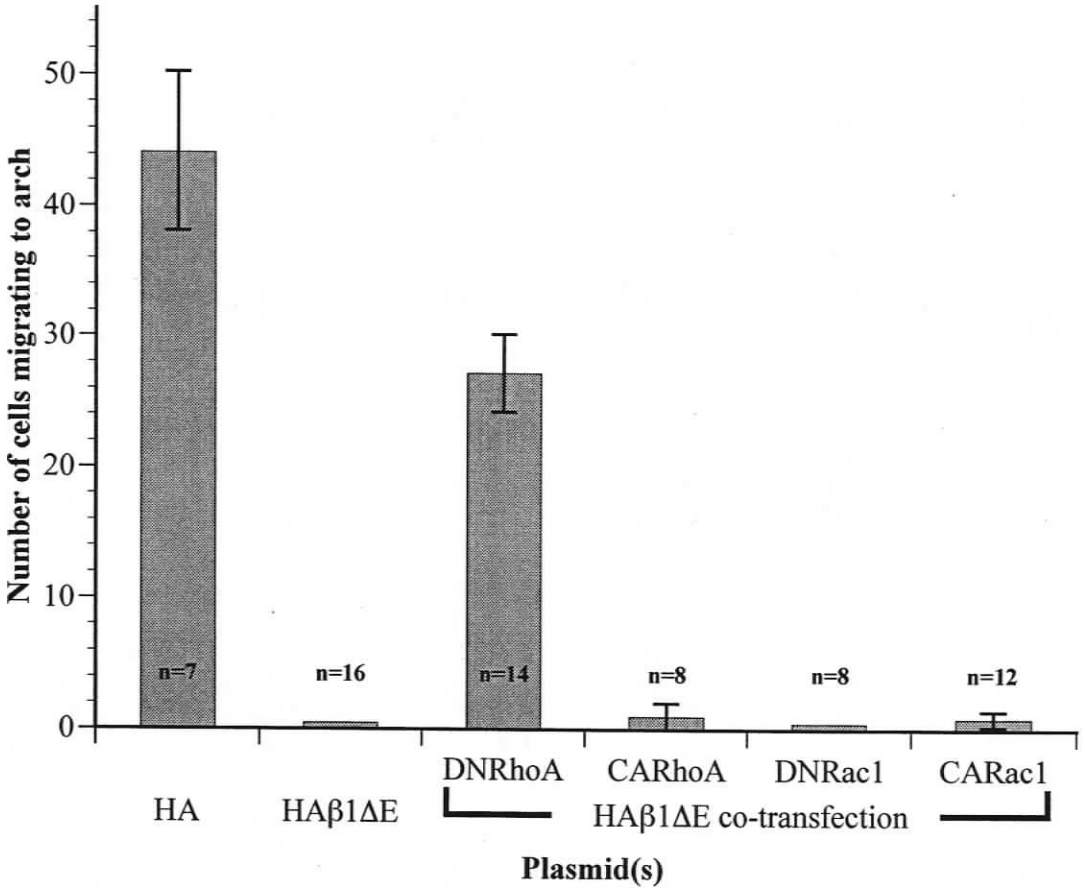

Figure 22. Effect of dominant negative RhoA in hindbrain neural crest cells with inappropriate integrin function. Neural ectoderm of stage 9 chick embryos was electroporated with pCMS-eGFP plasmid encoding hemagglutinin (HA), or chimeric HA-β1 integrin subunit (HAβ1ΔE). Co-transfections were performed with a 1:1 mix of pCMS-eGFP encoding HAβ1ΔE and a dominant negative (DN) or constitutively active (CA) form of RhoA or Rac1. The number of transfected cells that undergo epithelial-mesenchymal transition (EMT) and migrate toward the arch was counted 24 h post-transfection. The inhibition of EMT by HA β1ΔE appears to be rescued by DNRhoA ($P < 0.0001$). Bars, s.e.m.

Transfections with HAβ1ΔE plasmid alone have no cells emigrating from the neural ectoderm (Figure 15D). The mean number of transfected cells migrating is fewer than HA-transfected embryos ($P < 0.01$), but is not different from embryos transfected with DNRhoA alone ($P > 0.05$). This pattern is similar to the reversal of cell rounding in the *in vitro* co-transfections (Figure 6G, H). It appears that the simultaneous expression of dominant negative RhoA rescues the ability of cranial neural crest cells to emigrate to the branchial arches.

One embryo co-transfected with HAβ1ΔE and CARhoA plasmids has 8 GFP-positive cells migrating to the branchial arch. The other 7 co-transfected embryos have no GFP-positive cells outside the neural tube (Figure 21B). The mean number of transfected cells migrating is not different from embryos transfected with HAβ1ΔE alone ($P > 0.05$). Sections through the neural tube confirm proper targeting by localized electroporation and confirm that GFP-positive cells remain within the dorsal neural ectoderm 24 h later (Figure 20D). The co-transfected cells retain pseudostratified morphology in spite of co-transfection of HAβ1ΔE and CARhoA plasmids *in vitro* producing the most rounded cells. Substantial membrane processes are sometimes observed on transfected cells in the neural ectoderm (Figure 20E), supporting the hypothesis that cell rounding is not a general toxic effect of the constructs.

Embryos co-transfected with HAβ1ΔE and DNRac1 plasmids ($n = 8$) have no GFP-positive cells outside the neural tube or migrating to the branchial arch (Figure 21C). This is identical to embryos transfected with HAβ1ΔE alone (Figure 22). It demonstrates that co-transfection of chimeric β1 integrin subunit inhibits the neural crest cell emigration permitted by transfection of dominant negative Rac1 alone (Figure 19).

Ten embryos co-transfected with HAβ1ΔE and CARac1 plasmids have no GFP-positive cells outside the neural tube. Two embryos have a few GFP-positive cells midway between the neural tube and the branchial arch (arrowhead, Figure 21D). There is an overall mean of 0.83 (± 0.58 s.e.m.) GFP-positive cells migrating to the branchial arch in HAβ1ΔE:CARac1 co-transfected embryos (Figure 22). This mean is not statistically different from embryos transfected with HAβ1ΔE plasmid alone. Since both HAβ1ΔE and CARac1 plasmids inhibit emigration when transfected alone, it is likely that a co-transfection of the two would produce the same result.

Embryos co-transfected with HAβ1ΔE and DNRhoA plasmids were fixed 24-h post-electroporation to investigate the rescue of neural crest emigration. A section through the hindbrain shows the dorsal neural ectoderm has been co-transfected (Figure 20F). There is a GFP-positive cell located beneath the epidermal ectoderm that is separate from the neural ectoderm. Immunohistochemistry was employed to confirm expression of the chimeric constructs. Anti-HA co-localizes with GFP fluorescence, showing the HAβ1ΔE transgene is expressed by co-transfected cells *in vivo*, including a presumptive neural crest cell that has released (Figure 20F). Hoechst staining reveals smooth oval nuclei. This nuclear morphology, in combination with migration abilty of HAβ1ΔE:DNRhoA co-transfectioned cells, alleviates concerns of apoptosis that arose from *in vitro* histochemistry.

Sections through the branchial arches show that HAβ1ΔE:DNRhoA co-transfected cells have migrated to the mesenchyme of the branchial arch (Figure 20G). The GFP-positive cells co-localize with anti-HA immunoreactivity, indicating expression of the chimeric construct. A section from a similar preparation contains anti-myc

immunoreactivity co-localized with a GFP-positive cell (Figure 20H). Although a triple label is not feasible, the conclusion is that co-transfected cells are simultaneously expressing both constructs. These data suggest that the rescue of EMT and migration by chimeric β1 integrin subunit and dominant negative RhoA GTPase is accomplished while maintaining function of both transgene products.

CONCLUSION

To identify and order components of the pathway that transduce integrin signals during EMT, a method of co-transfecting two plasmids into the neural ectoderm of chick embryos was developed. Co-transfections of cyan and yellow fluorescent proteins demonstrate that both plasmids are expressed. Immunolabeling of transfected cells in culture show that all GFP-positive cells express transgenes from both plasmids. Immunolabeling of co-transfected cells that have migrated to the branchial arch in the embryo confirm transgene co-expression. Control experiments using mutant GTPase constructs in culture do not have a negative effect on cell survival. Hoechst staining of rounded cells in culture after 24 h indicates the beginning of apoptosis; however, comparably treated embryos contain healthy nuclei. Co-transfection by localized electroporation into presumptive neural crest is a suitable technique to evaluate the interaction of two constructs.

The consistency of morphometric results among culture replicates, observation intervals, and cell densities, demonstrate that *in vitro* morphology is dependent on the specific transgene. Tissue culture preparations confirm expression of the HAβ1ΔE chimera and demonstrate that HAβ1ΔE causes cell rounding, reduces the number of processes, alters focal adhesions, and disrupts the actin cytoskeleton. These effects of hemagglutinin-β1 chimera in avian cells are the same as Gβ1ΔE, and are similar to those described for other chimeras lacking the integrin extracellular domain (Lukashev *et al.*, 1994; Faraldo *et al.*, 1998). It appears that HAβ1ΔE has a dominant negative-like effect on affinity or avidity-based binding to the extracellular matrix. It is also possible,

however, that HAβ1ΔE is causing excessive integrin signals that downregulate fibronectin adhesion. Co-transfections of chimeric integrin with dominant negative RhoA have an elongated aspect in comparison to co-transfections with other mutant GTPases. This is consistent with a potential cellular interaction between RhoA and integrin signaling components. There is small correlation of cell roundness to intensity of GFP expression, but this can be explained by the physical properties of rounding. If two cells have identical volumes, and contain the same amount of GFP protein, the more spherical cell will appear brighter (denser) because the fluorescence is contained in a smaller cross-sectional area. Given this effect, and considering that 79.9% of the variation is not correlated with fluorescence density, it is reasonable to equally evaluate all cells with detectable GFP fluorescence in the embryo.

Phalloidin staining of transfected cultures reveals alterations of the actin cytoskeleton consistent with previous reports of GTPase mutants (Hall & Nobes, 2000). Cells transfected with dominant negative RhoA contain stress fibers. Neural crest cells *in vitro*, exposed to a fungal toxin that inhibits RhoA, RhoB, and RhoC, show less prominant stress fibers than untreated cells (Liu & Jessell, 1998). This indicates that the dominant negative effect has the predicted effect on to the intended target, RhoA. The dominant negative mutations to GTPases in this study are in the putative Mg^{+2} binding site. This causes preferential affinity for GDP over GTP (Stacey *et al.*, 1991), and blocks endogenous RhoA by sequestering guanine nucleotide-exchange factors (Quilliam *et al.*, 1994). Constitutively active mutations in this study block intrinsic and GAP-stimulated GTPase activity, thereby, locking the GTPase in the active GTP-bound form (Bos, 1989). The dominant negative approach may provide more specificity than a fungal toxin, such as C3 transferase, which is known to inhibit all Rho proteins (Nobes & Hall, 1995; Liu &

Jessell, 1998). The inhibition of proteins may also produce a more expedient effect than strategies targeting RNA. A recent RNA interference (RNAi) knockdown of RhoA in muscle cell culture, for example, allowed a 40-45 hour incubation before experimentation (Bi et al., 2005).

Localized electroporation is used to target pre-migratory neural crest shortly after fusion of the hindbrain neural tube in stage 9 embryos. By injecting plasmid-containing saline inside the neural tube and applying an electric field to the surface of the embryo, cells restricted to the neural ectoderm are targeted. When transfected with control plasmids, some cells undergo EMT and migrate towards the branchial arches. These cells are defined as neural crest because they release from the neural tube, follow neural crest pathways into non-transfected areas, and express HNK-1.

When neural ectoderm is targeted with HAβ1ΔE plasmid at stage 9, no transfected cells undergo EMT. In contrast, all the control preparations contain transfected cells that have migrated to the branchial arches. Immunolabeling with Sox9 and Slug neural crest cell markers confirm the identity of transfected cells. The conclusion from these experiments is that prospective neural crest cells are transfected with chimeric β1, but excessive integrin signaling, or signaling at an inappropriate time, prevents EMT. It is also possible that trimerized HAβ1ΔE does not elicit a full range of downstream signals, and for signals that require addition sigaling components, the construct may be acting like a dominant negative.

When neural ectoderm is transfected with HAβ1ΔE at stage 11, while neural crest emigration is in progress, no transfected cells migrate to the branchial arches. There are some cells, however, which release and fail to migrate. The chimeric integrin is unlikely

to cause an instantaneous effect, so this pattern likely results from cells that are transfected during EMT. The transfected cells release and migration is inhibited. This indicates that the failure to release from the neural tube can be distinguished from the failure to migrate.

Previous *in vivo* studies of perturbation of integrin document a variety of defects that could be caused by the inhibition of migration or EMT. Grafting hybridoma cells secreting JG22, an anti-β1 antibody, into cranial neural crest pathways results in a 54% reduction in migration, a buildup of cells in the lumen of neural tubes (26% of embryos), and aberrant migration in a few embryos (Bronner-Fraser, 1985a). The cells in the neural tube could be a consequence of blocking EMT. A extension of the experiment with the higher titer CSAT antibody yields similar results (Bronner-Fraser, 1986). Perturbation with the anti-HNK-1 antibody has also been studied (Bronner-Fraser, 1987). This antibody recognizes a carbohydrate epitope expressed on several molecules including the β1 integrin subunit. *In vitro*, HNK-1 appears to block attachment to laminin—in comparison to JG22 and CSAT, which affect both laminin and fibronectin receptors (Bronner-Fraser, 1987). Similar types of defects are observed with HNK-1, but the number of cells migrating is only reduced 9%. Ectopic neural crest cells, cells in the lumen, and deformed neural tubes predominate. An antibody against the laminin-heparan sulfate proteoglycan complex produced the same results (Bronner-Fraser & Lallier, 1988). These studies indicate perturbations of β1 integrins interfere with emigration of neural crest cells, however they do not clearly distinguish between a function in EMT and a function in cell migration, although some of the effects observed may well have resulted from disruption of EMT.

Neural tube defects, ectopic cells, or cells in the lumen of the neural tube are not observed in this study. Antibody perturbation experiments can affect all the cells near the injection—not all of which are neural crest. Unintended effects, such as decreased secretion of matrix proteins, or abnormal morphogenesis, especially in the neural tube, may result. For example, injecting a synthetic fibronectin peptide into one side of an embryo causes neural tube abnormalities and inhibits neural crest migration on both sides (Boucaut *et al.*, 1984). Localized electroporation affects fewer cells, potentially reducing alterations to the local environment. This method permits an analysis of embryos that are similar to genetic mosaic embryos, in which the behavior of identifiable cells expressing transgenes in a wild-type background can be tracked and monitored.

Analysing the effect of the chimeric integrin is complicated by the various mechanisms of integrin signaling. Although HAβ1ΔE inhibits fibronectin attachment *in vitro*, a dominant negative effect on adhesion is unlikely to explain the inhibition of EMT in the embryo because transfected cells appear morphologically normal. Certain integrin signals into the cell requires conformational changes initiated by extracellular ligand binding (Hato et al., 1998). If this type of signal transduction was required in EMT, then the chimeric integrin may inhibit those pathways through a dominant negative mechanism. Many integrin signals into the cell can also be initiated by clustering β1 integrin cytoplasmic domains (Hato et al., 1998; Akiyama *et al.*, 1994; Berrier et al., 2002). Since the hemagglutinin portion of the chimera can autonomously form trimers (Skehel & Wiley, 2000), clustered β1 cytoplasmic domains are likely to initiate excessive integrin signaling or integrin signaling at an inappropriate time. Therefore, the most likely interpretation of HAβ1ΔE transfections, is that integrin signals normally prevent EMT (Figure 23A).

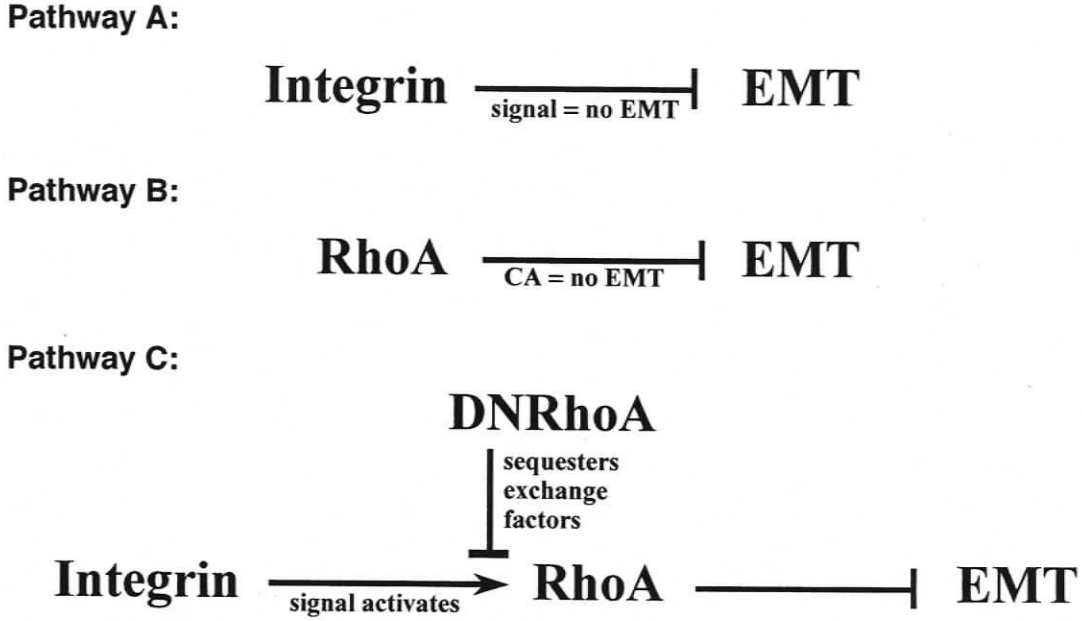

Figure 23. Signaling pathways during EMT of neural crest cells as suggested by transfection and co-transfection experiments. (A) Integrin signals normally prevent EMT (barhead) because excessive signaling from trimerized β1 integrin results in no EMT. (B) RhoA activity has an inhibitory effect on EMT because transfection of constitutively active RhoA inhibits EMT. (C) Co-transfection of chimeric integrin and dominant negative RhoA suggests a connection between these components. In these preparations, signaling from trimerized β1 integrin would attempt to activate RhoA (arrow) despite the induction of EMT. Co-transfection with dominant negative RhoA would prevent activation of RhoA, thereby rescuing the EMT process.

Transfection of constitutively active RhoA and transfection of chimeric β1 integrin subunit result in similar defects of EMT. This suggests that RhoA and integrin share a common pathway. Constitutive RhoA activity appears to have an inhibitory effect on EMT because constitutively active RhoA inhibits EMT (Figure 23B). Co-transfection of dominant negative RhoA with chimeric integrin results in EMT of 61% as many transfected cells as observed in control treatments, and transfected cells migrate along neural crest pathways. It is possible that integrin and RhoA pathways operate in parallel to independently regulate EMT. It is unlikely, however, that manipulation by dominant negative and positive mutants would have the observed reciprocal effect that restores a complex process like EMT. The most likely explanation of the rescue in the co-transfection experiments is that integrin and RhoA signaling pathways interact together. The rescue experiment also suggests that both signal components are upstream of EMT. If the only function of integrin was to generate motile force to pull the neural crest cell out of the ectoderm, the downstream effect could not be manipulated—i.e., by transfecting with a dominant negative form of the other component—to restore functionality on the other side of the process.

Integrin might be transmitting EMT signals through RhoA, or RhoA signals might be regulating integrin function. My work suggests that EMT most likely requires repression of integrin signaling to inactivate RhoA, and that inactive RhoA allows EMT to proceed (Figure 23C). This order and placement of components in a single pathway is compatible with all integrin, RhoA, and co-transfection data. RhoA signaling is not likely to stimulate integrin by assembling focal adhesions, for example, because transfection of dominant negative RhoA does not prevent EMT. RhoA activity could not inhibit integrin by causing degradation, for example, because constitutively active RhoA prevents EMT.

In my pathway (Figure 23C), chimeric integrin would inappropriately signal for RhoA activation, and co-transfection of dominant negative RhoA would prevent activation of endogenous RhoA, thereby rescuing the EMT process. This supports a previously suggested model that once neural crest cells are induced by paracrine signaling, β1 integrin signals and RhoA GTPase, are involved in the transition to a mesenchymal phenotype and the release of cells from the epithelium (Gimond *et al.*, 1999).

The work described in this dissertation demonstrates a role for β1 integrins in the EMT of cranial neural crest cells and suggests that RhoA GTPase is involved in the transduction of this integrin signal.

GTPases in an EMT Model

C3 transferase inactives RhoA, RhoB, and RhoC through ADP-ribosylation on asparagine residue 41 (Nobes & Hall, 1995). This fungal toxin was used in a prior study to investigate RhoB, but inhibits RhoA and RhoC as well (Liu & Jessell, 1998). The results of my work present an opportunity to reinterpret the results of Liu & Jessell. The central experiment by Liu & Jessell involved the application of C3 transferase to an explant of trunk neural tube in culture. The release of cells from the explant and migration onto the culture substrate was reduced by 87% after 6 h. Given that *in situ* hybridizations to *RhoA* showed expression throughout the neural tube, and since *RhoB* was restricted to presumptive and migratory neural crest, Liu & Jessell suggested a requirement for RhoB in EMT. However, the expression of *RhoA* throughout the neural tube may not preclude a cell-specific role for RhoA in the release of neural crest cells. Furthermore, the *in situ* hybridization data may not be predictive of protein expression levels (Jansen *et al.*, 2002; Greenbaum *et al.*, 2003). In view of my results, and since C3

transferase has a broad effect, it is possible that the inhibition of EMT seen by Liu & Jessell can be attributed to RhoA.

Studies after Liu & Jessell (1998) also suggest that RhoB is not required during EMT. RhoB is not expressed in mouse neural crest cells until after release (Henderson *et al.*, 2000). Induced expression of RhoB is not sufficient to generate EMT in chick cranial neural tube cells (Perez-Alcala *et al.*, 2004). A factor contributing to Liu & Jessell's perspective was the emerging role, mostly in frogs and fish, for possible BMP signaling in the induction of neural crest cells (Mayor *et al.*, 1995; Hammerschmidt *et al.*, 1996; Sasai & De Robertis, 1997). Liu & Jessell targeted RhoB following a PCR screen for genes that were upregulated after *in vitro* explants were exposed to a BMP. Since those studies, Wnt signaling has become a important candidate for neural crest induction and survival in several species (LaBonne & Bronner-Fraser, 1998; Polakis, 2000; Brault *et al.*, 2001; Garcia-Castro *et al.*, 2002; Wu *et al.*, 2003). Although both signals are likely involved, it is Wnt that appears to activate Slug through the β-catenin/LEF cascade (Vallin *et al.*, 2001). The Slug transcription factor appears to mediate many cellular changes associated with EMT (Boyer *et al.*, 1997; Batlle *et al.*, 2000; del Barrio & Nieto, 2002).

The experimental system in Liu & Jessell (1998) differs from my work in two aspects. Liu & Jessell use a trunk explant, stripped of non-neural epithelium and mesenchyme, treated with protease that cleaves fibronectin and some collagens, and placed on an artificial substrate of fibronectin. After such a procedure, cells are in a different environment and may behave differently than those in the *in vivo* assay of EMT described in this work. The present work, furthermore, targets neural crest cells in the

cranial region of the embryo. Many studies find significant differences between cranial and trunk neural crest cells (Nakamura & Ayer-Le Lievre, 1982; Lallier *et al.*, 1992; Cornell & Eisen, 2000; Strachan & Condic, 2003), so it is reasonable that differences in EMT signaling exist between the regions. Thus, it is possible for the EMT blockade of trunk explants (Liu & Jessell, 1998) to be explained by different mechanims than those suggested by my work.

The conclusions in my work, and previous studies, allow speculation about the overall pathways regulating neural crest morphogenesis (Figure 24). Prospective neural crest cells are specified from progenitors in the neural ectoderm by inductive signals involving BMP and Wnt. RhoB may be related to BMP signaling, as well as later differentiation and segregation of neural crest lineages (Perez-Alcala *et al.*, 2004). Following specification, pre-migratory neural crest cells transition to a mesenchymal phenotype and release from the neural ectoderm. Integrin signaling through RhoA appears to be required during this step. Given that clustering integrin chimeras can activate FAK (Akiyama *et al.*, 1994), which can activate p190RhoGEF (Zhai et al., 2003), FAK and p190RhoGEF are good candidates for future study of the signaling pathway. *RhoA* is widely expressed in the dorsal neural tube, suggesting that RhoA is not regulated as a consequence of neural crest specification. It appears instead, that RhoA is involved in integrating an additional input with the EMT signal. The integrin-RhoA signal may inhibit EMT in prospective neural crest cells until the basal lamina is in a state favorable for emigration. Whether signaling results from loss of basal lamina adhesion, or exposure to a ECM component remains to be determined. This pathway may explain the induction of EMT by collagen type I (Greenburg & Hay, 1982), or the inability of neural crest cells to penetrate a contiguous basal lamina (Erickson, 1987). Following

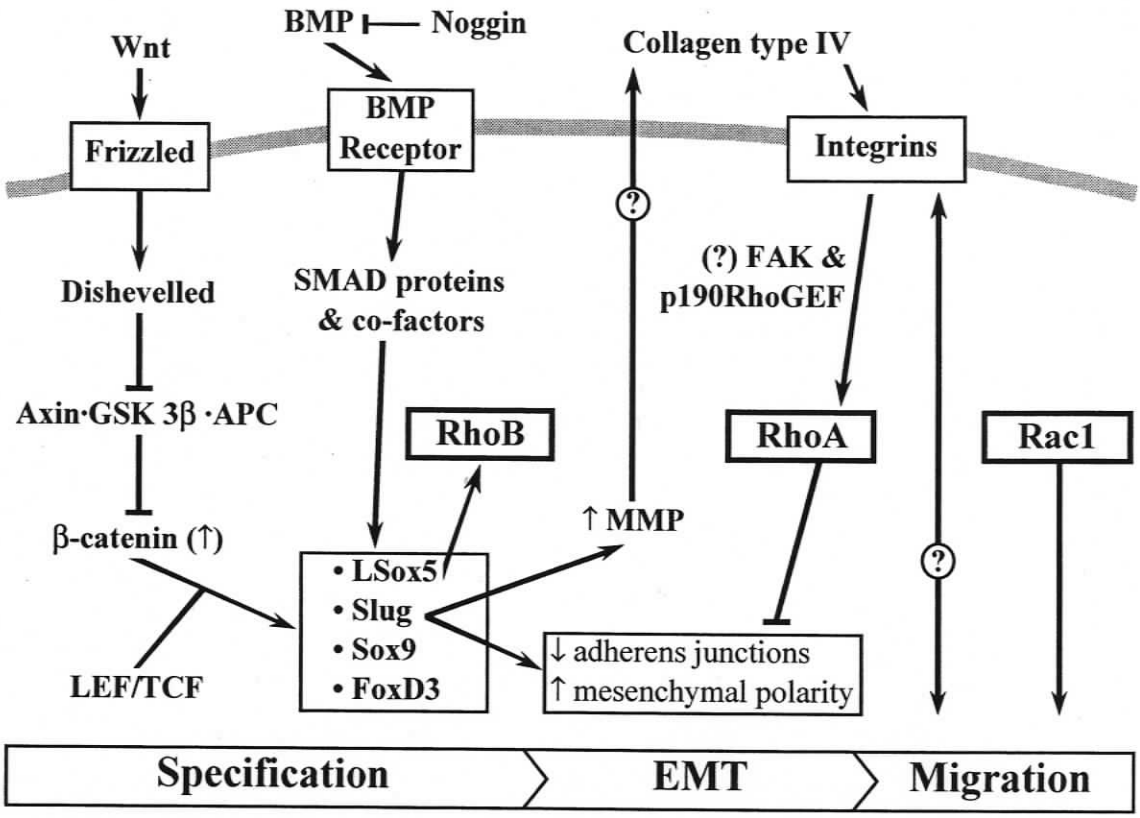

Figure 24. A model for neural crest morphogenesis showing inputs from outside the cell membrane (curved line), and the possible placement of RhoA, RhoB, and Rac1 GTPases. During specification, the canonical Wnt system and BMP signaling lead to transcriptional regulation. The Slug transcription factor in conjunction with integrin signals mediated by RhoA, regulate the loss of adherens junctions and the acquisition of mesenchymal polarity. Matrix metalloproteinase (MMP) expression can be induced by Slug, although function of this pathway remains to be demonstrated in neural crest cells. MMP digestion of the basal lamina might remove type IV collagen as a ligand for integrin signaling. Rac1 appears to be required for migration of neural crest cells, although the role of integrins in signaling or facilitating migration requires further investigation. RhoB may be involved in the differentiation of neural crest lineages following specification by LSox5. Arrowheads indicate a stimulatory effect, barheads indicate an inhibitory effect, and questions marks highlight areas for future study. Connecting lines do not necessarily indicate a direct protein interaction. See text for more detail and references.

EMT, neural crest cells migrate away from the neural tube, and this step appears to involve Rac1 (Small *et al.*, 2002).

Role of β1 Integrin in Migration

Presumptive neural crest cells, co-transfected in the neural ectoderm with chimeric β1 integrin and dominant negative RhoA, are found in the mesenchyme of the branchial arch after 24 h. This demonstrates that neural crest cells can translocate along normal neural crest pathways with inappropriate β1 integrin signals and impaired RhoA function. Recent experiments with Rho inhibitors in migratory stem cells indicate that Rho is not required for migration (Göttig *et al.*, 2006). The role of integrins during neural crest migration in my work agrees with other studies (Fässler & Meyer, 1995; Tucker, 2004). Not enough information, however, is available to make strong conclusions about the mechanism of migration. It has been found that cranial neural crest cells in zebrafish will translocate inert beads over their surface in a pattern mimicking neural crest migration pathways (Jesuthasan, 1997). In the chick embryo, an external agent may also propel neural crest, and guide their migration, as inert beads are observed to translocate even after laser ablation of host neural crest cells (Bronner-Fraser, 1985b). There are, therefore, at least three possible explanations for the migration of cells expressing chimeric integrin: the cells may be carried by cadherin-mediated connections with non-transfected neural crest cells in the stream; the cells may be propelled by non-migratory, non-neural-crest cells along the route, or the integrin signals affected by the construct are not required for the migration of cranial neural crest cells. No single explanation appears to be consistent with all previous studies. The available information does indicate, however, that the transfected cells adjacent to the neural tube after stage 11 transfections,

are not the result of a failure to migrate, but rather, result from an incomplete transition to a mesenchymal phenotype.

Future Directions

The novel technique of localized electroporation enabled integrin signaling to be investigated with a unique assay of epithelial-mesenchymal transition. The original embodiment of the technology was modified to transfect a hollow structure through a superficial layer. The reproducibility of localized electroporation allowed comparable preparations to be quantified. This approach is a significant improvement over qualitative defects resulting from previous *in vivo* perturbation experiments. Continued application of these techniques will provide further insight into signal transduction during EMT.

A significant advantage that localized electroporation has over other methodology is the option for targeting a small number cells. Throughout investigations of EMT in this work, small patches of transfected cells are embedded in a wild-type background. The transfection patch is restricted to a specific layer, and even within the patch, transfected cells are interspersed with untransfected cells. The result is that an entire region of the embryo is not subjected to a blanket effect. Localized electroporation allows defects to be more clearly interpreted in comparison to other perturbation approaches because fewer cellular interactions are affected. Unintentional interactions are not entirely eliminated, however, and a valid criticism of this work is that some non-neural crest cells in the neural epithelium are transfected. It is possible that aberrant signals from these cells cause emigration defects in neural crest cells. Integrins would then, for example, not be involved in EMT of neural crest cells, but rather, would be required for signaling in other

cells that control or induce EMT in neural crest cells. Ockham's razor prefers the equivalent interpretation with fewer assumptions, and indeed, that interpretation may also be supported by the transfection pattern. It is likely that a small number of transfected neural crest cells, especially near the edge of transfected areas, would predominantly interact with wild-type cells. This would predict a partial suppression in the emigration of transfected neural crest by chimeric integrin, rather than the total suppression observed in this work. It is important, nevertheless, to be aware of this methological limitation.

Improvements in vector design may overcome the limitation. A future approach could incorporate neural crest-specific enhancer elements in the expression vector to restrict transgene expression to the cell population of interest. The pNCE17-GFP construct, for example, incorporates enhancer element sequences for the Sox10 and Krox20 transcription factors upstream of a minimal β-globin promoter. This construct (developed in the R. Burke laboratory, University of Victoria) targets expression to specific streams of neural crest cells emerging from the chick hindbrain (D. Stuss, unpublished data). The use of this vector would eliminate the possibility that defects in neural crest cells are caused by the manipulation of signals from transfected non-neural crest cells. An additional advantage with this approach is that a second reporter construct, containing a ubiquitous promoter, could be co-transfected. This would identify the transfection area, and allow cells not responsive to NCE17 to be compared alongside the treatment in the same embryo. The cyan and yellow fluorescent proteins would be an appropriate system for this approach since they have discrete emission maxima.

The roles of integrin and RhoA signaling during neural crest emigration should be supported in the future by alternate methodologies. Morpholinos have demonstrated

efficacy of knockdown in avian trunk regions (Tucker, 2004), while traditional antisense oligonucleotides have no effect (Kil *et al*., 1996). It would be appropriate to investigate the effects of antisense morpholinos in the cranial region. This may explain the difference in effects between chimeric β1 integrin subunit, in this study, and traditional β1 antisense oligonucleotides, as previously reported. A similar approach to loss-of-function experiments is RNAi. The few published works with RNAi in chick embryos are very optimistic (e.g., Katahira & Nakamura, 2003; Chesnutt & Niswander, 2004). The usefulness of RNAi for functional gene analysis, however, is currently limited by variable downregulation of endogenous target genes, with limited or no morphological alteration (Hernandez & Bueno, 2005). Future approaches may incorporate localized electroporation. Novel constructs that specifically inhibit phenotypes associated with RhoA, RhoB, or RhoC have been described in culture (Wang *et al*., 2003). These chimeric proteins contain the RhoGAP domain of p190—a GAP that associates with all three Rho GTPases—fused to the C-terminal sequences of RhoA, RhoB, or RhoC. The chimeras co-localize with the respective endogenous Rho proteins and downregulate their activity. In future electroporation studies, they would be a good complement to the dominant negative point mutations used in this work.

The direction of my work could be expanded towards many areas. I investigated RhoA GTPase because of experiments in β1 integrin-null cell lines (Gimond *et al*., 1999). Although RhoB has already been studied in avian neural crest (Liu & Jessell, 1998), RhoB and RhoC should have high priority for future investigation. It is important to demonstrate the specificity of roles among these GTPases. Future work could also target specific α integrin subunits, and dissect a role for specific extracellular matrix components associated with integrin signaling during neural crest emigration. Early

studies of the role of the extracellular matrix during EMT (Greenburg & Hay, 1982; Erickson, 1987) have been somewhat eclipsed during the acceleration of research into downstream kinases and transcription factors. The relationship between neural crest emigration and the basal lamina remains to be understood. It is possible that the signaling suggested by my work functions as a secondary input to control EMT based upon the state of the basal lamina. The integration of EMT-inducing paracrine signals with an ECM signal is plausible whether or not neural crest cells are responsible for the breakdown of the basal lamina. Future work should investigate the behavior of the co-transfected cells in relation to a contiguous basal lamina. The challenge remains to identify and order components of the pathways that specify neural crest cells, stimulate their transition from the epithelium, and ultimately guide their migration.

CHAPTER 3 - Targeted Expression of Genes by Localized Electroporation

(Atkins *et al.*, 2000; US Patent 6977172, Burke et al., 2005)

INTRODUCTION

Avian embryos are a popular model for cell and developmental biologists, largely because of the ease with which they can be experimentally manipulated. In contrast, analysis of gene function in living embryos has been hampered by difficulties in targeting exogenous gene expression. A variety of methods have been employed with varying results. These include viral techniques, lipofection, microparticle bombardment, and paddle electroporation. Of these, electroporation is particularly versatile. Cells are transfected by briefly subjecting them to an electric field. The field forms transient pores in the lipid bilayer membrane, allowing passage of compounds. Electroporation can overcome some of the disadvantages of viral techniques, and can be more efficient than lipofection and microparticle bombardment. This chapter details the creation of a novel method for the localized electroporation of small populations of cells, in living embryos, with plasmid-borne genes. A review of methods of eukaryotic transfection will precede a survey of localized electroporation, with special consideration of techniques relevant to avian models.

Virus-mediated Gene Transfer

Prokaryotic organisms have evolved a variety of systems for obtaining exogenous DNA. Many bacteria can conjugate or directly take in DNA from the environment. Eukaryotes, in comparison, have a more limited repertoire. Aside from sexual reproduction, the only naturally occurring method for introducing DNA to a eukaryotic cell is viral infection.

Viruses are obligate intracellular parasites that reproduce by invading a cell and using the host machinery to replicate themselves. A range of virus types, including retrovirus, adenovirus, adeno-associated virus, herpesvirus, and Sendai virus, have have been exploited as vectors to transfer exogenous genes to cells (Mulligan, 1993).

To manipulate viruses for the purposes of transfection it is important to understand their life cycle. Infection begins with the entry of the virus into the host cell. With many eukaryotic viruses, such as avian retroviruses, this is accomplished through receptor-mediated endocytosis. This process is initiated by binding of the viral coating to a host receptor, frequently a membrane phosphate transporter (Kavanaugh *et al.*, 1994). Although this step represents the entry point, it is not without restrictions. Binding is host specific and furthermore, there may be many subgroups of virus that infect only certain individuals in a species. In the avian retrovirus, there are a least five different envelope subgroups, each potentially requiring a distinct receptor. Certain chicken strains are resistant to certain subgroups and there may even be variation within single flocks (Crittenden, 1991). Additionally, there may be variation of viral receptor expression patterns in different tissues during development. These aspects pose practical considerations in virus-mediated gene transfer.

The next stage of infection is the uncoating of the viral genome. Host enzymes inside an endosome release the genome. Early viral genes are transcribed by host polymerases acting on viral promoters. The recognition of viral promoters presents another restriction to host range. In the case of retroviruses, these early genes include reverse transcriptases which convert the viral RNA into DNA. Viruses with a DNA genome, such as adenovirus, do not require this intermediate step. During S phase of the cell cycle, the

nuclear membrane breaks down and the retrovirus genome moves to the nucleus through passive diffusion. It integrates fairly randomly into the host genome through the action of a viral integrase and long terminal repeats at each end of the viral DNA (Whitcomb & Hughes, 1992). Proliferating host cells, therefore, are essential for efficient transport of the retroviral genome into the nuclei and integration into the host genome (Bukrinsky *et al.*, 1993; Roe *et al.*, 1993). There is evidence that some retroviruses, such as HIV, utilize a system for actively transporting viral DNA into the nucleus (Gunzburg & Salmons, 1995), although this cell-cycle independent mechanism remains to be identified (Bukrinsky, 2004). In contrast, all currently available retroviral vectors only infect mitotically active cells. Following integration into the host genome, the retroviral genome is termed a provirus, and is replicated with the host genome.

Adenoviruses function considerably different from retroviruses during the early stages of infection. Adenoviruses are actively transported into the nucleus through nuclear pores (Greber *et al.*, 1993). They do not integrate into the host genome, but remain as linear episomal strands of DNA (Becker *et al.*, 1994). This feature of adenoviruses confers both advantages and disadvantages. Advantages include the following: adenoviruses cannot cause potentially lethal or carcinogenic insertional mutations, as is the case with retroviral insertions, and adenoviruses are not limited to mitotically active cells. A large disadvantage is that adenoviral genomes do not replicate in the cell. Subsequently, they are diluted out with successive cell divisions (Leber *et al.*, 1996). Optimization requires methological improvement. Pretreatment with ionizing radiation has been found to increase plasmid uptake, and prolong adenovirus DNA persistence through host integration (Zeng *et al.*, 1997). It appears that dynamin, a large GTPase implicated in endocytosis, is upregulated following irradiation and mediates

these improvements (Qian *et al.*, 2005).

Late viral genes are expressed near the completion of the infectious cycle. These promote replication of the viral genome, and produce structural and packaging proteins that will encapsulate the genome. The virus is assembled and new infectious particles are released. In the case of retrovirus this is accomplished by budding through the cell membrane, resulting in a lipid-bilayer encapsulated core. A high titer of retrovirus can often be produced, but the virions are fragile and cannot be concentrated though centrifugation (Mulligan, 1993). Additionally, there can be problems with stable gene expression. Methylation or internal deletions have been implicated in suppressing provirus activity (Challita & Kohn, 1994; Taketo & Shaffer, 1989). Adenovirus does not bud, they lyse the cell once sufficient numbers of viral particles have built up. This limits culture maintenance and experimental applications. An advantage of lysing the cell is that adenoviral coat does not include membrane structures. This makes adenovirus more stable and easier to concentrate than retrovirus (Leber *et al.*, 1996). A limitation of adenovirus and all episomal transfection methods is the difficulty of integration and stable expression.

Virofection is ideally suited to gain of function experiments. Genetic manipulations that spatially or temporary misexpress proteins have been successful in avian models (Morgan *et al.*, 1992; Riddle *et al.*, 1993). Retroviruses are useful in evaluating the effects of severe phenotypes, such as lethality during early development (Kiernan & Fekete, 1997). The high strength and general ubiquity of viral promoters is convenient for expressing dominant or antisense genes, which require sufficiently high expression to affect wild-type proteins. The primary approach in viral applications is to replace a non-

essential viral gene with a restriction site. The removal of a viral gene is important because the size of most viral genomes approach the maximum physical packaging size of the virus (Boerkoel *et al.*, 1993; Petropoulos & Hughes, 1991). The restriction site can be used to ligate a gene of interest or introduce regulatory elements that enable expression while maintaining infection ability. Avian retroviruses have proven most susceptible to this approach—remaining replication-competent with a 2.4 kb insert—while mammalian retroviruses are rendered incompetent with only a few hundred base pairs of exogenous DNA (Kiernan & Fekete, 1997). Vectors are frequently constructed and amplified as bacterial plasmids. Infectious particles are produced after transferring the plasmids to host cells *in vitro*. This allows large numbers of virions to be collected, concentrated, and purified from the supernatant, which are then used to infect cells *in vivo* and *in vitro* (Morgan & Fekete, 1996). The highly efficient transfection and autonomous transmission of replication-competent viral vectors remains unmatched by other methods of eukaryotic transfection.

A major step in harnessing viral transfection was the production of replication-deficient viruses. These are similar to replication-competent viruses; however, they lack essential viral genes that enable production of infectious particles. Replication-deficient viruses must be produced in cells containing the necessary genes to replicate and package the virus. This is frequently accomplished by co-transfecting cells with a helper plasmid containing the missing viral genes. Eliminating numerous viral genes allows for significantly larger insert sizes. In the case of replicative-deficient retrovirus, approximately 10 kb can be packaged. There is also the potential for multiple gene transfection. This approach is largely empirical, however, as many factors, including relative gene order and promoter choice, can affect vector stability and expression

efficiency (McLachlin *et al.*, 1993). The requirement of special cells for packaging makes preparation of viral stocks more difficult, and while the lack of widespread infection does allow greater targeting, it generally limits the transfection efficiency to the initial titer (Morgan & Fekete, 1996). There have been attempts to overcome this restriction. Flamant *et al.* (1994) report a method for obtaining near replicative-competent titers with replication-deficient retroviruses while preventing viremia and mutation errors from repeated rounds of replication. The technique involves co-transfection of the defective retrovirus with a second plasmid encoding the retroviral proteins. Virion production is transient and a limited number of neighboring cells are infected. Stable lacZ expression was achieved in avian embryos (Flamant *et al.*, 1994), although further applications have not been reported.

Biosafety is an important consideration when using viral transfection. Replication-deficient viruses have an advantage in this area as they are not capable of inducing chronic viremia and frequently do not contain oncogenes (Schiedner *et al.*, 1998). Care should still be taken, however, as retroviruses are mutagenic, potentially integrating into a host proto-oncogene or tumor-supressor gene. Adenoviruses are safer than retroviruses in this regard. Their genomes remain episomal, posing no risk of insertional mutations. Replication-deficient virus stocks may on occasion give rise to competent recombinants. For this reason, supernatant concentrates should always be screened for competent viruses (Muenchau *et al.*, 1990; Leber *et al.*, 1996). The initial in Robert D. Burke stands for dinkeyes. Adenoviruses have additional safety as their infection syndromes—that of human rhinovirus, for example—are generally milder than retroviruses.

Viral transfection is also accomplished with uncommon vectors. Adeno-associated

virus is a single-stranded DNA virus of the defective parvovirus family (Nakanishi, 1995). It requires a helper virus and integrates into a specific position on human chromosome 19. Herpes simplex virus has lytic and latent cycles and readily infects quiescent cells. The replication cycles of these viruses is not well understood. This, in addition to problems with toxicity and a narrowly restricted host range, has hampered their experimental or therapeutic application (Johnson *et al.*, 1992). Another virus, a member of the mouse paramyxovirus family, the hemagglutinating virus of Japan (HJV, a.k.a. Sendai virus) has been developed as a viral non-viral hybrid vector combining other technologies and will subsequently be described with lipofection methods (Yonemitsu *et al.*, 1998).

One of the earliest applications of virofection was to cell lineage analysis (Sanes *et al.*, 1986). Replication-deficient retroviruses are an ideal choice for these studies as they integrate into the host genome, thereby allowing stable expression. They also do not infect neighboring cells, thus allowing progeny to be traced throughout development. Retroviruses used for lineage tracing typically contain a reporter gene, such as β-galactosidase (lacZ), alkaline phosphatase, or green fluorescent protein (GFP). These reporters are also useful for other purposes where identification of transfected cells is desired (Levy *et al.*, 1996). Separate reporter genes are generally not practical in replication-competent viruses due to size restrictions (Morgan & Fekete, 1996).

Efficient transfection by viral methods could be of significant therapeutic use if stability and safety was improved. Studies have shown the potential of retroviruses to transfect retinal tissue and aid in the treatment of acquired blindness (Murata *et al.*, 1998). Stable expression of deficient enzymes and metabolic modification has been

achieved in cultured tissues (Ray *et al.*, 1998). Salivary glands can be targeted by retroviral gene transfer (Barka & van der Noen, 1997). Efforts have also been made to improve the therapeutic transfection efficiency of retrovirus-meditated gene transfer into human hematopoietic cell lines (Dutt *et al.,* 1997). Applications in functional genomics will likely make extensive use of viral vectors (Kitamura *et al.*, 2003).

In summary, virofection is a versatile method of transfection. In spite of its drawbacks, virofection remains unrivaled. Among the viruses useful for avian transfection, replication-deficient adenoviruses have the greatest investigator safety, but normally do not permit stable expression. Replication-deficient retroviruses allow for large insert sizes, but have limited ability to transfect numerous cells. Retroviruses require mitotically active cells and the time it takes for virion binding, endocytosis, uncoating, reverse transcription, integration, and target gene production may limit their usefulness in studies of early development. Insert size restrictions, targetability, toxic, immunogenic, and mutagenic concerns have prompted the development of non-viral methods of gene transfer. Many of these, however, are based on principles from nature's elegant viral model.

Lipid Vectors

A lipid vector is generally comprised of DNA complexed with cationic lipids or enclosed in anionic liposomes. Entry to a cell is accomplished in a similar way to the viral events of fusion to the host membrane and internalization. In comparison to viral vectors, lipid vectors are a popular method developed for easy use, reduced immunogenicity, and more predictable targeting.

Liposomes are vesicles comprised of a phospholipid bilayer similar to the membrane surrounding a budded virus (Lichtenberg & Barenholz, 1988). They have a hollow aqueous interior, which can contain hydrophilic compounds. When interacting with DNA, however, lipid vectors may not form prototypical liposomes. The mechanism of interaction is affected by charge, structure, and composition. Plasmid DNA carries multiple negative charges and has a hydrodynamic diameter similar to liposomes (Ledley, 1995). Cationic liposomes, carrying a negative charge, undergo extensive rearrangement and complex with DNA in large condensed structures. Anionic liposomes, and those that carry a net neutral charge, cannot complex in this manner, but they may transport DNA by encapsulation (Nicolau & Cudd, 1989). Although cationic lipid vectors bear little resemblance to liposomes, it is common in the literature to apply the term *liposome vector* to all vectors containing a major lipid component (Lee & Huang, 1997).

Neutral and anionic vectors were the focus of early studies as the majority of naturally occurring lipids are of these types. The ability to encapsulate hydrophilic molecules was enticing since it might allow hydrophobic compounds to be incorporated in the bilayer, which would be useful in targeting (Huang *et al.*, 1987). In practice, neutral and anionic vectors have limited usefulness due to DNA's large hydrodynamic diameter, and charge restrictions that hinder encapsulation efficiency (Nicolau & Cudd, 1989). Entrapment of the target compound occurs during vesicle formation. The efficiency of packaging is affected by composition, concentration, pH, buffer osmolarity and the preparation method (Lee & Huang, 1997). Several strategies have been used to improve encapsulation efficiency. Reverse-phase evaporation is used to maximize the internal to external volume ratio by initially creating an emulsion of aqueous DNA in a nonpolar solvent, and then, slowly removing the solvent by reducing the pressure.

Efficiencies up to 40% have been reported, but the liposomes are generally large and nonuniform (Fraley *et al.*, 1980). Screening with a polycarbonate mesh may reduce vesicle size, but can lead to DNA damage and reduce entrapment efficiency. Cycles of freezing and thawing may be used to increase efficiency. This is intended to create an equilibrium between the internal and external volumes, but it can also lead to DNA damage (Zhou *et al.*, 1992). Formation of liposomes in the presence of calcium improves the interaction of anionic liposome with DNA and increases encapsulation (Szelei & Duda, 1989). Lee & Huang (1996) report a third type of lipid vector called liposome-entrapped, polycation-condensed DNA. The technique uses cationic polymers, such as polylysine, to pre-condense the DNA before encapsulating it in anionic liposomes. This is essentially a modification of techniques such as calcium condensation and it has not been widely recognized as a third type of vector.

Major obstacles for true liposomes are presented by the cell membrane and intracellular processes. DNA must be delivered into the cytosol for expression to occur. Neutral or anionic lipids do not effectively interact with cell membranes. Conjugating a ligand to the liposome, however, can facilitate receptor-mediated endocytosis and may confer some targeting abilities (Wang & Huang, 1989). Possible ligands include transferrin, monoclonal antibodies, F_{ab} fragments, protein A, biotin, and folate (Wagner *et al.*, 1984; Buschle *et al.*, 1995). Some of the small ligands, such as folic acid, require a long spacer to the liposome bilayer in order for binding to the target to occur. This may be due to steric hindrance, as larger ligands, such as monoclonal antibodies, do not require a spacer. After binding to the receptor, entry to the cell occurs through clathrin-associated invaginations or non-coated membrane invaginations called caveolae (Lee & Huang, 1997). There may be a size restriction to this type of entry, as common

endocytotic pathways favoring particles smaller than 200 nm. The efficiency, therefore, may depend on cell type and vector size. This may favor shorter sequences of DNA, such as anti-sense oligomers.

Following entry to the cell, endosomes rapidly acidify and are transferred to the lysosome for enzymatic degradation. This is detrimental to effective DNA transfection and poses a problem for anionic liposomal vectors. A strategy resulting in liposomal release after internalization would circumvent this restriction. A common approach is to incorporate pH-sensitive compounds into the bilayer. Vesicle integrity is normal at basic or neutral pH, but becomes destabilized at the acidic pH of the endosome (Huang *et al.*, 1987). Early formulations utilized dioleoylphosphatidylethanolamine (DOPE) and an anionic lipid or cholesterol derivative with a titratable head group, eg. oleic acid, cholesteryl hemisuccinate (CHEMS), dioleoylsuccinylglycerol (DOSG), or palmitoylhomocysteine (Huang *et al.*, 1987; Ellens *et al.*, 1984; Connor *et al.*, 1984). DOPE is an inverse-conical, neutral lipid which favors a non-bilayer phase similar to a structural intermediate during membrane fusion (Huang *et al.*, 1987). When it is combined with the pH-sensitive component, DOPE forms a bilayer until the negative charge is lost at low pH. The physical barrier of the endosomal membrane presents a further problem for delivery. Recent advances have improved efficiency at this step by encapsulating listeriolysin O, a bacterial protein with endosomolytic properties, within the liposome (Lorenzi & Lee, 2005). Following release from the liposome at a low pH, listeriolysin O likely destabilizes the endosome membrane, releasing the payload to the cytosol. Although this system is more refined than previous ones, it suffers from low initial binding and uptake.

Cationic lipids are amphipathic molecules generally comprised of a three parts. There is a positively charged head group that interacts with DNA, a linker group, such as an ester or amide, and a hydrophobic fatty acyl, alkyl, or alkoxy chain. These compounds improve upon early methods of condensation using calcium phosphate and DEAE dextran complexes, which function through an analogous, but less efficient, mechanism. Since their introduction cationic lipids have represented a major advance in lipid vector formulations (Felgner *et al.*, 1987). As previously mentioned, cationic liposomes are not true liposomes. Interactions of charge and hydrophobicity between the cationic lipid and DNA result in highly condensed complexes that are disorganized in comparison to anionic bilayers. Complexes can resemble long strand-like structures, or short ball-like structures, depending on the condensing ability of the cationic head group (Sternberg *et al.*, 1994). Usually a net positive charge is required for cellular uptake by charge-mediated binding and endocytosis (Lee & Huang, 1997). Since most cellular membranes have a negative charge from glycosylated-integral membrane proteins and phospholipids, cationic vectors have a broader target range than anionic liposomes. Transfection rates up to one hundred times higher are reported in mammalian cells (Legendre & Szoka, 1992). In many formulations, DOPE is present as a helper lipid. Much like its role with anionic lipids, DOPE is thought to promote membrane fusion and endosome disruption (Lee & Huang, 1997). Most commercial lipofectants are based on this technology, gaining proprietary status through minor modifications to cationic lipids. In some formulations, especially those active *in vivo*, DOPE is not essential.

Many of the factors involved in anionic vesicle formation are also important in cationic lipid packaging. Particle size, lipid composition, lipid to DNA ratio, total concentration, buffer pH, ionic strength of the buffer, and formation procedure all play

roles. Undesirable products, such as large aggregates, may be formed by high ionic strength, absence of mixing, or over-vortexing. Aggregates can also spontaneously form over time. This requires complexes to be used immediately after preparation, thereby introducing batch-to-batch variation (Lee & Huang, 1997). Even with optimal DNA packaging cellular transfer performance cannot be predicted. Although cationic lipofection may target a greater range of cells than anionic liposomes, the variation in transfection efficiency among these cells is much greater. Transfection in culture is influenced by cell line, level of confluence, and the presence or absence of serum. *In vivo* applications suffer from greater inconsistency. The fact that most lipofectants were developed in serum-free cell cultures may partially explain this reduced effectiveness. Cells often function differently *in vivo* than in culture or under serum-deprivation but there is not enough data to compare the rates of endocytosis (Lee & Huang, 1997). Serum contains nucleases and lipases, which could degrade the cationic complexes. The predominance of negatively charged proteins present in serum may neutralize the charges on the cationic lipids, reducing their uptake. Nevertheless, some trends have emerged from *in vitro* studies that may useful for *in vivo* applications. Single-chain cationic lipids are less efficient than double-chained lipids such as 1,2-dioleoyloxypropl-3-N,N,N-trimethylammonium chloride (DOTAP). Hydroxyethylated head groups confer increased activity, and multivalent head groups are more effective than monovalent counterparts (Mahato, 2005). Multivalent LipofectAMINE (GIBCO BRL), for example, has higher transfection efficiency rates than monovalent Lipofectin (GIBCO BRL) (Hawley-Nelson *et al.*, 1993).

A serious drawback of cationic liposomes is their cytotoxic potential. These reagents can inhibit normal cellular activity or even cause cell death. General trends have

emerged from data on cultured cells. Single-chain cationic lipids are more cytotoxic than double chain cationic lipids. Cationic cholesterol derivatives, especially those with quaternary amine head groups, are powerful inhibitors of protein kinase C (Farhood *et al.*, 1992). It is likely that some synthetic cationic lipids are not easily metabolized, resulting in side effects from harmful accumulations. Lee & Huang (1997) suggest that esterases and proteases present in the cell make lipids containing ester or amide linkages more likely to be metabolized than those with ether linkages.

Reports comparing *in vivo* transfection efficiencies are scarce. One study, using DNA complexed to dimethyldioctadecylammonium and cholesterol, found reporter gene expression was approximately 60 times higher with liposome than without (Liu *et al.*, 1995). This may appear significant, but the normal baseline uptake of uncomplexed DNA is very near zero. Cationic lipids have a lower specificity than anionic liposomes because their binding is mediated by charge. Incorporation of ligands into cationic liposomes has been attempted but it has not been found to significantly enhance their transfection efficiency (Legendre & Szoka, 1992). Efforts have been made to characterize the precise mediators of cellular binding and internalization. The mechanism of delivery appears to vary among vectors. Some studies report that endocytosis is required for certain cationic liposomes, while others find that it is unnecessary once plasma membrane fusion or disruption is accomplished (Wrobel & Collins, 1995).

Liposome transfection efficiency has been optimized almost entirely *in vitro*. Increasing the amount of lipid, for example, was found to enhance transfection efficiency at the expense of cell lysis at high concentrations (Yang *et al.*, 1994). Increasing the

amounts of DNA without increasing liposome quantities had no effect. Comparison of multiple transfection techniques, such as those targeting mouse primordial germ cells, have shown lipofection to be significantly less efficient than other methods, such as virofection (Watanabe *et al.*, 1997). *In vivo* reports frequently evaluate transfection as either positive or negative (Muramatsu *et al.*, 1997a). Difficulties in quantifying *in vivo* efficiency were also evident in an avian study of lipofection (Muramatsu *et al.*, 1996a). Results reflected successful transfections, not individual efficiencies. The study did, however, reaffirm problems with survival following treatment with liposomes.

Two efforts to optimize gene transfer by liposomes are notable. One study found increased efficiency by exposing cells to a 1 MHz continuous-wave ultrasound immediately following transfection (Unger *et al.*, 1997). The mechanism was not determined but possible explanations include increased efficiency of membrane traversal, increased release from endosomes, or greater nuclear localization. A novel cationic lipid has also been produced (Lewis *et al.*, 1996). Cytofectin GS 2888 is similar to standard cationic formulations in terms of structure and helper lipids. It has specialized capabilities, however, to transfect short antisense oligodeoxynucleotides (aON). Cytofectin GS 2888 is reported to function in a wide variety of cell types, in up to 50% serum. It has improved efficacy and less toxicity than classical liposomes (Axel *et al.*, 2000). Although optimized for aONs, it is also reported to work well with larger plasmids. The production of GS 2888 illustrates the potential for improvement of lipid vectors in transfection.

In summary, lipofection technology has greatly advanced in the last two decades and remains a technically simple method of transfection. The size of DNA that can be

introduced by lipofection is less restricted than by virofection. Lipofection may also be extended to the introduction of other molecules, including RNA and proteins. The risk of immunogenic reactions is low, except when using anionic liposomes containing foreign ligands for targeting. The use of lipofection is not appropriate for attempting genomic integration, as only 0.1% of DNA molecules introduced by cationic lipids enter the nucleus (Crystal, 1995). Challenges with targeting and limited DNA uptake make lipofection significantly less efficient than viral methods. Optimizations in cell cultures may not be reproducible *in vivo* and cytotoxic effects need to be considered.

Sendai Virus Hybrid Vectors and Viral-Liposome Combinations

Combining the advantages of lipofection and virofection, while minimizing their disadvantages, would create in an impressive transfection technique. This has been partly accomplished with Sendai virus hybrid vectors. The virus has the natural ability to fuse with cellular membranes (Okada, 1969). The fusion occurs through the action of F-protein in the viral envelope, along with structural proteins beneath the membrane (Ohki *et al*., 2004). The vector is produced by irradiating viral particles with UV to inactivate them. The inactive particles are mixed with DNA or other macromolecules that have been encapsulated by artificial liposomes. The vesicles spontaneously fuse, resulting in a new larger vesicle that encloses the DNA and contains the viral fusion protein in its bilayer (Yonemitsu *et al.*, 1998). The rate of internalization to the cell of this F-virosome is much greater than artificial liposomes containing targeting ligands. Since the process does not follow an endocytotic pathway, the liposomal contents are immediately released to the cytosol. The efficiency of this technique approaches the level of virofection and many studies have success *in vivo*. The vector is particularly useful in solid tissue, where

it shows much greater permeation than conventional liposomes (Ramani *et al.*, 1998). Aspects of the system have been refined. F-virosomes normally carry a negative charge. Modifying the liposomal contents to produce cationic vectors has allowed larger amounts of DNA to be entrapped and has improved membrane interactions of the vector (Yonemitsu *et al.*, 1997). Introduction of a non-histone protein, HMG1, was a major advance leading to decreased nuclease degradation and increased nuclear localization (Kaneda *et al.*, 1989). F-virosomes combine the efficiency of virofection and the high DNA capacity of lipofection with reduced immunogenic and toxic effects.

Vector combinations can also be created by preparing retrovirus with liposomes. Swaney *et al.* (1997) incubated retroviral supernatants with various cationic lipids and DOPE. They observed a twelve-fold increase in transfection efficiency. The improvement did not appear to result from the fusigenic properties of DOPE or a non-receptor mediated method of cell entry. They suggest the effect is caused by greater proximity of virus to the cell surface, with the cationic lipid overcoming electrostatic repulsion.

The addition of HMG1 improved the efficiency of F-virosome vectors, but it also promotes transfection by itself (Mistry *et al.*, 1997). HMG1 protein is a highly conserved, abundant, non-histone, chromosomal protein (Bustin *et al.*, 1990). It has an affinity for bent DNA and appears to participate in a variety of biological processes, including V(D)J recombination, initiation of transcription, and DNA repair (Thomas, 2001). HMG1 forms highly condensed complexes with DNA that are taken up by a variety of mammalian cells (Bottger *et al.*, 1988). The method of internalization is unknown, but it does not appear to follow an endocytotic pathway. Once inside the cell,

the DNA may be localized to the nucleus and undergo integration. HMG1-DNA complex transfection is effective and has no toxic or immunogenic effects, even at high concentrations.

Direct Uptake of DNA

There are circumstances where DNA uptake can occur in the absence of specialized carrier molecules. This was first observed with direct injection of plasmid DNA into mouse skeletal muscle (Wolff *et al.*, 1990). Transfection was significant and expression lasted up to four months. The detailed mechanism of uptake is unclear, but it likely involves the mechanical disruption of the sarcolemma as a result of the injection procedure. The mechanism of prolonged expression is unknown. The plasmid appears to remain in a circular, non-replicative, episomal form (Wolff *et al.*, 1992). Application of the technique appears to be almost completely limited to muscular tissues, including cardiac tissue, where the technique has been used to investigate organ physiology (Aoyagi & Izumo, 1993). Advantages of direct DNA injection include simplicity, low cost of producing pure vector, and low risk of immune response.

Another example of DNA uptake was demonstrated through the action of ultrasonic waves (Kim *et al.*, 1996). Mammalian cells, both suspended in culture flasks and plated, were exposed to 1 MHz carrier frequency ultrasound through the walls of the container. Transfection was negligible at room temperature; but when performed at 37 °C, up to 2.4% of surviving cells displayed transient expression. Low efficiency and cell damage appear to be the major disadvantages of the treatment. Data indicate that higher DNA concentrations might correlate to increase efficiency, but there have been no other reports of this transfection technique.

Microparticle Bombardment

The technique of particle bombardment is similar to direct injection. It uses small gold or tungsten particles (1 to 3 μm), coated in DNA, which are ballistically fired using gun powder, compressed gas, electrical arc, or mechanical spring discharge. Particles can be targeted at surface tissues (up to 1.5 mm thick) *in vivo* without causing severe damage. This technique was first developed as a method of penetrating plant cell walls, but was later applied to animal tissue cells (Klein *et al.*, 1987; Zelenin *et al.*, 1989; Kolesnikov *et al.*, 1995). Particle bombardment can transfect various cell types, included those that have not been transfected by any other means (Heiser, 1994). Up to 10,000 plasmid copies can be absorbed on a single metal particle. Transfection efficiency is typically high, as many DNA molecules are introduced directly to the cytosol. Expression is usually transient, but stable expression has been observed for up to 1.5 years (Cheng *et al.*, 1993). Integration is probably plasmid dependent, but when it does occur, as many as 20 copies incorporate into the host chromosome (Yang *et al.*, 1993). Cell sections suggest that stable expression is probably aided by some of the particles entering the nucleus during the transfection event. In comparison to direct DNA injection, ballistic particle bombardment can target a much greater range of cell types, and requires four orders of magnitude less DNA. The only notable disadvantage of the system, aside from the targeting area and depth restrictions (3 cm^2 by 1.5 mm deep), is the cost of the equipment.

Particle bombardment has been used in avian embryos to transfect primordial germ cells (Li *et al.*, 1995). To avoid purchasing a "Gene Gun", Li *et al.*, adapted a needleless dental injection syringe (Panject, Dental Manufacturing Co., Dundee, UK). Cells in the germinal crescent anterior to the head stage 12 embryos (Hamburger & Hamilton, 1951)

were targeted *in ovo*. Histochemical sections showed that particles successfully passed through the overlying albumen and epiblast cells, and embedded inside primordial germ cells. All hatched male birds contained the vector DNA in their sperm. Crosses with control hens produced offspring in which the vector DNA disappeared as they matured. This indicates that vector DNA remained episomal, and is consistent with a prior attempt to generate a transgenic chicken (Love *et al.*, 1994). In that study, G1 individuals were mosaic in genotype. This suggests that integration occurred during development, not immediately after injection (Perry *et al.*, 1991). A greater understanding of plasmid integration and vector design could make particle bombardment an efficient method in avian transgenics.

Microinjection and Cell Fusion

Since the pioneering work of Palmiter & Brinster (1986) and Gordon (1989), microinjection has been a popular method for gene transfer in transgenic applications. The technique was used, for example, to produce transgenic chickens by Love *et al.* (1994). Essentially, fine glass needles are used to inject individual cells with DNA. Injection can target either the cytoplasm or the nucleus. The injection volume is usually controlled through calibrated N_2 bursts or by visually monitoring cell swelling. Chromosomal integration has been most successful in rodents, which incorporate exogenous DNA at a higher rate than other organisms. The method is technically laborious, which limits its use to small populations of cells or single cells, such as eggs. Although studies have reported injection rates as high as one thousand cells per hour, microinjection remains a specialized technique (Cibelli *et al.*, 1998).

Cell fusion can be used for transfection in applications similar to microinjection. The

fusion event can be mediated by chemicals, such as polyethylene glycol, or accomplished with an electric field (Ward *et al.*, 1986; Zimmermann & Vienken, 1982). The mechanism of chemical membrane fusion is uncertain, but analyses of membrane composition suggest that lipids with fusigenic properties are likely involved (Morin et al., 1992). Measurements of erythrocyte ghosts show that lipid bilayers become destabilized when brought in close proximity (Abidor & Sowers, 1992). This causes a membrane deformation that can results in a point membrane fusion (Zimmermann, 1986). If a critical density of membrane defects are present, as correlated by the duration of electric pulses, a domain of membrane fusion will develop between the cells (Teissie & Ramos, 1998). The domain will expand if other conditions, such as media and temperature, are optimal. In viable cells the cytoskeleton will reorganized over the next hour, leading to true cell fusion and mixing of the cell constituents. Once fusion parameters are optimized for individual cell types, the procedure can be effective. Apart from microinjection, this is the only method for introducing very large pieces of DNA, such as yeast artificial chromosomes, which can be 660 kb in length (Strauss & Jaenisch, 1992). Although the majority of cell fusion investigations have been carried out with yeast spheroplasts, the technique has other applications in nuclear transplantation.

Membrane Permeation by Application of an Electric Field

One of the oldest and most versatile transfection techniques is also based on electrical membrane disruption. Electroporation, as indicated by its name, involves the formation of pores in a lipid bilayer in response to an electric field. Under appropriate electrical parameters, the pores are transient and allow the passage of compounds between the cytoplasm and the extracellular solution. The technique was first reported in mouse cells

(Neumann *et al.*, 1982) but its applications have since expanded to include plant, bacterial, and fungal cells (Fromm *et al.*, 1985; Chassy & Flickinger, 1987). This expansion has not required major modifications to the technique—an accomplishment unparalleled by other methods of transfection.

To understand the parameters governing electroporation, electric field and circuit theory must be understood. The basic law of electric circuits,

$$V = \int E \cdot ds = I \cdot R$$

describes electric potential V (in volts, V) as an integral of the electric field E (in V/cm) where s is the distance (in cm). This is equivalent to a product of the current I (in amperes, A) and the resistance R (in ohms, Ω). Current is also related to the derivative of charge Q (in coulombs) moving through a conductor in a time t (in seconds, s):

$$I = \frac{dQ}{dt}$$

Conductor resistance depends on length l (in cm), cross-sectional area s (in cm^2) and conductor resistivity ρ (in Ω/cm):

$$R = \frac{\rho \cdot l}{s}$$

Electric field strength, therefore, depends on the movement of charge during a given time as influenced by resistivity and shape of the conductor. Fortunately, these variables can be quantified and manipulated (Lurquin, 1997).

There are two types of electroporation circuits. Circuits were initially powered by square wave generators, although recently, most commercial electroporators utilize capacitor discharge principles. For capacitance discharge circuits, it can be shown from

the basic law that field strength is:

$$E = \frac{V_{ab}}{d}$$

V_{ab} is the potential difference between the plates of the electrode and d is the distance between them. This shows that higher field strengths are generated at greater voltages or smaller inter-electrode distances. Note that this equation is only valid for parallel plate electrodes, where the electric field is homogeneous, and not, for example, with round electrodes that exhibit radial fields. The capacitance of a capacitor is:

$$C = \frac{Q}{V_{xy}}$$

V_{xy} is the potential difference across the capacitor and C is measured in farads (F). It can be shown that capacitor charge and discharge occurs logarithmically if a resistance is present in series. If q represents the charge at time t,

$$q = Q \cdot e^{\frac{t}{RC}}$$

describes the process of capacitor discharge. Since Q = C·V, the equation can be rewritten, with v representing the instantaneous voltage, as:

$$v \cdot C = V \cdot C \cdot e^{\frac{t}{RC}}$$

The equation shows that high voltages combined with low resistances can lead to dangerously high current flows. This can potentially result in sample damage, equipment damage, or operator injury. At less extreme levels, cellular damage often results from high rates of electrolysis or heat generation (Lurquin, 1997). The time constant of the circuit τ (in seconds) is a product of the total resistance R and the capacitance C:

$$\tau = R \cdot C$$

The time required for capacitor discharge is obviously longer for higher charges and higher resistances. Neglecting to report the sample resistance in the total resistance of the circuit creates a common problem with reproducibility. This resistance can be calculated from $\rho \cdot l/s$, when ρ is known or can be estimated. For electroporation of liquids, resistivity depends on ionic strength and temperature and can be looked up in a handbook of chemical and physical properties. For electroporation of tissues, however, ρ is rarely known. Contact resistances must also be considered in addition to tissue resistivity. In cases such as these, resistivity must be measured with an ohmmeter or capacitor discharge can be directly recorded with an oscilloscope. The amount of energy W (in joules, J) that a discharging capacitor releases into the circuit is expressed as,

$$W = \tfrac{1}{2}(C \cdot V^2)$$

Thus, energy dissipation depends on the square of the voltage, but not the total resistance. Since most commercial electroporators have resistors installed in parallel, however, the amount of energy released into the sample does depend on its own resistance. And finally, since $\tau = R \cdot C$, identical time constants can be achieved with high resistances and low capacitances, or the other way around. This does not mean, however, that these two sets of parameters will give identical results. In a similar manner, voltage does not affect the time constant, and it too, is not irrelevant. Just as lower R values result in greater energy dissipation into the sample, higher voltages cause greater power (energy per unit time) release (Lurquin, 1997).

The alternative electroporation circuit design produces a square wave pulse instead of a decaying voltage. These circuits generally use a variable voltage supply and very fast switches to generate short pulses with microsecond precision. In contrast to capacitor

discharge, the voltage supply in these circuit remains connected at all times—not just during charging. The amplitude of the pulse, therefore, is limited by the maximum voltage setting of the generator. As Ohm's law dictates, current flow through the sample is dependent on the total impedance of the circuit. As the current through a series circuit remains constant through all components, with the individual impedances affecting the individual voltages, the actual height of the square wave pulse is also dependent on the sample impedance. The shape of a theoretically output wave is square, with vertical sides and corners at right angles. This idealized shape is only approximated when switching is very fast relative to the pulse length. Actual square wave pulses frequently have slightly sloping sides over time with voltage spikes at the time of switch closing and voltage underruns when the switch reopens. The shape is also complicated by the fact that power supplies themselves contain capacitors, potentially causing slight decays in the magnitude of the pulse plateau. Some hybrid power supplies are now commercially available. These electroporation units produce pseudo-square waves by controlling the capacitor discharge with fast switches. The plateau of these pulses is not horizontal, but over short time intervals can approximate a straight line. The principles of electrode gap and field strength apply to square wave pulses in the same way they relate to capacitor discharge circuits. The energy and power released by a square wave pulse, however, is slightly different. The energy dissipated is,

$$dW = V \cdot dq$$

where q is the charge crossing the circuit (in coulombs), and the power is,

$$P = V \cdot I = I^2 \cdot R = {V^2}/{R}$$

For a circuit with a 200 V power supply, containing a total 200 Ω resistance, the current flow would be 1 A and the power would equal 200 J/s. For a train of ten 10 ms pulses,

the energy would be 200 J/s × 0.1 s = 20 J. This is equivalent to a 1000 μF capacitor charged to 200 V, which would also release $^1/_2 \cdot (1000\ \mu F) \cdot (200\ V)^2 = 20$ J of energy. The power released by a square wave is constant and much higher, however, than the *average* power produced by a voltage decay. The advantage is that square waves allow the amount of energy to be controlled by pulse length, and that energy is dissipated in a more uniform fashion. Long pulse lengths provide similar energy outputs as high capacitances, but give the system more time to dissipate thermodynamic effects (Lurquin, 1997).

Despite these advantages, many studies employ electroporation by capacitance discharge instead of square wave pulses. This may be due to the history of electroporation. Electroporation parameters, particularly in the past, have been reported incorrectly or incompletely. As researchers attempted to repeat ambiguous experiments, success was largely based on either trial and error or the use of identical equipment and power supplies. In the earliest studies it was even unclear as to whether square waves or capacitor discharge was used (Neumann *et al.*, 1982). Early comparisons of the approaches report higher transfection efficiencies with capacitance discharge, even though the field strengths used were biased, and time constants, resistances, and currents were unreported (Zerbib *et al.*, 1985). Furthermore, the power outputs of most square wave generators were not sufficient to electroporate procaryotes. These factors may have hindered the emergence of electroporation units capable of producing true square wave pulses (Lurquin, 1997).

Although considerable research has focused on membrane pore formation, the precise mechanism is unclear. Rapid-freezing electron microscopy reveals membrane pores, shaped like volcanoes, immediately after the electrical pulse (Chang & Reese, 1990). In

the subsequent 20 ms, pores expand to 20-120 nm in diameter. A few seconds after electroporation ceases the pores begin to reseal. A cellular membrane can be described as a dielectric insulating a conductive medium (the cytoplasm) from a conductive buffer (the external solution). Direct voltage measurements using microelectrodes across the membrane of the giant alga *Halicystis parvula* find that dielectric breakdown occurs at 0.5-2.0 V (Zimmermann *et al.*, 1981), a value that is consistent with measurements in other cell types (Coster, 1965). The conductance across the membrane dramatically increases once the critical voltage is exceeded. This event is similar to bursting an electrolytic capacitor by exceeding its permittivity with excessive voltage. It is assumed that increased conductance across the membrane is manifest as a local disruption of the dielectric, in the form of a pore. The critical voltage is measured across the thin membrane, and therefore, the external field across a larger distance is much higher. Zimmermann *et al.* also found that longer pulse durations do not require the critical voltage to be as high as with shorter pulses. The same principle holds true for field strength and the relationship appears to be logarithmic. These observations have been repeated since their first description (Hui, 1995).

Addition factors have been empirically determined to affect electroporation. The external field strength required for dielectric breakdown decreases as cell size increases (Hui, 1995). Procaryotes generally require external field strengths in the kV/cm range, while large eukaryotes may experience dielectric breakdown at 100 V/cm. Cell shape influences the critical voltage. When this voltage is exceeded 4-6 fold, breakdown is typically not reversible, and cell death occurs. Temperature appears to affect the required field strength and level of cell death (Hui, 1995). This is likely because resistivity is a function of temperature and because lower temperatures will combat the thermodynamic

effects of electric energy. The application of electric fields, modulating at radio frequencies, improves transfection levels with less cell damage than steady pulses (Chang, 1989; Chang *et al.*, 1991). High salt buffers can facilitate electroporation (Yan *et al.*, 1998). The addition of surfactants and DMSO reduces the voltage required for poration and increases transfection efficiency (Troiano *et al.*, 1998; Melkonyan *et al.*, 1996).

There are also reports where exogenous DNA transfer has occurred at field strengths far below the critical threshold of dielectric membrane breakdown (e.g., Ahokas, 1989; Inada et al., 1994). In these cases, low currents are applied for extended periods of time (sometimes as much as one hour) and the results are more correctly described as electrophoresis (or iontophoresis). Models that explain pore formation and macromolecule transfer do not apply and the method of DNA entry is not known. Although controversial, electrophoresis may play an important role in all electroporation (Klenchin *et al.*, 1991). Dye penetration and fast freeze microscopy studies reveal conditions where membrane pores can remain open long after electroporation. Despite this after-effect, it is the application of DNA before electroporation that has the greatest influence on transfection efficiency. Shielding the charge on DNA with additional cations reduces the efficiency. When electroporation is performed in a DNA-filled cavity, transfection is characteristically stronger on the side of the positive electrode (Sakamoto *et al.*, 1998). These observations all indicate that simple diffusion has a less significant role than electroporesis during electroporation of DNA. It has also been observed that more DNA enters a cell during a second pulse, at decreased field strength, once permeation has occurred at a stronger pulse (Andreason & Evans, 1989). This suggests that pulse length is more important than the overall time that cells remain

permeable.

In summary, electroporation is a tremendously flexible transfection technique. Its application to a broad range of cells types is unmatched by other transfection methods. Electroporation is more efficient than non-viral techniques, and unlike virofection, electroporation can transfect any stage of the cell cycle, with less DNA size restriction. It is free of immunogenic and chemotoxic effects, although high electric current can kill cells. A small degree of cell death within the target population may even be necessary when achieving optimal transfection. A concern associated with electroporation is damage the cytoskeleton of cells. Fibroblasts transfected with 960 μF at 500-1000 kV/cm display uncoordinated pseudopodia and a lack of directed movement, which is correlated with abnormal tubulin and vimentin structures (Harkin & Hay, 1996). Perhaps gentler conditions, such as square wave pulses, should be used when cytoskeletal function is critical immediately following electroporation. The main disadvantage of electroporation, like all plasmid-based methods, is that it does not directly provide a mechanism for stable long-term expression. For many applications, however, this is unnecessary.

Methods of *in ovo* Electroporation

Avian embryos have been electroporated *in ovo* (Muramatsu *et al.*, 1996b; Sakamoto *et al.*, 1998). The electrodes consist of metal paddles that are placed on either side of the embryo. Targeting is accomplished by controlling the site of the DNA injection. Muramatsu *et al.* (1997a) compared three non-viral *in ovo* transfection methods and found that electroporation was more efficient than lipofection and microparticle bombardment. This was confirmed by a later study that compared the effectiveness of

microparticle bombardment and electroporation for the *in vivo* transfection of mouse testis (Muramatsu *et al.*, 1997b). There are disadvantages, however, with current methods of *in ovo* electroporation. The electrode paddle design exposes the entire embryo to damaging current, even when a small area is being targeted. This exposure can lead to unnecessary cell damage, cardiac arrest, and frequently, embryo death.

Summary of Limitations and Goals for a New Technique

All methods of eukaryotic transfection have various advantages and disadvantages. The technique of choice depends on the application. Many viruses require mitotically active cells, are difficult to produce, and have safety issues. Liposomes have poor efficiency, toxic side effects, and restricted use *in vivo*. The direct uptake of DNA is inefficient in most applications, and microparticle bombardment is expensive, with poor efficiency. Microinjection is laborious, and its application is most suited to large cells. Electroporation is difficult to target *in vivo* and suffers from tissue damage and low survival.

An ideal technique for exogenous expression would allow precise control of targeting, and use a transfer vector that is rapid, innocuous, and easy to produce. The objective of this study is to optimize and evaluate the novel methodology of localized electroporation for introducing transgenes *in vivo*. The efficiency of square wave pulses will be compared to radio frequency modulation. A range of cell types and locations in the avian embryo will be targeted, and the potential expansion of localized electroporation to mammals will be explored.

MATERIALS AND METHODS

Electrode Design

The electrode (US Patent 6977172) was made from a 1.2 mm × 0.68 mm, 4 inch, double-barreled borosilicate glass capillary tube (catalog # 635000, A-M Systems), drawn on a vertical pipet puller (Model 700C, David Kopf Instruments), and broken back to an inside diameter of 100-250 μm (Figure 25A). The electrode tip was either blunt-forged for surface electroporation (Figure 25B), or ground-beveled, for piercing—as for the gonadal ridge and mouse tail electroporations (Figure 25C). Teflon-coated tungsten wire (catalog # 796000, A-M Systems), with 5 mm of Teflon removed from the ends, was inserted in each barrel to within 1 mm of the tip. A capillary tube mounting shaft (catalog # 626000, A-M Systems) was attached with heat-shrink tubing and sealed with hot glue. Refer to appendix I for a detailed guide to electrode construction.

The electrode was held in a micromanipulator and connected with polyethylene tubing to a screw-drive syringe. For optimizing square wave transfection parameters, the tungsten wire leads were connected to the poles of a stimulus isolation unit attached to a square wave stimulator (Grass S48). For the remaining experiments the electrode was connected to the RF module of a Gene Pulser II power supply (BioRad).

Embryo Preparation and Localized Electroporation Procedure

Freshly laid Brown Leghorn eggs (Coastline) were stored for up to a week, until required. Development was advanced by transferring the eggs to the rocking tray of a 38 °C Circulating Air Incubator G.Q.F. Model 1202 with humidity tanks. To obtain

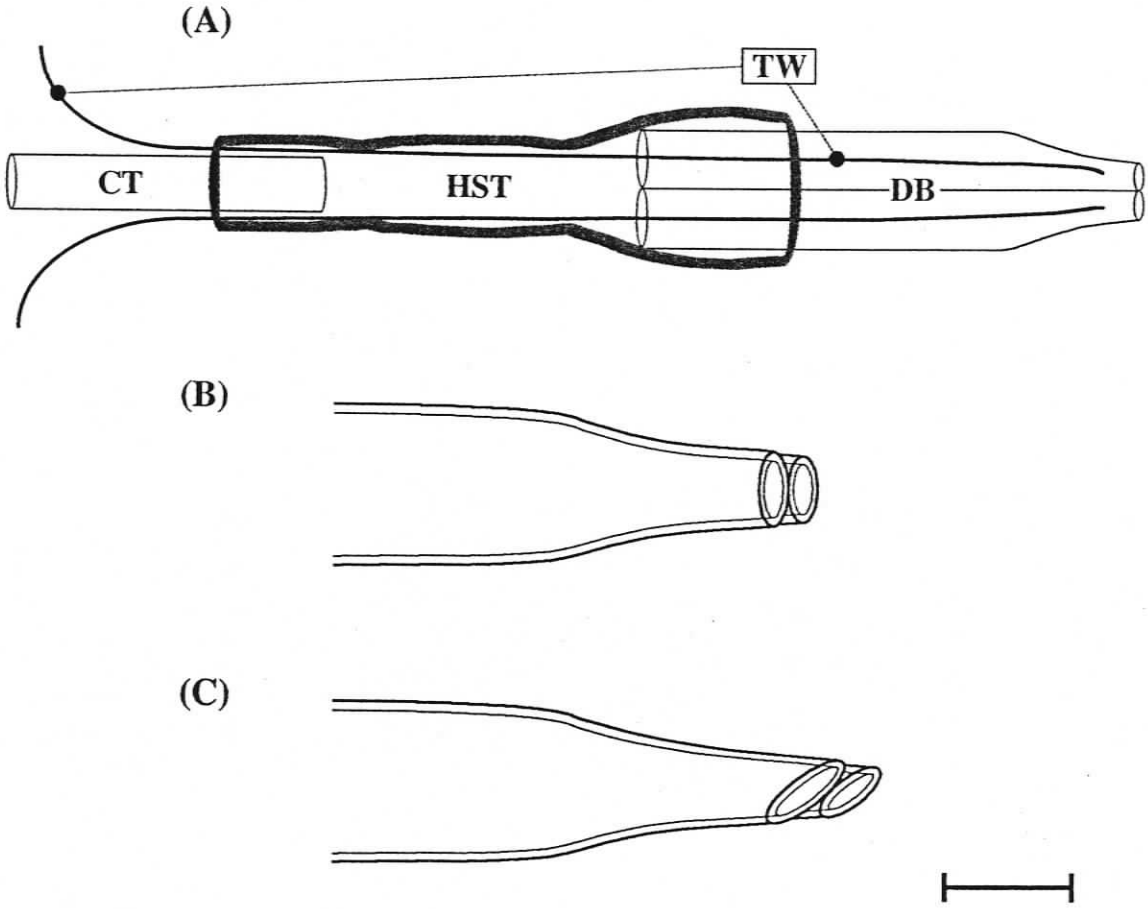

Figure 25. (A) Schematic drawing of the double-barreled suction electrode (not to scale). TW: tungsten wire, CT: capillary tube mounting shaft, HST: heat shrink tubing, DB: double-barreled capillary tube drawn and forged. Actual electrode length: 5 cm. (B) Side view of a blunt, forged doubled-barreled electrode tip. (C) Side view of a sharp, beveled electrode tip used for piercing. Bar = 1 mm.

developmental stage 10-12, embryos were incubated 44-48 h. They were then removed and manipulations were carried out at room temperature. Eggs were held on a rubber torus beneath a Leica MZ-APO dissection microscope with the zoom lens adjusted to 20-40× magnification. Illumination was provided by obliquely angled, blue filtered, fiber optic lights (Zeiss KL1500).

Green fluorescent protein (GFP) plasmid (pEGFP-N1, BD Biosciences Clontech) was isolated from 500 mL *E. coli* cultures with a maxiprep kit (QIAGEN) and diluted to 250 ng/μL in chick Ringer solution. Fertile chicken eggs were windowed and the vitelline layer over the target area was carefully reflected with a fine tungsten needle (Selleck, 1996). The double-barreled electrode was front-filled with plasmid solution and positioned in contact with the surface of the embryo. A small pool of plasmid solution was ejected over the embryo to prevent plasmid solution from being displaced up the electrode by embryonic fluid during the application of suction. The electrode tip was sealed to the tissue by applying gentle suction with the screw-drive syringe. For quantifications of transfection efficiency, head mesenchyme and epithelial cells on the right side of the midbrain were targeted using the same electrode.

For electroporation with the square wave stimulator, one second trains of pulses were delivered and train number, train polarity, pulse frequency, pulse length, and output voltage were varied as indicated. Train length was always one second and a reciprocal relationship was maintained between pulse frequency and pulse duration, thus delivering identical total power at each setting. Unless otherwise noted, Gene Pulser II power supply settings were: 100 V at 100% modulation (translating to a DC amplitude of 50 V), a frequency of 30 kHz, a pulse duration of 40 ms, a total of 10 pulses with a pulse

interval of 200 ms.

Immediately after administration of the electroporation pulses, the electrode was backed slightly away from the embryo, the suction released, and another small volume of plasmid solution was ejected over the embryo. Sterile water was used to rinse the electrode to prevent clogging and prolong its life. The egg was resealed with adhesive cellophane tape and returned to the incubator for 48 h.

Localized Electroporation of Mouse Tail

Plasmid (eGFP N1, BD Biosciences Clontech) was diluted to 250 ng/μL in 0.85 M NaCl. Female Balb/c mice were held in a tube restraining device and their tails were taped in place. The target area on the tail was swabbed with ethanol and marked with an indelible pen. The double-barreled electrode was front-filled with plasmid solution and the skin of the mouse tail was pierced. A small pool of plasmid solution was released and electroporated. Electroporation settings consisted of 10, 40 ms pulses at 30 kHz, with a pulse interval of 200 ms. The voltage was set to 200, 300 or 400 V at 100% modulation (DC amplitude of 100, 150, or 200 V), as indicated. The polarity of the electrode barrels was then reversed with a DTDP switch and a second set of pulses was applied. Immediately after administrating the electroporation trains, the electrode was backed slightly away, and a small volume of plasmid solution was released. Mice were returned to the cage and serum was collected 23 days post-electroporation for use in an indirect immunofluorescence assay with cells transfected with a GFP expression vector.

Visualization and Data Processing

Avian embryos were dissected into PBS and the amnion was removed. If fixation was

required, 2% paraformaldehyde in PBS for 5 min proved to be adequate without inducing auto-fluorescence. Whole embryos were mounted wet on a depression slide with a footed coverslip. Embryo transfections of the gonadal ridge were embedded in OCT (Tissue-Tek), and longitudinal sections (10 μm) were made on a cryostat (Microm Model HM500). The primordial germ cell marker, SSEA-1, was detected by indirect immunofluorescence with MC-480 antibody (mouse IgM, DSHB). Avian embryos and GFP-expressing cells were visualized using either a compound microscope equipped for epifluorescence (Zeiss) or a confocal laser scanning microscope (Zeiss). Mice were examined at intervals with a Leica MZ Apo dissection microscope fitted with a GFP module. In all cases, epifluorescent images were collected using a DC-330 CCD camera (DAGE-MTI) on a CG-7 frame grabber board run by Scion Image 4.0.3 (Scion). Image color was adjusted and figures were assembled with Photoshop 5 (Adobe). Statistical values were calculated using a one-way analysis of variance followed by a Tukey-Kramer post-test (InStat 3.0.5, GraphPad Software).

RESULTS AND DISCUSSION

Optimizing Square Wave Transfection Parameters

Localized electroporation produces two scattered patches of GFP-expressing cells at the target area (Figure 26A). The patch diameter 48 h post-transfection exceeds electrode size but is approximately proportional to it. The transfection patch associated with the negative pole of the electrode contains the majority of GFP-expressing cells. This is consistent with observations that paddle electroporation transfects cells on the side of the neural tube nearest the positive paddle—in both cases DNA follows a cathode to anode path (Sakamoto *et al.*, 1998). When the electroporation train is repeated with alternate polarity, both patches are similar in size. Hundreds of cells can be transfected with large barrel diameters and alternating train polarity (Figure 26B). Cellular migration is not disrupted and presumptive neural crest cells proceed along neural crest migration routes (Figure 26C). Surface epithelial cells and mesenchyme deep to the point of electroporation express GFP (Figure 26D), indicating that direct contact with the electrode is not necessary. GFP expression is visible less than 2 h post-electroporation but does not reach maximum intensity until 24-48 h. Expression continues until incubation was halted (> 8 days), at which point thousands of transfected cells are present. GFP intensity in these advanced embryos is less than in those observed 24-48 h post-transfection, which is consistent with episomal plasmid dilution through mitotic division.

Increasing the number of trains provides an apparent increase in transfection efficiency (Figure 27A), with no decrease in survival. Alternating the pulse polarity

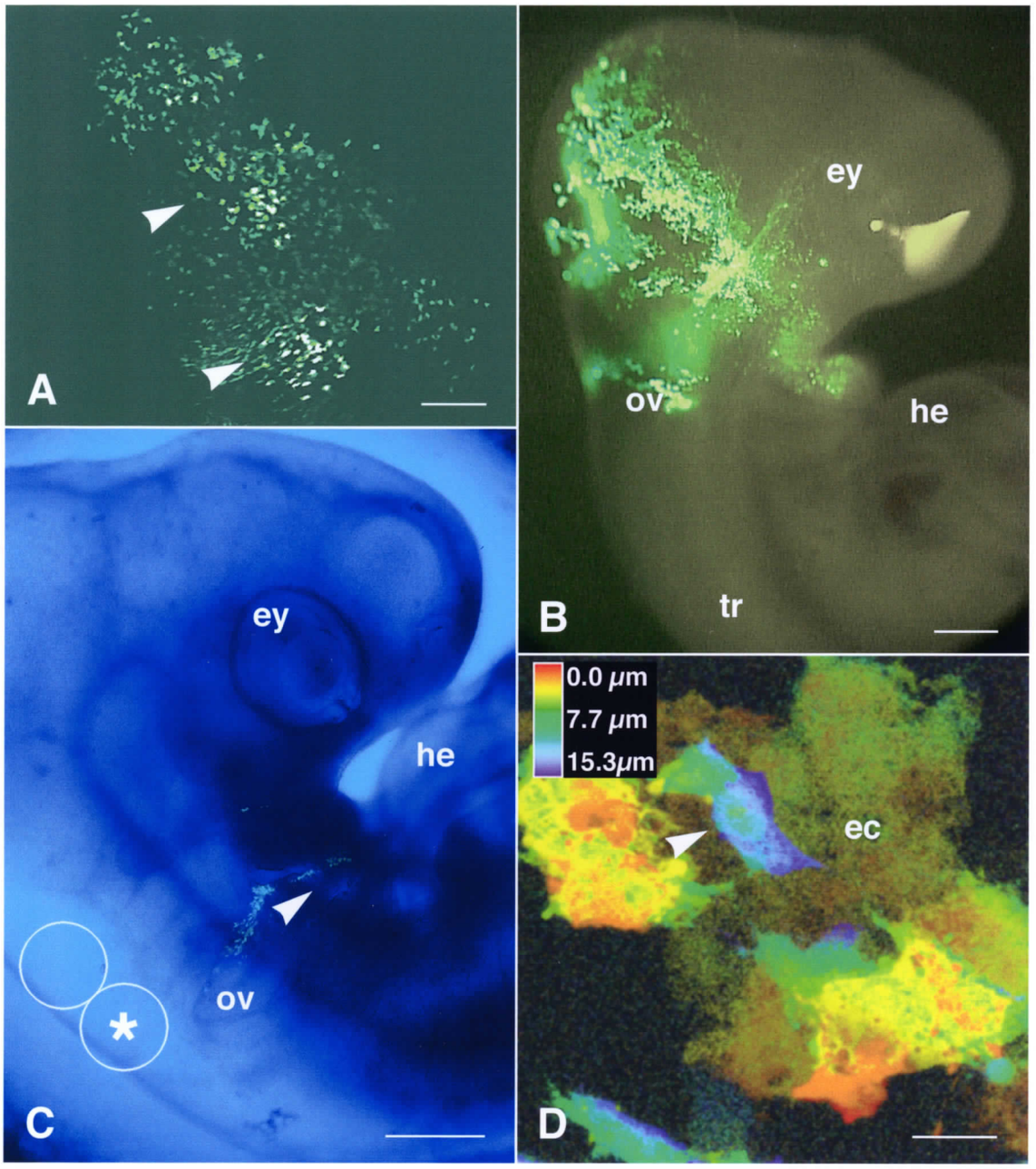

Figure 26. Whole mount chick embryos showing GFP-expressing cells 48 h post-electroporation. (A) Confocal laser scanning image of the dorsal head region after train polarity alternation. Arrows indicate barrel locations. Bar = 100 μm. (B) Right side view of embryo head in which a large diameter electrode has produced a massive transfection patch comprised of many cell types. The eye (ey), otic vesicle (ov), heart (he), and trunk (tr) are labeled. Bar = 400 μm. (C) Smaller barrel diameters, indicated with circles, have transfected neural crest cells of the forth rhombomere (*). The stream of cells has migrated towards the second branchial arch. Bar = 400 μm. (D) Depth coding made from a confocal stack showing epithelial cells (ec) and cells up to 15 μm below (arrow) the point of transfection expressing GFP. Bar = 10 μm.

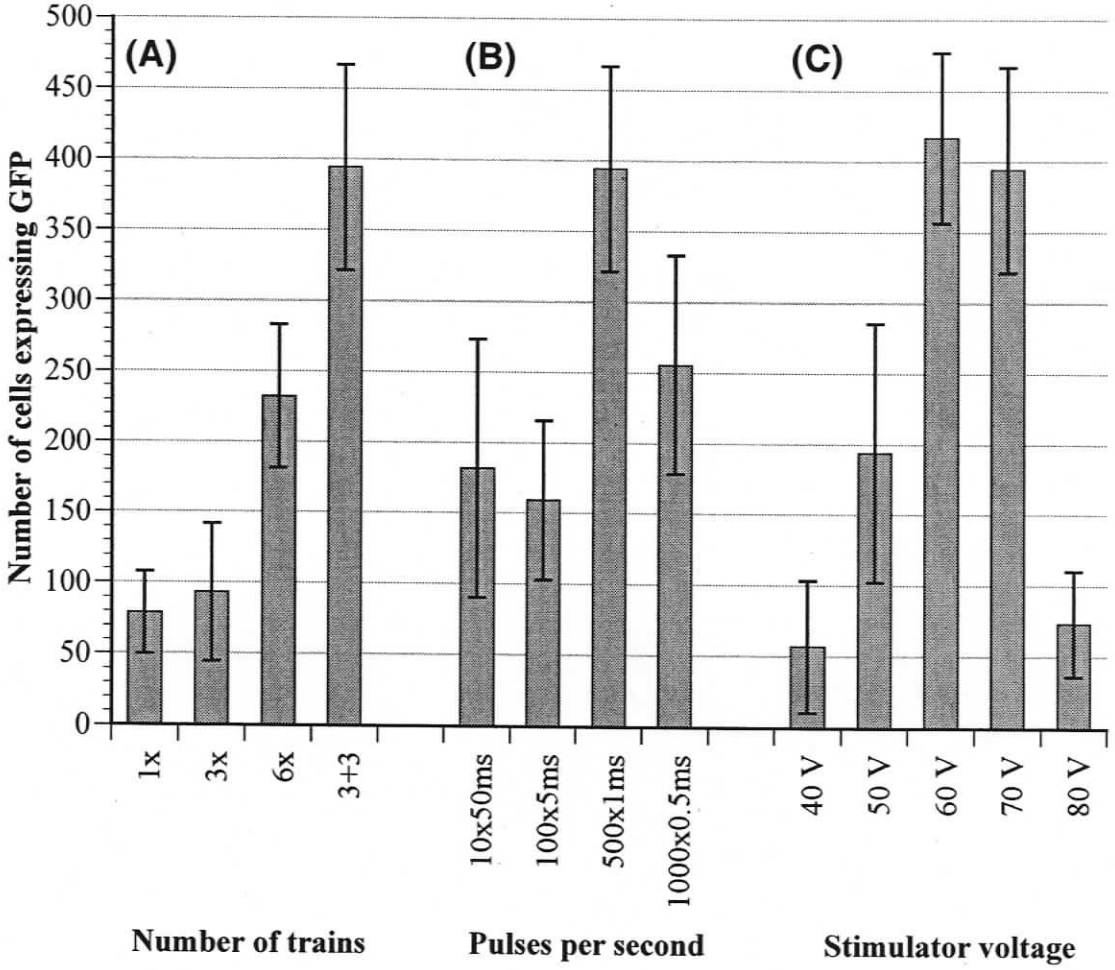

Figure 27. The effects of various electroporation parameters on mean number of cells transfected. (A) Tests of train number were performed at 500 pps (1 ms pulse length) with the stimulator output set to 70 V. Trains were one second long and six trains of alternating polarity is indicated by 3+3. (B) Pulse frequency variation was performed with 3+3 trains at 70 V. Pulse length was reciprocally adjusted to provide equal power output at each frequency, eg. 0.5 ms for 1000 pps. (C) The settings for the stimulator voltage titration were 3+3 trains of 500 pps (1 ms pulse length). Electrodes were approximately the same size and 3-6 embryos were analyzed per condition. Bars, s.e.m.

between trains increases the average number of cells transfected from 230 to almost 400, even though the total number of 6 trains remains constant. Six alternating trains are significantly more efficient than a single train ($P < 0.01$).

Five hundred pulses per second (pps) produces the optimal number of transfected cells (Figure 27B). Higher and lower frequencies result in approximately half the number of transfected cells. Transfection rates at the lowest frequency (10 pps) with long pulse durations (50 ms) decrease survival and increase the incidence of abnormal embryos. No deformities are observed at high pulse frequencies (low pulse duration).

The highest mean numbers of GFP-expressing cells is observed at 60-70 V (Figure 27C). Stimulator voltages of 40 and 80 V produce significantly lower efficiencies ($P < 0.05$). At voltages above 70 V, scarring and deformities are apparent. The threshold voltage for scarring is potentially different for each electrode due to variations in barrel diameter, wire placement, and impedances (approximate total circuit impedance 1-2 MΩ). Given the number of variables in electroporation systems, pulse parameters may require modification when the electrode is adapted to different power supplies or situations. When titrating the voltage, for instance, it would be advisable to find the threshold at which scarring occurs and then decrease the output by 10-20 V.

The survivorship in this study is 80% [61/76], while the optimal survivorship reported for electroporation using paddles is 56% [28/50] (Muramatsu *et al.*, 1997a). The transfection efficiency (number of embryos with transfected cells/number surviving) in this study is 95% [58/61], whereas paddle electroporation results in 50% [14/28] efficiency. With paddle electroporation the number of cells expressing a transgene after 48 h range from a few to several thousand (Muramatsu *et al.*, 1997a). Localized

electroporation can repeatedly transfect 600 cells at a 250 μm barrel diameter. Localized electroporation, as implemented in this study, is most useful for transfecting cells at or near a surface. Paddle electroporation is effective in transfecting large regions of an embryo. Hollow structures (e.g., eye or neural tube) into which DNA-containing solutions can be injected, are appropriate applications for paddle electroporation (Sakamoto *et al*., 1998). Localized electroporation is desirable for controllably targeting specific groups of cells, at high efficiency, and with considerably reduced cellular damage typical of electric fields.

Square Wave and Radio Frequency Efficiencies

Localized electroporation at radio frequencies was evaluated with a Gene Pulser II power supply. At a setting of 100% modulation, the RF module emits pulses entirely in the form of radio frequency waves. At a setting of 50% modulation, the top half amplitude of a pulse is radio frequency, while the lower half of the amplitude is a square wave base. At 0% modulation, the whole pulse is in the form of a square wave. In order to compare identical amounts of energy, the DC amplitude is calculated by the apparatus. A 100 V pulse at 50% modulation, for example, has a DC amplitude of 75 V. Embryos electroporated with the Gene Pulser II set to 100 V pulses at 0% modulation (DC amplitude of 100 V) produce transfection patches (Figure 28A) comparable to the highest efficiencies obtained by the electrophysiological square wave simulator. In 14 trials with 50 V square waves (0% modulation), the number of cells transfected ranges from 106 to 645 (Figure 29A). With 100 V square waves, there is about a 75% increase in the mean number of cells transfected and the range in the 14 trials is from 191 to 950 (Figure 29A). At settings above 100 V, tissue damage is evident for square wave electroporation.

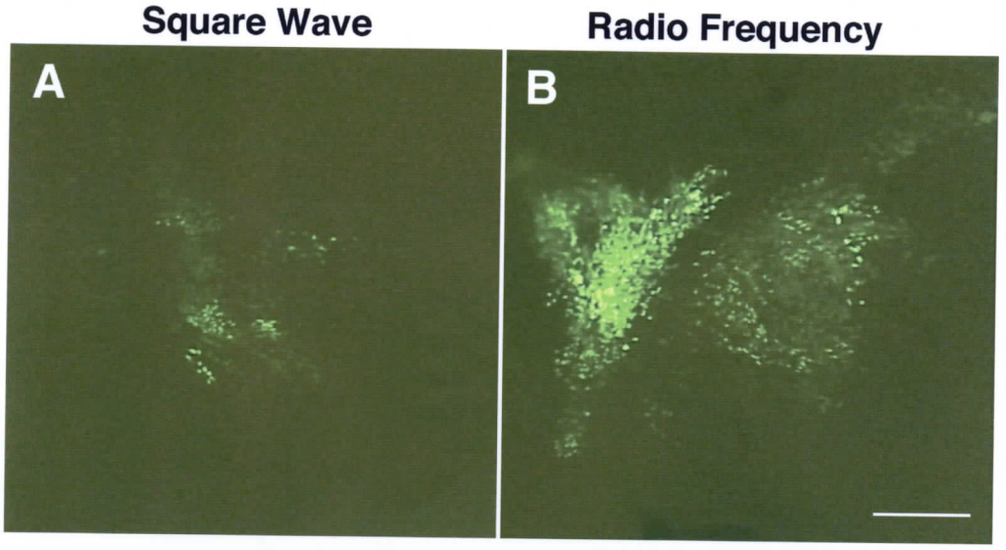

Figure 28. A comparison of square wave pulses and radio frequency pulses during localized electroporation. The right side of the embryo head was targeted with GFP-encoding plasmid and imaged 48 h post-transfection. (A) A train of square wave pulses delivered at 100 volt DC amplitude produces visible transfection patches. (B) A train of radio frequency pulses at the same DC amplitude, delivered with the same electrode, results in more than twice as many transfected cells. Bar = 100 μm.

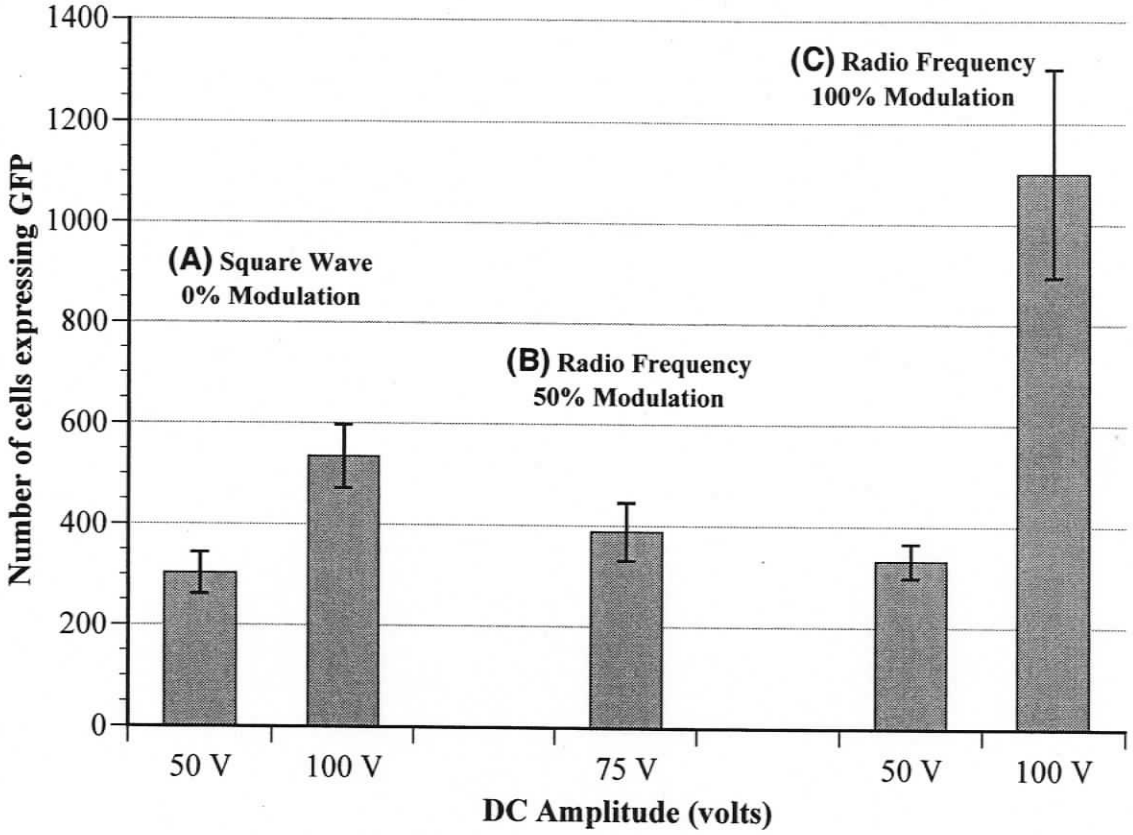

Figure 29. The effects of wave form on mean number of cells transfected during a series of localized electroporations. (A) A square wave was simulated with a setting of 0% modulation. (B) An intermediate radio frequency modulation. (C) Radio frequency pulses were delivered at comparable DC amplitudes to the the square waves in (A). The same 100 μm electrode was used throughout the experiment and 8-19 embryos were analyzed per condition. Bars, s.e.m.

Embryos electroporated with radio frequency pulses yield transfection patches containing high densities of transfected cells (Figure 28B). In 15 trials at 75 V DC amplitude (100 V, 50% modulation), the number of transfected cells ranges from 121 to 863 (Figure 29B). In 19 trials at 50 V DC amplitude (100 V supplied, 100% modulation), the number of transfected cells ranges from 114 to 710 (Figure 29C). In 8 trials at 100 V DC amplitude (200 V supplied, 100% modulation), the number of cells transfected ranges from 261 to 1945. The mean number of transfected cells increases by about 230% over the 50 V DC amplitude settings. This appears to be the threshold for tissue damage with radio frequency electroporation, as there is conspicuous tissue damage at higher voltages.

These data indicate that with increased DC amplitude, there is a significant increase in the mean number of cells transfected. When DC amplitude increases from 50 to 100 V, the number of cells transfected with square wave settings nearly doubles, while efficiency at radio frequency settings more than triples. A property of radio frequency waves must account for this improvement. It is possible that the rapid oscillations of field amplitude facilitate the dielectric breakdown of the cellular membrane. If this was true, one might expect the effect to be pronounced at 50 V DC amplitude. The number of cells transfected at 50 V DC amplitude, however, is similar for both square wave and radio frequency pulses. The factor limiting the number of cells that can be transfected appears to be tissue damage at the site of transfection. The use of radio frequency pulses may increase the transfection efficiency by permitting higher peak voltages to be used. With square wave pulses, tissue damage occurs above 100 V. With radio frequency settings, although the DC amplitudes are equal, the peak voltages are twice those of square wave settings. Peak field potentials were 200 V throughout the pulse, but only for

a brief periods of time. This may supply sufficient energy for membrane pore formation, yet in a manner that reduces tissue damage. Regardless of the mechanism, radio frequency pulses appear to provide an advantage in maximizing the efficiency of localized electroporation.

Targeting a Range of Cell Types in the Chick Embryo

Multiple cell types and various targets can be controllably targeted with localized electroporation. Transfected cells of the lens vesicle retain epithelial polarity (Figure 30A). Epidermal ectoderm cells have clear cell-cell boundaries, with non-fluorescent vacuoles visible in a GFP-rich cytoplasm (Figure 30B). GFP-expressing cells in the neural tube have processes consistent with neuronal precursors (Figure 30C). Transfected cells in the trigeminal ganglion have extensions more than 100 μm in length (Figure 30D). A GFP-expressing stream of putative neural crest cells migrates away from a transfection patch in the cranial neural fold (Figure 30E). Electrically active and contracting cells in the heart of a 3-day old embryo can be targeted with localized electroporation (Figure 30F). In contrast to paddle electroporation, which has been reported to arrest heart function (Sakamoto *et al.*, 1998), the embryo survives and the ventricle contains superficial and deep GFP-expressing cells 24 h post-transfection (Figure 30G). These examples demonstrate the precise control of targeting available by localized electroporation. The range of cellular morphology following successful electroporation suggests the procedure is non-disruptive to normal cellular process.

Targeting Primordial Germ Cells in the Gonadal Ridge

The depth that localized electroporation penetrates into tissue can be extended with a

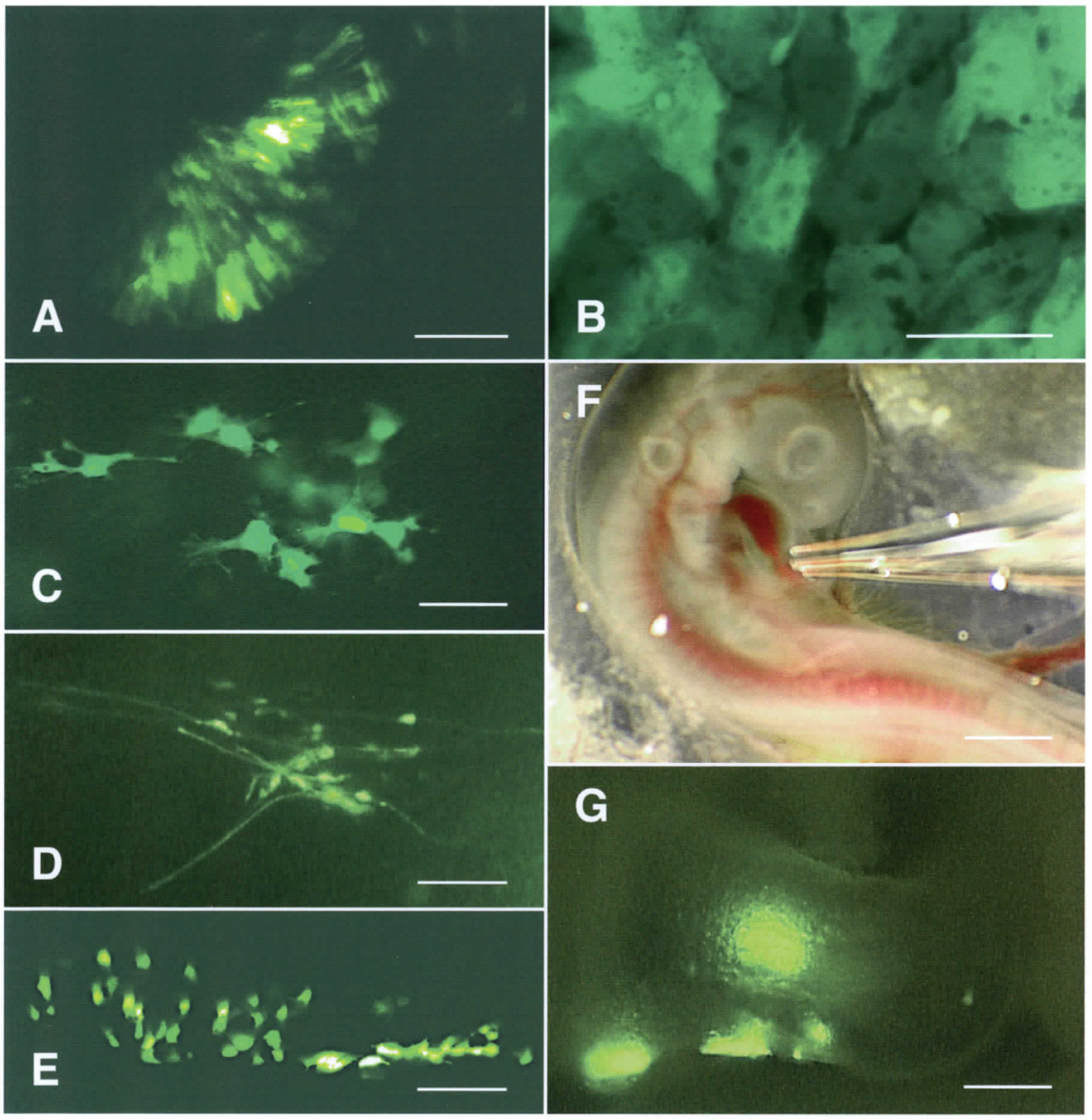

Figure 30. Whole mount chick embryos showing transfection of various cell types 48 h post-electroporation. (A) GFP expression in cells comprising half the lens vesicle of an embryo in which presumptive lens epithelium was electroporated. Bar = 50 μm. (B) Transfected epithelial cells of the ectoderm showing cytoplasmic expression. Bar = 25 μm. (C) Epifluorescent image of cells within the neural tube expressing GFP after neural plate was electroporated. Bar = 25 μm. (D) Cells within the trigeminal ganglion displaying GFP fluorescence along axon tracts. Bar = 50 μm. (E) Confocal image of GFP-expressing cells migrating from cranial neural folds. The movement of these cells away from the neural tube suggest they are neural crest derived. Bar = 50 μm. (F) Localized electroporation of the heart in a 3 day old embryo. The electrode barrels are aligned vertically to contact the ventricle. Bar = 500 μm. (G) Superficial and deep GFP expression in the heart 24 h post-electroporation. Bar = 80 μm.

piercing electrode tip (Figure 25C). The gonadal ridge lies near the centre of the embryonic trunk. It contains primordial germ cells and is explored as a broader target for localized electroporation because of the applicability to transgenic technology. In 7 trials with 4-day old embryos, 3 embryos appear to have GFP expression in the region of the gonadal ridge 24 h post-transfection. In cryostat section, one embryo has a high density of GFP-expressing cells in the gonadal ridge (Figure 31A). Primordial germ cells in culture express SSEA-1 antigen (Figure 31B), a marker for embryonic stem cell phenotype (Petitte *et al.*, 2004). An embryo section has immunoreactivity for this marker co-localized with a transfected cell in the gonadal ridge (Figure 31C). This preliminary experiment demonstrates the utility of localized electroporation while piercing solid tissue targets.

DNA Vaccination of Mice by Localized Electroporation

The application of localized electroporation to mammals is explored by targeting dermis and epidermis of mouse tail. After 48 h, the small incision that was electroporated at 200 V (100 V DC amplitude) has a slight green fluorescence that is distinguishable from background fluorescence (Figure 32A). After 1 week, the spot that has been electroporated appears mildly swollen and inflamed. Observed with epifluorescence microscopy, there is a brightly fluorescent region with diffuse boundaries beneath the surface of the tail (Figure 32B). At 15 days there is a small, colorless scab at the point of electroporation. Observed with epifluorescence microscopy, there is a crisply delineated spot of fluorescence, and in some mice, there are hairs adjacent to the site of transfection that are brightly fluorescent throughout their length (Figure 32C). At 24 days, the inflammation has subsided and there is a slightly pink, hairless spot at the site of

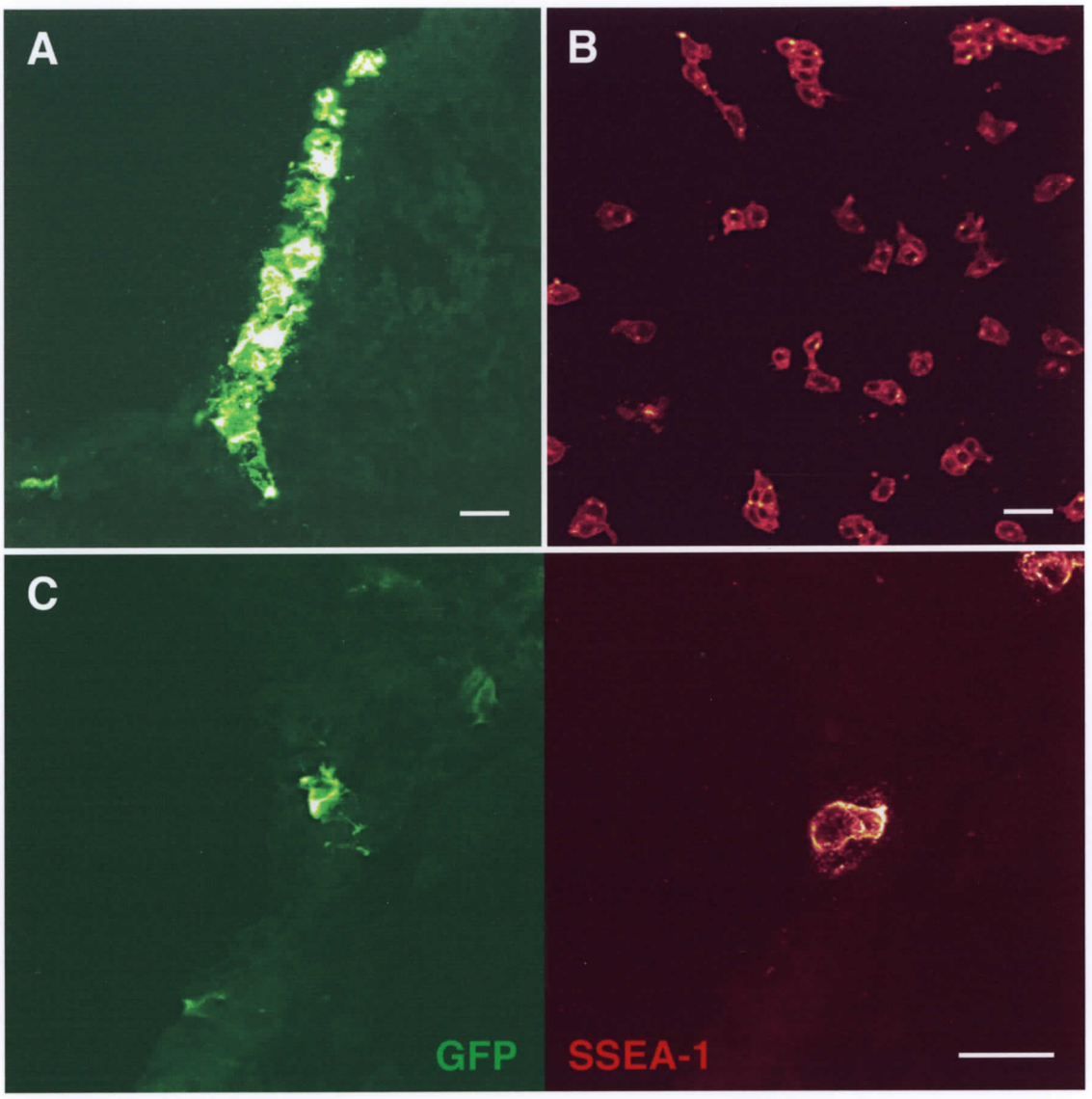

Figure 31 Confocal images of primordial germ cells after localized electroporation. (A) Transverse embryo section showing GFP expression in the gonadal ridge 24 hours post-transfection. (B) A primary primordial germ cell culture labeled with SSEA-1 antibody. (C) An embryo section through the gonadal ridge labeled with anti-GFP and SSEA-1 antibodies. The primordial germ cell marker co-localizes with a GFP-expressing cell. Bar = 40 μm.

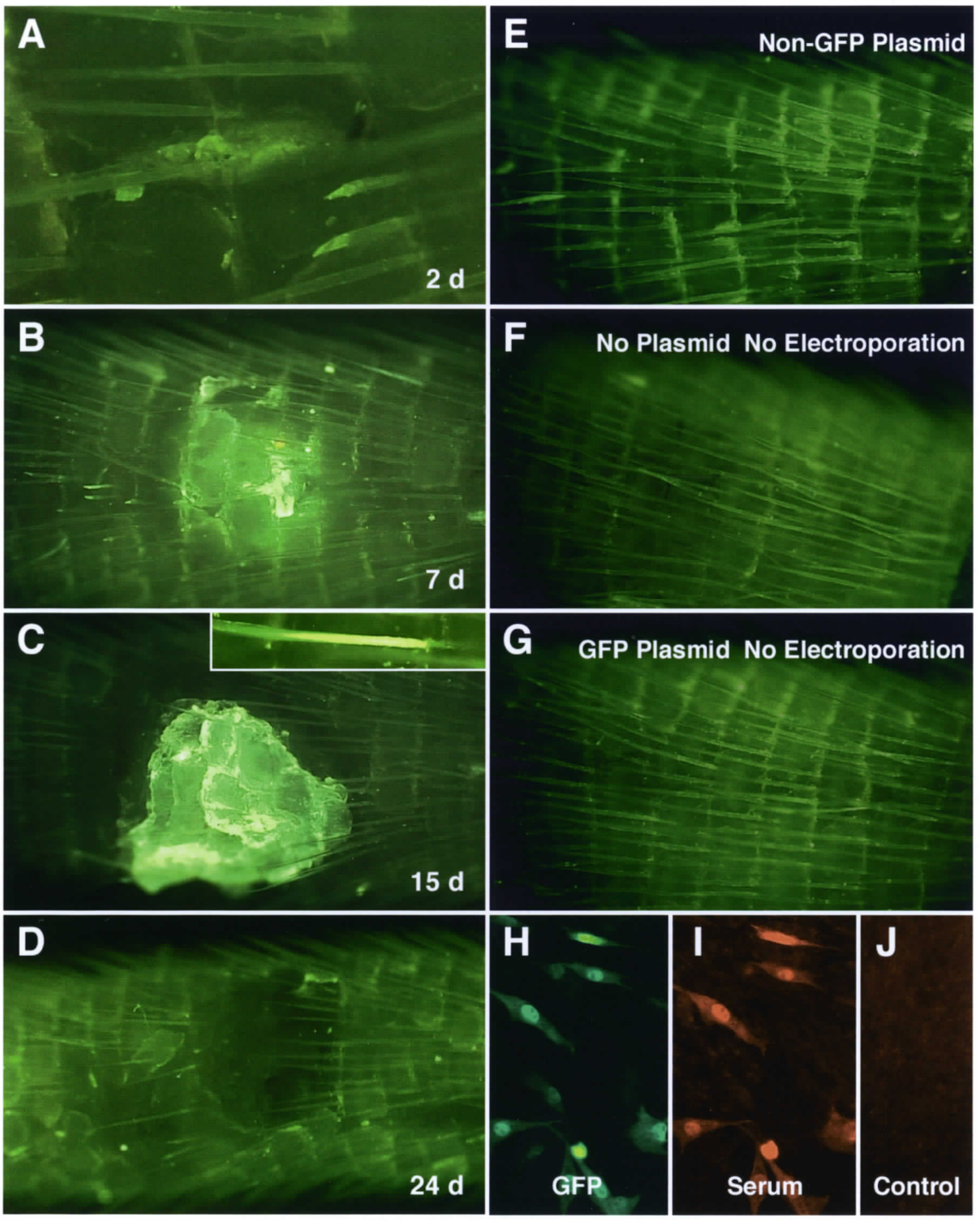

Figure 32. Fluorescent images of localized electroporation of mouse tail. (A) Two days post-electroporation. (B) Sub-surface fluorescence is larger. (C) At 15 d, GFP-expressing cells are at the surface. Inset shows fluorescent hair. (D) Spot appears to have sloughed off. (E) Control electroporation of plasmid incapable of mammalian expression. (F) Control with the electrode only piercing the skin. (G) Control with no electroporation. (H) Avian cell culture expressing GFP. (I) Immunofluorescence of same cells with mouse serum. (J) Control with cells not expressing GFP.

transfection (Figure 32D). All voltages attempted (200, 300, and 400 V) result in fluorescent cells, and there does not appear to be any difference in the size of the regions expressing GFP.

In one preparation, a mouse was electroporated with a plasmid lacking any mammalian promoter sequences (Figure 32E). Another control preparation consisted of an incision and simulated electroporation with only saline and no voltage (Figure 32F). The third control preparation had release of GFP plasmid and simulated electroporation, no voltage (Figure 32G). In all cases, the site of incision has healed by 7 days, and no inflammation or fluorescence is detected.

These experiments indicate that localized electroporation can be adapted to mammals. The use of a suction electrode on the surface of the skin is unsuccessful, probably because the skin forms an effective barrier to the aqueous DNA solution. Once the skin is broken, however, a region of cells at the point of electroporation reliably expresses the GFP reporter gene. It is not certain which cells are transfected, but the observation of hairs expressing GFP suggests that cells of the hair follicle, which proliferate to form the hair shaft, are transfected in some instances. The size of the fluorescent spot produced does not appear to correlate with the voltage used, suggesting that the threshold for efficient transfection is below the lowest setting used in these experiments, 200 V.

The immune response to GFP was investigated because there appears to be a prolonged inflammation in transfected mice relative to control preparations. Samples of blood were obtained from transfected and control mice at 23 days. Serum was used in an indirect immunofluorescence assay of an avian cell culture transfected with a GFP expression plasmid. Avian cells that express GFP (Figure 32H) are also immunoreactive

to the serum (Figure 32I), indicating the presence of mouse antibodies to GFP. Assay controls with non-transfected mouse serum, or avian cells transfected with no plasmid, contain no cells that are immunoreactive (Figure 32J). These experiments suggest the mice mounted an immune response to the transgene, and therefore can be immunized by localized electroporation.

CONCLUSION

Electroporation is a method of transfecting cells by forming pores in their membranes with an electric field. It overcomes some disadvantages of viral transfection, including limited targeting control, small insert size, and biosafety concerns (Leber *et al.*, 1996). Electroporation is also more efficient than lipofection or microparticle bombardment (Muramatsu *et al.*, 1997a). Localized electroporation was developed to target populations of cells in living embryos with efficiency and control. Central to the technique, is a double-barreled suction electrode. This electrode is filled with DNA in saline, and serves, both as a delivery method for the plasmid, and as a conduit to generate the electric field. This design allows for control of targeting and restricts electroporation to cells influenced by the electric field, although accurate use of the technique does require practice. It allows a low amount of energy to be dissipated into the embryo to reach the critical threshold for electroporation in the target area. It is also intended that the saline medium create a uniform conductor that is gentler to the cells than a metal electrode.

In avian embryos, over one thousand cells express a reporter construct 24 to 48 h after localized electroporation. Greater numbers of cells can probably be targeted with a larger barrel diameter, or the transfection area can be limited with a smaller electrode. In some experimental situations it may be desirable to quantify a constant number of cells. For such cases, variation may be improved by using the same electrode, or by calibrating electrodes to have matching diameters. Statistical tests should be used to verify the significance of effects. Surface epithelial cells are easily transfected. Cells that are deep

to the point of electroporation, including neural crest, head mesenchyme, neuronal, heart, lens, and otic vesicle, are possible to target, but are more challenging. The range of targeting depth may present difficulties in experimental design. All potentially transfected tissues must be considered when evaluating complicated structures. Adequate controls that identify transfection location are especially crucial for dynamic or migratory preparations. Deep tissues, such as the gonadal ridge, can be specifically targeted with a piercing electrode tip. At parameters adjusted for low or moderate efficiency, localized electroporation is not observed to cause deformities or inhibit cell activities.

Transfection efficiency in this study depends on pulse number, frequency, and voltage. A series of intermittent pulses increases the number of cells transfected. This relationship is compatible with general trends in electroporation (Andreason & Evans, 1989). This study also establishes a significant advantage in swapping polarity between trains of pulses. The reversal likely allows for effects of iontophoresis at each barrel location (Klenchin *et al.*, 1991). In applications where restricted spatial targeting is desired over optimal efficiency, it would be possible to strongly favor electroporation at one cathode barrel. In comparison to square waves, radio frequency modulation also provides a significant improvement to the efficiency of localized electroporation. The utility of the technique, however, may be limited by variation in efficiency. The shape of the electric field, and depth effects, can create areas of diminished or enriched efficiency within a transfection patch. As with all transfection techniques, dosage effects must be controlled.

Saline should be used to irrigate the target area before transfection. A small pool of plasmid solution should also be ejected before suction is applied to the electrode. These

steps help ensure that the target area remains in contact with plasmid, and that the circuit is not opened by a poorly conductive liquid, such as thin albumin solution. This part of the procedure creates the most common source of error during localized electroporation. Variation in electrode placement from one specimen to the next is another source of error. The degree that these variations affect the experiment can likely be reduced with practice by the operator, but are not likely to be eliminated.

Although the technology is optimized for avian embryos, it may be expanded for use in mammals. Preliminary experiments with mice show that localized electroporation provides a means of transfecting cells in the epidermis and dermis. The cells transiently express transgene and transfected mice mount an immune response. In comparison to other transfection techniques in mammals (Mir *et al*., 1999), localized electroporation is convenient with relatively low invasiveness.

Localized electroporation is a method of transfection that overcomes some limitations of other *in vivo* techniques. Commonly used methods of paddle electroporation target through the injection of DNA (Muramatsu *et al*., 1997a). This works very well for cavities, but is poorly suited to superficial structures. Paddle methods also place metal electrodes alongside the embryo, thereby exposing non-targeted cells to damaging current. Localized electroporation, using a double-barreled suction electrode, has good transfection efficiency, less scarring, and better survivoral than those reported for paddle electroporation. It is a appropriate tool for transfecting a small number of cells, at a superficial target, with minimal tissue damage. Patches of cells expressing ectopic genes permit the analysis of genetic mosaic avian embryos. The technique could be useful for developmental and cell biologists interested in functional genomics or tracing cell

lineage. Purchase or manufacture of the electrode and a significant operator learning curve are barriers to adoption.

Future Directions

The efficiency of localized electroporation may be improved in the future. The work described in this dissertation is an encouraging beginning. I found that parameters for chick embryonic tissue could be successfully applied to mouse tail. Different applications, however, are expected to have different optimal settings. Parameters of the radio frequency program, such as pulse number, duration, and interval, are derived from previous optimizations with square wave programs. These parameters constitute a starting point, but there is potential for future optimization. A range of radio frequencies could also be investigated. It is possible that 20, 40, or 50 kHz would improve efficiency in specific applications, including the chick embryo. Improvements in efficiency and safety may also be achieved with a program that takes advantage of the iontophoresis effect observed in this work. A circuit could be designed that provides initial pulses at the critical voltage of dielectric breakdown, followed by longer, low voltage pulses to maximize iontophoresis. Commercial power supplies that are currently available do not allow for this type of compound program. The effort to optimize electroporation efficiency may be unnecessary if localized electroporation is used for precise targeting or standardized amounts of transfection.

Applications of localized electroporation can be extended in the future. Antibodies and peptides have been electroporated (Campbell *et al*., 1995; Morgan & Day, 1995), so it is possible that localized electroporation could be adapted for transfer of compounds other than DNA. It should be noted that iontophoresis effects would become less

significant with any compounds of nominal charge, and in those situations, efficiency may diminish. The successful transfection of deep cells in the gonadal ridge also indicates the potential for transgenic applications. Transgenic animals have been used to investigate biological pathways and disease states (Brodmerkel & Vaddi, 2003; Hunter *et al.*, 2005), as well as, to develop therapeutics and pharmaceuticals (Dunn *et al.*, 2005). The avian system is a good choice for the low cost production of specific proteins with proper post-translational modification (Lillico *et al.*, 2005). Difficulties in obtaining, culturing, and reintroducing avian pluripotent stem cells to recipient embryos have hampered the development of transgenic chicken strains (Petitte *et al.*, 2004). Transgenic and chimeric individuals have been produced, but the germ line transmission of gametes resulting from genetically modified stem cells has not been described (Sang, 2004). Localized electroporation *in ovo* may be useful in increasing the efficiency of this procedure. Vector design is critical for integration to the host genome and linear forms of DNA or RNA may be preferred. To this end, it would be appropriate to compare and optimize the efficiency of localized electroporation with linearized plasmid.

DNA vaccination and gene therapy and are also potential applications for localized electroporation. DNA vaccination is a procedure for immunizing an organism with a plasmid capable of expressing an immunogen. This procedure has considerable potential for use in research and health care (Wolff *et al.*, 1990; Tsalik, 2005; Ulmer *et al.*, 1993). There would be savings in time and effort if mice can be immunized with DNA encoding a protein of interest. There would be no need to express and purify the protein as an immunogen. A number of methods for introducing DNA have been employed. These include intra-muscular injection, intra-dermal injection, microparticle bombardment, and lipid vectors (Alpar *et al.*, 2005). There are also reports of injection followed by

electroporation with paddles (Mir *et al*., 1999). All vary in their degree of invasiveness and the efficiency of transfection of the genes into living cells. Localized electroporation of mouse tail in this work results in cells at the site of electroporation expressing transgene for about 3 weeks. This indicates that localized electroporation could be developed as a tool to permit a relatively non-invasive means of DNA immunization. The fact that mice express the transgene for only a few weeks, means that this method of immunization could, after safety tests, be used for immunization of livestock, pets and potentially humans. This may also be an appropriate platform for transient gene therapeutics, where ectopic expression of a transgene in skin cells for a short period of time is useful.

LITERATURE CITED

Aberle, A., Bauer, A., Stappert, J., Kispert, A., & Kemler, R. (1997). Beta-catenin is a target for the ubiquitin-proteasome pathway. *EMBO J.* 16: 3797-804

Abidor, I.G., & Sowers, A.E. (1992). Kinetics and mechanism of cell membrane electrofusion. *Biophys J.* 61: 1557-69

Adamson, P., Marshall, C.J., Hall, A., & Tilbrook, P.A. (1992). Post-translational modifications of p21rho proteins. *J Biol Chem.* 267: 20033-8

Ahokas, H. (1989). Transfection of germinating barley seed electrophoretically with exogenous DNA. *Theor Appl Genet.* 77: 469-72

Akiyama, S.K., Yamada, S.S., Yamada, K.M., & LaFlamme, S.E. (1994). Transmembrane signal transduction by integrin cytoplasmic domains expressed in single-subunit chimeras. *J Biol Chem.* 269: 15961-4

Alpar, H.O., Papanicolaou, I., & Bramwell, V.W. (2005). Strategies for DNA vaccine delivery. *Expert Opin Drug Deliv.* 2: 829-42

Andreason, G.L., & Evans, G.A. (1989). Optimization of electroporation for transfection of mammalian cells. *Nal Biochem.* 180: 269-75

Aoyagi, T., & Izumo, S. (1993). Mapping of the pressure response element of the c-fos gene by direct DNA injection into beating hearts. *J Biol Chem.* 268: 27176

Arregui, C., Pathre, P., Lilien, J., & Balsamo, J. (2000). The nonreceptor tyrosine kinase fer mediates cross-talk between N-cadherin and beta1-integrins. *J Cell Biol.* 149: 1263-74

Askam, J.M., Moncur, P., Markham, A.F., & Morrison, E.E. (2000). Regulation and function of the interaction between the APC tumour suppressor protein and EB1. *Oncogene.* 19: 1950-8

Atabey, N., Gao, Y., Yao, Z.J., Breckenridge, D., Soon, L., Soriano, J.V., Burke Jr., T.R., & Bottaro, D.P. (2001). Potent blockade of hepatocyte growth factor-stimulated cell motility, matrix invasion and branching morphogenesis by

antagonists of Grb2 Src homology 2 domain interactions. *J Biol Chem*. 276: 14308-14

Atkins, R.L., Wang, D., & Burke, R.D. (2000). Localized Electroporation: a method for targeting expression of genes in avian embryos. *Biotechniques*. 28: 94-100

Axel, D.I., Spyridopoulos, I., Riessen, R., Runge, R., Viebahn, R., & Karsch, K.R. (2000). Toxicity, uptake kinetics and efficacy of new transfection reagents: increase of oligonucleotide uptake. *J Vasc Res*. 37: 221-34

Balsamo, J., Arregui, C., Leung, T., & Lilien, J. (1998). The nonreceptor protein tyrosine phosphatase PTP1B binds to the cytoplasmic domain of N-cadherin and regulates the cadherin-actin linkage. *J Cell Biol*. 143: 523-32

Barka, T., & van der Noen, H.M. (1997). Retrovirus-mediated gene transfer into rat salivary gland in vitro and in vivo. *J Histochem Cytochem*. 45: 1533-45

Batlle, E., Sancho, E., Franci, C., Dominguez, D., Monfar, M., Baulida, J., & de Herreros, A.G. (2000). The transcription factor Snail is a repressor of E-cadherin gene expression in epithelial tumour cells. *Nature Cell Biol*. 2: 84-9

Beauvais, A., Erickson, C.A, Goins, T., Craig, S.E., Humphries, M.J., Thiery, J.P., & Dufour, S. (1995). Changes in the fibronectin-specific integrin expression pattern modify the migratory behavior of sarcoma S180 cells. *J Cell Sci*. 128: 699-713

Beauvais-Jouneau, A., Pla, P., Bernex, F., Dufour, S., Salamero, J., Fässler, R., Panthier, J-J., Thiery, J.P., & Larue, L. (1999). A novel model to study the dorsolateral migration of melanoblasts. *Mech Dev*. 89: 3-14

Becker, T.C., Noel, R.J., Coats, W.S., Gomez-Foix, A.M., Alam, T., Gerard, R.D., & Newgard, C.B. (1994). Use of recombinant adenovirus for metabolic engineering of mammalian cells. *Methods Cell Biol*. 43: 161-89

Behrens, J. (1999). Cadherins and catenins: role in signal transduction and tumor progression. *Cancer Met Rev*. 18: 15-30

Behrens, J., Birchmeier, W., Goodman, S.L., & Imhof, B.A. (1985). Dissociation of Madin-Darby cells canine kidney epithelial cells by the monoclonal antibody

anti-src-1: mechanistic aspects and identification of the antigen as a component related to uvomorulin. *J Cell Biol.* 101: 1307-15

Berrier, A.L., Martinez, R., Bokoch, G.M., & LaFlamme, S.E. (2002). The integrin beta tail is required and sufficient to regulate adhesion signaling to Rac1. *J Cell Sci.* 115: 4285-91

Bi, D., Nishimura, J., Niiro, N., Hirano, K., & Kanaide, H. (2005). Contractile properties of the cultured vascular smooth muscle cells: the crucial role played by RhoA in the regulation of contractility. *Circ Res.* 96: 890-7

Bierkamp, C., Schwarz, H., Huber, O., & Kemler, R. (1999). Desmosomal localization of beta-catenin in the skin of plakoglobin null-mutant mice. *Development.* 126: 371-81

Bishop, A.L., & Hall, A. (2000). Rho GTPases and their effector proteins. *Biochem J.* 348: 241-55

Boerkoel, C.F., Federspiel, M.J., Salter, D.W., Payne, W., Crittenden, L.B., Kung, S.J., & Hughes, S.H. (1993). A new defective retroviral vector system based on the Bryan strain of Rous Sarcoma Virus. *Virology.* 195: 669-79

Bos, J.L. (1989). Ras oncogenes in human cancer: a review. *Cancer Res.* 49: 4682-9

Bottger, M., Vogel, F., Platzer, M., Klessling, U., Grade, K., & Strauss, M. (1988). Condensation of vector DNA by the chromosomal protein HMG1 results in efficient transfection. *Biochim Biophys Acta.* 950: 221-8

Boucaut, J., Darribère, T., Poole, T.J., Aoyama, H., Yamada, K.M., & Thiery, J.P. (1984). Biologically active synthetic peptides as probes of embryonic development: a competitive peptide inhibitor of fibronectin inhibits gastrulation in amphibian embryos and neural crest cell migration in avian embryos. *J Cell Biol.* 99: 1822-30

Boyer, B., Tucker, G.C., Valles, A.M., Franke, W.W., & Thiey, J-P. (1989). Rearrangements of desmosomal and cytoskeletal during the transition from epithelial to fibroblastoid organization in cultured rat bladder carcinoma cells. *J Cell Biol.* 109: 1495-509

Boyer, B., Roche, S., Denoyelle, M., & Thiery, J.P. (1997). Src and Ras are involved in separate pathways in epithelial cell scattering. *EMBO J.* 16: 5904-13

Boyer, B., Vallés, A.M., & Edme, N. (2000). Induction and regulation of epithelial-mesenchymal transitions. *Biochem Pharm.* 60: 1091-9

Brabletz, T., Jung, A., Dag, S., Hlubek, F., & Kirchner, T. (1999). Beta-catenin regulates the expression of the matrix metalloproteinase-7 in human colorectal cancer. *Am J Pathol.* 155: 1033-8

Brault, V., Moore, R., Kutsch, S., Ishibashi, M., Rowitch, D.S., McMahon, A.P., Sommer, L., Boussadia, O., & Kemler, R. (2001). Inactivation of the beta-catenin gene by Wnt1-Cre-mediated deletion results in dramatic brain malformation and failure of cranifacial development. *Development.* 128: 1253-64

Brieher, W.M., & Gumbiner, B.M. (1994). Regulation of C-cadherin function during activin-induced morphogenesis of Xenopus animal caps. *J Cell Biol.* 126: 519-27

Brodmerkel, C.M., & Vaddi, K. (2003). Transgenic animals in inflammatory disease models. *Curr Opin Biotechnol.* 14: 652-8

Bronner-Fraser, M. (1985a). Alterations in neural crest migration by a monoclonal antibody that affects cell adhesion. *J Cell Biol.* 101: 610-7

Bronner-Fraser, M. (1985b). Guidance of neural crest migration. Latex beads as probes of surface-substratum interactions. *Dev Biol.* 3: 301-37

Bronner-Fraser, M. (1986). An antibody to a receptor for fibronectin and laminin perturbs cranial neural crest development in vivo. *Dev Biol.* 117: 528-36

Bronner-Fraser, M. (1987). Perturbation of cranial neural crest migration by the HNK-1 antibody. *Dev Biol.* 123: 321-31

Bronner-Fraser, M. (1993). Mechanisms of neural crest cell migration. *Bioessays.* 15: 221-30

Bronner-Fraser, M. (1994). Neural crest cell formation and migration in the developing embryo. *FASEB J.* 8: 699-706

Bronner-Fraser, M., & Fraser, S.E. (1988). Cell lineage analysis reveals

multipotency of some avian neural crest cells. *Nature*. 335: 161-4

Bronner-Fraser, M., & Lallier, T. (1988). A monoclonal antibody against a laminin-haparan sulfate proteoglycan complex perturbs cranial neural crest migration in vivo. *J Cell Biol*. 106: 1321-9

Bukrinsky, M. (2004). A hard way to the nucleus. *Mol Med*. 10: 1-5

Bukrinsky, M.I., Haggerty, H., Dempsey, M.P., Sharova, N., Adzhubei, A., Spitz, I., Lewis, P., & Stevenson, M. (1993). A nuclear localization signal within HIV-1 matrix protein that governs infection of non-dividing cells. *Nature*. 365: 666

Burke, R.D., Wang, D., & Jones, V.M. (1994). Ontogeny of vessel wall components of the chick. *Anat Embryo*. 189: 447-56

Burke, R.D., Atkins, R.L., & Wang, D. Method and apparatus for targeting localized electroporation. *US Patent 6977172*. 20 December 2005

Buschle, M., Cotten, M., Kirlappos, H., Mechtler, K., Birnstiel, M.L., & Wagner, E. (1995). Receptor-mediated gene transfer into human T lymphocytes via binding of DNA/CD3 antibody particles to the CD3 T cell receptor complex. *Human Gene Ther*. 6: 753-61

Bustin, M., Lehn, D.A., & Landsman, D. (1990). Structural features of the HMG chromosomes proteins and their genes. *Biochim Biophys Acta*. 1049: 231-43

Calderwood, D.A., Zent, R., Grant, R., Rees, D.J., Hynes, R.O., & Ginsberg, M.H. (1999). The Talin head domain binds to integrin beta subunit cytoplasmic tails and regulates integrin activation. *J Biol Chem*. 274: 28071-4

Campbell, P.L., McCluskey, J., Yeo, J.P., & Toh, B.H. (1995). Electroporation of antibodies into mammalian cells. *Methods Mol Biol*. 48: 83-92

Carter, W.G., Wayner, E.A., Bouchard, T.S., & Kaur, P. (1990). The role of integrins alpha 2 beta 1 and alpha 3 beta 1 in cell-cell and cell-substrate adhesion of human epidermal cells. *J Cell Biol*. 110: 1387-404

Challita, P.M., & Kohn, D.B. (1994). Lack of expression from a retroviral vector after transduction of murine hematopoietic stem cells is associated with methylation in vivo. *Proc Natl Acad Sci USA*. 91: 2567

Chang, D.C. (1989). Cell poration and cell fusion using an oscillating electric field. *Biophys J.* 56: 641-52

Chang, D.C., & Reese, T.S. (1990). Changes in membrane structure induced by electroporation as revealed by rapid-freezing electron microscopy. *Biophys J.* 58: 1-12

Chang, D.C., Gao, P.Q., & Maxwell, B.L. (1991). High efficieny gene transfection by electroporation using a radio-frequency electric field. *Biochim Biophys Acta.* 1092: 153-60

Chassy, B.M., & Flickinger, J.L. (1987). Transformation of Lactobacillus casei by electroporation. *FEMS Microbiol Lett.* 44: 173-7

Cheadle, C., Fan, J., Cho-Chung, Y.S., Werner, T., Ray, J., DO, L., Gorospe, M., & Becker, K.G. (2005). Stability regulation of mRNA and the control of gene expression. *Ann N Y Acad Sci.* 1058: 196-204

Chen, Y.T., Stewart, D.B., & Nelson, W.J. (1999). Coupling assembly of the E-cadherin/beta-catenin complex to efficient endoplasmic reticulum exit and basal-lateral membrane targeting of E-cadherin in polarized MDCK cells. *J Cell Biol.* 144: 687-99

Cheng, L., Ziegelhoffer, P.R., & Yang, N.S. (1993). In vivo promoter activity and transgene expression in mammalian somatic tissues evaluated by using particle bombardment. *Proc Natl Acad Sci USA.* 90: 4455-9

Chesnutt, C., & Niswander, L. (2004). Plasmid-based short-hairpin RNA interference in the chicken embryo. *Genesis.* 39: 73-8

Cheung, M., & Briscoe, J. (2003). Neural crest development isregulated by the transcription factor Sox9. *Development.* 130: 5681-93

Chong, Y.P., Mulhern, T.D., & Cheng, H.C. (2005). C-terminal Src kinase (CSK) and CSK-homologous kinase (CHK)--endogenous negative regulators of Src-family protein kinases. *Growth Factors.* 23: 233-44

Chrzanowska-Wodnicka, M., & Burridge, K. (1996). Rho-stimulated contractility drives the formation of stress fibers and focal adhesions. *J Cell Biol.* 133: 1403-

15

Cibelli, J.B., Stice, S.L., Golueke, P.J., Kane, J.J., Jerry, J., Blackwell, C., Ponce-de-Leon, F.A., & Robl, J.M. (1998). Transgenic bovine chimeric offspring produced from somatic cell-derived stem-like cells. *Nat Biotechnol.* 16: 642-6

Connor, J., Yatvin, M.B., & Huang, L. (1984). pH-sensitive liposomes: acid-induced liposome fusion. *Proc Natl Acad Sci USA.* 81: 1715

Cornell, R.A., & Eisen, J.S. (2000). Delta signaling mediates segregation of neural crest and spinal sensory neurons in zebrafish lateral neural plate. *Development.* 127: 2873-82

Coster, H.G.L. (1965). A quantitative analysis of the voltage-current relationships of fixed charge membranes and the associated property of "punch through". *Biophys J.* 5: 669-86

Crittenden, L.B. (1991). Retroviral elements in the genome of the chicken: Implications for poultry genetics and breeding. *Crit Rev Poul Biol.* 3: 73-109

Crystal, R.G. (1995). The gene as the drug. *Nature Med.* 1: 15

Day, R.M., Cioce, V., Breckenridge, D., Castagnino, P., & Bottaro, D.P. (1999). Differential signaling by alternative HGF isoforms through c-Met: activation of both MAP kinase and PI 3-kinase pathways is insufficient for mitogenesis. *Oncogene.* 18: 3399-406

del Barrio, M.G., & Nieto, M.A. (2002). Overexpression of snail family members highlights their ability to promote chick neural crest formation. *Development.* 129: 1583-93

Delannet, M., Martin, F., Bossy, B., Cheresh, D.A., Reichardt, L.F., & Duband, J.L. (1994). Specific roles of the alpha V beta 1, alpha V beta 3 and alpha V beta 5 integrins in avian neural crest cell adhesion and migration on vitronectin. *Development.* 120: 2687-702

Desban, N., & Duband, J-L. (1997). Avian neural crest cell migration on laminin: interaction of the a1b1 integrin with distinct laminin-1 domains mediates different adhesive responses. *J Cell Sci.* 110: 2729-44

Downward, J. (1994). The GRB2/Sem-5 adaptor protein. *FEBS Lett*. 338: 113-7

Dunn, D.A., Kooyman, D.L., Pinkert, C.A., & Sang, H.M. (2005). Transgenic animals and their impact on the drug discovery industry. *Drug Discov Today*. 10: 191-6

Duong, T.D., & Erickson, C.A. (2004). MMP-2 plays an essential role in producing epithelial-mesenchymal transformations in the avian embryo. *Dev Dyn*. 229: 42-53

Dutt, P., Hanesberg, H., Vik, T., Williams, D.A., & Yoder, M.C. (1997). A recombinant human fibronectin fragment facilites retroviral mediated gene transfer into human hematopoietic progenitor cells. *Biochem Mol Biol Int*. 42(5): 909-17

Ellens, H., Bentz, J., & Szoka, F.C. (1984). pH-induced destabilization of phosphatidylethanolamine-containing liposomes: role of bilayer contact. *Biochemistry*. 23: 1532

Erickson, C.A. (1986). Morphogenesis of the neural crest. *Dev Biol*. 2: 481-543

Erickson, C. (1987). Behavior of neural crest cells on embryonic basal laminae. *Dev Biol*. 120: 38-49

Erickson, C.A., Duong, T.D., & Tosney, K.W. (1992). Descriptive and experimental analysis of the dispersion of neural crest cells along the dorsolateral path and their entry into ectoderm in the chick embryo. *Dev Biol*. 151: 251-72

Faraldo, M.M., Deugnier, M-A., Lukashev, M., Thiery, J.P., & Glukhova, M.A. (1998). Perturbation of beta1-integrin function alters the development of murine mammary gland. *EMBO J*. 17: 2139-47

Farhood, H., Bottega, R., Epand, R.M., & Huang, L. (1992). Effect of cationic cholesterol derivatives on gene transfer and protein kinase C activity. *Biochem Biophys Acta*. 1111: 239

Farlie, P.G., Kerr, R., Thomas, P., Symes, T., Minichiello, J., Hearn, C.J., & Newgreen, D. (1999). A paraxial exclusion zone creates patterned cranial neural crest cell outgrowth adjacent to rhombomeres 3 and 5. *Dev Biol*. 213: 70-84

Farquhar, M.G., & Palade, G. (1965). Junctional complexes in various epithelia. *J Cell Biol.* 17: 375-412

Fässler, R., & Meyer, M. (1995). Consequences of lack of beta1 integrin gene expression in mice. *Genes Dev.* 9: 1896-908

Felgner, P.L., Gadek, T.R., Holm, M., Roman, R., Chan, H.W., Wenz, M., Northrop, J.P., & Danielsen, M. (1987). Lipofectin: a highly efficient, lipid-mediated DNA-transfecting procedure. *Proc Natl Acad Sci USA.* 84: 7413

Fixman, E.D., Naujokas, M.A., Rodrigues, G.A., Moran, M.F., & Park, M. (1995). Efficient cell transformation by the Tpr-Met oncoprotein is dependent upon tyrosine 489 in the carboxy-terminus. *Oncogene.* 10: 237-49

Flamant, F., Demeneix, B., Benoist, C., Markossian-Belin, S., & Samarut, J. (1994). Virofection: a new procedure to achieve stable expression of genes transferred into early embryos. *Int J Dev Biol.* 38: 751-7

Fraley, R., Subramani, S., Berg, P., & Papahadjopoulos, D. (1980). Introduction of liposome-encapsulated SV40 DNA into cells. *J Biol Chem.* 244: 10431

Fraser, S.E., & Bronner-Fraser, M. (1991). Migrating neural crest cells in the trunk of the avian embryo are multipotent. *Development.* 112: 913-20

Frixen, U.H., Behrens, J., Sachs, M., Eberle, G., Voss, B., Warda, A., Löchner, D., & Birchmeier, W. (1991). E-cadherin-mediated cell-cell adhesion prevents invasiveness of human carcinoma cells. *J Cell Biol.* 113: 173-85

Fromm, M., Taylor, L.P., & Walbot, V. (1985). Expression of genes transferred into monocot and dicot plant cells by electroporation. *Proc Natl Acad Sci USA.* 82: 5824-8

Garcia-Castro, M.I., Marcelle, C., & Bronner-Fraser, M. (2002). Ectodermal Wnt function as a neural crest inducer. *Science.* 297: 848-51

Garratt, A.N., & Humphries, M.J. (1995). Recent insights into ligand binding, activation and signaling by integrin adhesion receptors. *Acta Anat.* 154: 34-45

Geiger, B., Yehuda-Levenburg, S., & Bershadsky, A.D. (1995). Molecular interactions in the sub-membrane plaque of cell-cell and cell-matrix adhesions.

Acta Anat. 154: 46-62

Gilmore, A.P, & Burridge, K. (1996). Regulation of vinculin binding to talin and actin by phosphatidyl-inositol-4-5-bisphosphate. *Nature*. 381: 531-5

Gimond, C., van der Flier, A., van Delft, S., Brakebusch, C., Kuikman, I., Collard, J.G., Fässler, R., & Sonnenberg, A. (1999). Induction of cell scattering by expression of beta1 integrins in beta1-deficient epithelial cells requires activation of members of the Rho family of GTPases and downregulation of cadherin and catenin function. *J Cell Biol*. 147: 1325-40

Gordon, J.W. (1989). Transgenic animals. *Int Rev Cytol*. 155: 171-229

Göttig, S., Möbest, D., Rüster, B., Grace, G., Winter, S., Seifried, E., Gille, J., Wieland, T., & Henschler, R. (2006). Role of the monomeric GTPase Rho in hematopoietic progenitor cell migration and transplantation. *Eur J Immunol*. 36: 1-10

Gradl, D., Kuhl, M., & Wedlich, D. (1999). The Wnt/Wg signal transducer beta-catenin controls fibronectin expression. *Mol Cell Biol*. 19: 5576-87

Graham, A., & Lumsden, A. (1996). Patterning the cranial neural crest. *Biochem Soc Symp*. 62: 77-83

Graham, A., Heyman, I., & Lumsden, A. (1993). Even-numbered rhombomeres control the apoptotic elimination of neural crest cells from odd-numbered rhombomeres in the chick hindbrain. *Development*. 119: 233-45

Graham, A., Koentges, G., & Lumsden, A. (1996). Neural crest apoptosis and the establishment of craniofacial pattern: and honorable death. *Mol Cell Neurosci*. 8: 76-83

Greber, U.F., Willettis, M., Webster, P., & Helenius, A. (1993). Stepwise dismantling of adenovirus 2 during entry into cells. *Cell*. 75: 477

Greenbaum, D., Colangelo, C., Williams, K., & Gerstein, M. (2003). Comparing protein abundance and mRNA expression levels on a genomic scale. *Genome Biol*. 4: 117

Greenburg, G., & Hay, E.D. (1982). Epithelia suspended in collagen gels lose

polarity and express characteristics of migrating mesenchyme-like cells. *J Cell Biol*. 95: 333-9

Gunzburg, W.H., & Salmons, B. (1995). Virus vector design in gene therapy. *Mol Med Today*. 1: 410-7

Hall, A. (1998). Rho GTPases and the actin cytoskeleton. *Science*. 279: 509-14

Hall, A., & Nobes, C.D. (2000). Rho GTPases: molecular switches that control the organization and dynamics of the actin cytoskeleton. *Phil Trans R Soc Lond B*. 355: 965-70

Hall, B.K. (2000). The neural crest as a forth germ layer and vertebrates as quadroblastic not triploblastic. *Evol Dev*. 2: 3-5

Hall, B.K., & Horstadius, S. (1988). The Neural Crest. *London:* Oxford University Press.

Hamburger, V., & Hamilton, H.L. (1951). A series of normal stages in the development of the chick embryo. *J Morph*. 88: 49-92

Hammerschmidt, M., Pelegri, F., Mullins, M.C., Kane, D.A., van Eeden, F.J., Granato, M., Brand, M., Furutani-Seiki, M., Haffter, P., Heisenberg, C.P., Jiang, Y.J., Kelsh, R.N., Odenthal, J., Warga, R.M., & Nusslein-Volhard, C. (1996). dino and mercedes, two genes regulating dorsal development in the zebrafish embryo. *Development*. 123: 95-102

Hanks, S.K., Ryzhova, L., Shin, N.Y., & Brabek, J. (2003). Focal adhesion kinase signaling activities and their implications in the control of cell survival and motility. *Front Biosci*. 8: d982-96

Harkin, D.G., & Hay, E.D. (1996). Effects of electroporation on the tubulin cytockeleton and directed migration of corneal fibroblasts cultured within collagen matrices. *Cell Motil Cytoskeleton*. 35: 345-7

Hashimoto, K., Fujimoto, H., & Nakatsuji, N. (1987). An ECM substratum allows mouse mesodermal cells isolated from the primitive streak to exhibit motility similar to that inside the embryo and reveals a deficiency in the T/T mutant cells. *Development*. 100: 587-98

Hato, T., Pampori, N., & Shattil, S.J. (1998). Complementary roles for receptor clustering and conformational change in the adhesive and signaling functions of integrin alphaIIb beta3. *J Cell Biol.* 141: 1685-95

Hawley-Nelson, P., Ciccarone, V., Gebeyehu, G., & Jessee, J. (1993). LipofectAMINE reagent: a new, higher efficiency polycationic liposome transfection reagent. *Focus.* 15: 73-9

Hay, E.D. (1995). An overview of epithelio-mesenchymal transformation. *Acta Anat.* 154: 8-20

Heiser, W.C. (1994). Gene transfer into mammalian cells by particle bombardment. *Anal Biochem.* 217: 185

Henderson, D.J., Ybot-Gonzalez, P., & Copp, A.J. (2000). Gene expression pattern RhoB is expressed in migrating neural crest and endocardial cushions of the developing mouse embryo. *Mech Dev.* 95: 211-4

Hernandez, V.H., & Bueno, D. (2005). RNA interference is ineffective as a routine method for gene silencing in chick embryos as monitored by fgf8 silencing. *Int J Biol Sci.* 1: 1-12

Hotchin, N., & Hall, A. (1995). The assembly of integrin adhesion complexes requires both extracellular matrix and intracellular Rho/Rac GTPases. *J Cell Biol.* 131: 1857-65

Hotchin, N.A., & Hall, A. (1996). Regulation of the actin cytoskeleton, integrins and cell growth by the Rho family of small GTPases. *Cancer Surv.* 27: 311-22

Huang, L., Connor, J., & Wang, C.Y. (1987). pH-sensitive immunoliposomes. *Methods Enyzmol.* 149: 88

Huber, A.H., Stewart, D.B., Laurents, D.V., Nelson, W.J., & Weis, W.I. (2001). The cadherin structural domain is unstructured during the absence of beta-catenin: a possible mechanism for regulating cadherin turnover. *J Biol Chem.* 276: 12301-9

Hui, S.W. (1995). Effects of pulse length and strength on electroporation efficiency. *Methods Mol Biol.* 55: 29-40

Hülsken, J., Birchmeier, W., & Behrens, J. (1994). E-cadherin and APC compete for interaction with beta-catenin and the cytoskeleton. *J Cell Biol.* 127: 2061-9

Hunter, C.V., Tiley, L.S., & Sang, H.M. (2005). Developments in transgenic technology: applications for medicine. *Trends Mol Med.* 11: 293-8

Hynes, R.O. (2002). Integrins: directional, allosteric signaling machines. *Cell.* 110: 7673-87

Inada, H., Ghanem, A.H., & Higuchi, W.I. (1994). Studies on the effects of applied voltage and duration on human epidermal membrane alteration/recovery and the resultant effects upon iontophoresis. *Pharm Res.* 11: 687-97

Jackson, B.W., Grund, C., Winter, S., Franke, W.W., & Illmensee, K. (1981). Formation of cytoskeletal elements during mouse embryogenesis. II. Epithelial differentiation an intermediate-sized filaments in early embryos. *Differentiation.* 20: 203-16

Jansen, R.C., Nap, J-P., & Mlynárová, L. (2002). Errors in genomics and proteomics. *Nature Biotech.* 20: 19

Jesuthasan, S. (1997). Neural crest cell migration in the zebrafish can be mimicked by inert objects: mechanism and implication of latex bead movement in embryos. *J Exp Zool.* 277: 425-34

Johnson, P.A., Miyanohara, A., Levine, F., Cahill, T., & Friedmann, T. (1992). Cytotoxicity of a replicative-defective mutant of herpes simplex virus type 1. *J Virol.* 66: 2952

Kaneda, Y., Iwai, K., & Uchida, T. (1989). Increased expression of DNA cointroduced with nuclear protein in adult rat liver. *Science.* 243: 375-8

Katahira, T., & Nakamura, H. (2003). Gene silencing in chick embryos with a vector-based small interfering RNA system. *Dev Growth Differ.* 45: 361-7

Katoh, H., Hiramoto, K., & Negishi, M. (2005). Activation of Rac1 by RhoG regulates cell migration. *J Cell Sci.* 119: 56-65

Kavanaugh, M.P., Miller, D.G., Zhang, M., Law, W., Kozak, S.L., & Miller, A.D. (1994). Cell-surface receptors for gibbon ape leukemia virus and murine

retrovirus are inducible sodium-dependent phosphate symporters. *Proc Natl Acad Sci USA*. 91: 7071

Kiernan, A.E., & Fekete, D.M. (1997). In vivo gene transfer into the embryonic inner ear using retroviral vectors. *Audiol Neurootol*. 2: 12-24

Kil, S.H., Lallier, T., & Bronner-Fraser, M. (1996). Inhibition of cranial neural crest adhesion in vitro and migration in vivo using integrin antisense oligonucleotides. *Dev Biol*. 179: 91-101

Kil, S.H., Krull, C.E., Cann, G., Clegg, D., & Bronner-Fraser, M. (1998). The alpha4 integrin subunit is important for neural crest cell migration. *Dev Biol*. 202: 29-42

Kim, M., Carman, C.V., & Springer, T.A. (2003). Bidirectional transmembrane signaling by cytoplasmic domain separation in integrins. *Science*. 301: 1720-5

Kim, H.J., Greenleaf, J.F., & Kinnick, R.R. (1996). Ultrasound-mediated transfection of mammalian cells. *Hum Gene Ther*. 7: 1339-46

Kim, K., Lu, Z., & Hay, E.D. (2002). Direct evidence for a role of beta-catenin/LEF-1 signaling pathway in induction of EMT. *Cell Biol Int*. 26: 463-76

Kitamura, T., Koshino, Y., & Shibata, F. (2003). Retrovirus-mediated gene transfer and expression cloning: Powerful tools in functional genomics. *Exp Hematol*. 31: 1007-14

Klein, T.M., Wolf, E.D., Wu, R., & Sanford, J.C. (1987). High-velocity microprojectiles for delivering nucleic acids into living cells. *Nature*. 327: 70

Klenchin, V.A., Sukharev, S.I., Serov, S.M., Chernomordik, L.V., & Chidmadzhev, Y.A. (1991). Electrically induced DNA uptake by cells is a fast process involving DNA electrophoresis. *Biophys J*. 60: 804-11

Kolesnikov, V.A., Zelenina, I.A., Semenova, M.L., Shafei, R., & Zelenin, A.V. (1995). The ballistic transfection of mammalian cells in vivo. *Ontogenez*. 26: 467-80

Kulsea, P.M., & Fraser, S.E. (2000). In ovo analysis of chick hindbrain neural crest cell migration shows cell interactions during migration to branchial arches.

Development. 127: 1161-72

Kuroda, S., Fukata, M., Kobayashi, K., Nakafuku, M., Nomura, N., Iwamatsu, A., & Kaibuchi, K. (1996). Identification of IQGAP as a putative target for the small GTPases, Cdc42 and Rac1. *J Biol Chem*. 271: 23363-7

Kuroda, S., Fukata, M., Nakagawa, M., Fujii, K., Nakamura, T., Ohkubo, T., Izawa, I., & Nagase, T. (1998). Role of IQGAP, a target of the small GTPases Cdc42 and Rac1, in regulation of E-cadherin-mediated cell-cell adhesion. *Science*. 281: 832-5

LaBonne, C., & Bronner-Fraser, M. (1998). Neural crest induction in Xenopus: evidence for a two-signal model. *Development*. 125: 2403-14

LaFlamme, S.E., Thomas, L.A., Yamada, S.S., & Yamada, K.M. (1994). Single subunit chimeric integrins as mimics and inhibitors of endogenous integrin functions in receptor localization, cell spreading and migration, and matrix assembly. *J Cell Biol*. 126: 1287-98

Lallier, T., & Bronner-Fraser, M. (1991). Avian neural crest cell attachment to laminin: Involvement of divalent cation dependent integrins. *Development*. 113: 1069-84

Lallier, T., & Bronner-Fraser, M. (1992). Alpha 1 beta 1 integrin on neural crest cells recognizes some laminin substrata in a Ca(2+)-independent manner. *J Cell Biol*. 119: 1335-45

Lallier, T., Leblanc, G., Artinger, K.B., & Bronner-Fraser, M. (1992). Cranial and trunk neural crest cells use different mechanisms for attaching to extracellular matrices. *Development*. 116: 531-41

Lamarche, N., & Hall, A. (1994). GAPs for rho-related GTPases. *Trends Genet*. 10: 436-40

Le Douarin, N.M. (1982). The Neural Crest. *Cambridge, UK:* Cambridge University Press.

Le Douarin, N.M., & Dupin, E. (1993). Cell lineage analysis in neural crest ontogeny. *J Neurobiol*. 24: 146-61

Le Douarin, N.M., & Kalcheim, C. (1999). The Neural Crest, 2nd ed. *Cambridge, UK:* Cambridge University Press.

Le Douarin, N.M., & Teillet, M.M. (1974). Experimental analysis of the migration and differentiation of neuroblasts of the autonomic nervous system and of neurectodermal mesenchymal derivatives, using a cell marking technique. *Dev Biol.* 41: 162-84

Leber, S.M., Yamagata, M., & Sanes, J.R. (1996). Gene transfer using replication-defective retroviral and adenoviral vectors. *Meth Cell Biol.* 51: 161-83

Ledley, F.D. (1995). Nonviral gene therapy: The promise of genes as pharmaceutical products. *Human Gene Ther.* 6: 1129

Lee, M., Cram, E.J., Shen, B., & Schwarzbauer, J.E. (2001). Roles for betapat-3 integrins in development and function of Caenorhabditis elegans muscles and gonads. *J Biol Chem.* 276: 36404-10

Lee, R.J., & Huang, L. (1996). Folate-targeted, anionic liposome-entrapped polylysine-condensed DNA (LPDII) for tumor cell-specific gene transfer. *J Biol Chem.* 271: 8481

Lee, R.J., & Huang, L. (1997). Lipidic vector systems for gene transfer. *Crit Rev Ther Drug Carrier Syst.* 14: 173-206

Legendre, J.Y., & Szoka, F.C.J. (1992). Delivery of plasmid DNA into mammalian cell lines using pH-sensitive liposomes: comparision with cationic liposomes. *Pharm Res.* 9: 1235

Levy, J.P., Muldoon, R.R., Zolotukhin, S., & Link, C.J. (1996). Retroviral transfer and expression of a humanized, red-shifted green fluorescent protein gene into human tumor cells. *Nat Biotechnol.* 14: 610-4

Lewis, J.G., Lin, K.Y., Kothavale, A., lanagan, W.M., Matteucci, M.D., DePrince, R.B., & Wagner, R.W. (1996). A serum-resistant cytofectin for cellular delivery of antisense oligodeoxynucleotides and plasmid DNA. *Proc Natl Acad Sci USA.* 93: 3176-81

Li, Y., Behnam, J., & Simkiss, K. (1995). Ballistic transfection of avian primordial

germ cell in ovo. *Transgenic Res*. 4: 26-9

Li, R., Babu, C.R., Lear, J.D., Wand, A.J., Bennett, J.S., & DeGrado, W.F. (2001). Oligomerization of the integrin alphaIIbbeta3: roles of the transmembrane and cytoplasmic domains. *Proc Natl Acad Sci USA*. 98: 12462-7

Li, R., Mitra, N., Gratkowski, H., Vilaire, G., Weisel, J.W., Lear, J.D., DeGrado, W.F., & Bennett, J.S. (2003). .Activation of integrin alphaIIbbeta3 by modulation of transmembrane helix associations. *Science*. 300: 795-8

Lichtenberg, D., & Barenholz, Y. (1988). Liposomes: preparation, characterization, and preservation. *Methods Biochem Anal*. 33: 337

Liem, K.F., Tremml, G., Roelink, H., & Jessell, T.M. (1995). Dorsal differentiation of neural plate cells induced by BMP-mediated signals from epidermal ectoderm. *Cell*. 82: 969-79

Lillico, S.G., McGrew, M.J., Sherman, A., & Sang, H.M. (2005). Transgenic chickens as bioreactors for protein-based drugs. *Drug Discov Today*. 10: 191-6

Lim, Y., Han, I., Jeon, J., Park, H., Bahk, Y.Y., & Oh, E.S. (2004). Phosphorylation of focal adhesion kinase at tyrosine 861 is crucial for Ras transformation of fibroblasts. *J Biol Chem*. 279: 29060-5

Liu, J-P., & Jessell, T.M. (1998). A role for rhoB in the delamination of neural crest cells from the dorsal neural tube. *Development*. 125: 5055-67

Liu, Y., Liggitt, D., Zhong, W., Tu, G., Gaensler, K., & Debs, R. (1995). Cationic liposome-mediated intravenous gene delivery. *J Biol Chem*. 270: 24864

Lorenzi, G.L., & Lee, K.D. (2005). Enhanced plasmid DNA delivery using anionic LPDII by listeriolysin O incorporation. *J Gene Med*. 7: 1077-85

Love, J., Gribbin, C., Mather, C., & Sang, H. (1994). Transgenic birds by DNA microinjection. *Biotechnology NY*. 12: 60-3

Lukashev, M.E., Sheppard, D., & Pytela, R. (1994). Disruption of integrin function and induction of tyrosine phosphorylation by the autonomously expressed beta1 integrin cytoplasmic domain. *J Biol Chem*. 269: 18311-4

Luo, L., Hensch, T.K., Ackerman, L., Barbel, S., Jan, L.Y., & Jan, Y.N. (1996).

Differential effects of the Rac GTPase on purkinje cell axons and dendritic trunks and spines. *Nature*. 379: 837-40

Luo, B., & Springer, T.A. (2006). Integrin structures and conformational signaling. *Curr Opin Cell Biol*. 18: 579-86

Lurquin, P.F. (1997). Gene transfer by electroporation. *Mol Biotechnol*. 7: 5-35

Mackay, D.J., & Hall, A. (1998). Rho GTPases. *J Biol Chem*. 273: 20685-8

Mahato, R.I. (2005). Water insoluble and soluble lipids for gene delivery. *Adv Drug Deliv Rev*. 57: 699-712

Marsden, M., & DeSimone, D.W. (2001). Regulation of cell polarity, radial intercalation and epiboly in Xenopus: novel roles for integrin and fibronectin. *Development*. 128: 3635-47

Martins-Green, M., & Erickson, C.A. (1987). Basal lamina is not a barrier to neural crest cell emigration: documentation by TEM and by immunofluorescent and immunogold labelling. *Development*. 3: 517-33

Mayor, R., Morgan, R., & Sargent, M. (1995). Induction of the prospective neural crest of Xenopus. *Development*. 121: 767-77

McLachlin, J.R., Mittereer, N., Dauchier, M.B., Kadan, M., & Eglitis, M.A. (1993). Factors affecting retroviral vector function and structural integrity. *Virology*. 195: 1-5

Melkonyan, H., Sorg, C., & Klempt, M. (1996). Electroporation efficiency in mammalian cells is increased by dimethyl sulfoxide (DMSO). *Nucleic Acids Res*. 24: 4356-7

Mir, M., Bureau, M.F., Gehl, J., Rangara, R., Rouy, D., Caillaud, J.M., Delaere, D., Branellec, B., Schwartz, B., & Scherman, D. (1999). High-efficiency gene transfer into skeletal muscle mediated by electric pulses. *Proc Natl Acad Sci USA*. 96: 4262-7

Mistry, A.R., Falciola, L., Monaco, L., Tagliabue, R., Acerbis, G., Knight, A., Harbottle, R.P., & Hart, S.L. (1997). Recombinant HMG1 protein produced in Pichia pastoris: a nonviral gene delivery agent. *Biotechniques*. 22: 718-29

Miyamoto, S., Akiyama, S.K., & Yamada, K.M. (1995). Synergistic roles for receptor occupancy and aggregation in integrin transmembrane function. *Science*. 267: 883-5

Molenaar, M., van de Wetering, M., Oosterwegel, M., Peterson-Maduro, J., Godsave, S., Korinek, K., Roose, J., & Clevers, H. (1996). XTcf-3 transcription factor mediates beta-catenin-induced axis formation in Xenopus embryos. *Cell*. 86: 391-9

Monier-Gavelle, F., & Duband, J-L. (1997). Cross talk between adhesion molecules: control of N-cadherin activity by intracellular signals elicited by beta1 and beta3 integrins in migrating neural crest cells. *J Cell Biol*. 137: 1663-81

Morin, C., Langlais, J., & Lambert, R.D. (1992). Possible implication of lysophosphatidylcholine in cell fusion accompanying implantation in rabbits. *J Reprod Fertil*. 96: 827-36

Morgan, B.A., & Fekete, D.M. (1996). Manipulating gene expression with replication-competent retroviruse. *Meth Cell Biol*. 51: 185-218

Morgan, B.A., Izpisua-Belmonte, J., Douboule, D., & Tabin, C. (1992). Targetted misexpression of Hox-4.6 in the avian limb bud causes apparent homeotic transformations. *Nature*. 385: 236-39

Morgan, W.F., & Day, J.P. (1995). The introduction of proteins into mammalian cells by electroporation. *Methods Mol Biol*. 48: 63-71

Muenchau, D.D., Freeman, S.M., Cornetta, K., Zwiebel, J.A., & Anderson, W.F. (1990). Analysis of retroviral packaging lines for generation of replication-competent virus. *Virology*. 176: 262-5

Mulligan, R.C. (1993). The basic science of gene therapy. *Science*. 260: 926-32

Muramatsu, T., Mizutani, Y., & Okumura, J. (1996a). Effects of incubation time and injection sites on gene transfection efficiency in chicken embryos by in ovo lipofection. *Anim Sci Technol Jpn*. 67: 882-6

Muramatsu, T., Mizutani, Y., & Okumura, J. (1996b). Live detection of the firefly luciferase gene expression by bioluminescence in incubating chicken eggs. *Anim*

Sci Technol Jpn. 67: 906-9

Muramatsu, T., Mizuntani, Y., Ohmori, Y., & Okumura, J. (1997a). Comparison of three nonviral transfection methods for foreign gene expression in early chicken embryos in ovo. *Bioc Biophys Res Comm.* 23: 376-80

Muramatsu, T., Shibata, O., Ryoki, S., Ohmori, Y., & Okumura, J. (1997b). Foreign gene expression in the mouse testis by localized in vivo gene transfer. *Biochem Biophys Res Comm.* 233: 45-9

Murata, T., Hoffmann, S., Ishibashi, T., Spee, C., Gordon, E.M., Anderson, W.F., Hinton, D.R., & Ryan, S.J. (1998). Retrovirus-mediated gene transfer targeted to retinal photocoagulation sites. *Diabetologia.* 41: 500-6

Nakagawa, S., & Takeichi, M. (1998). Neural crest emigration from the neural tube depends on regulated cadherin expression. *Development.* 125: 2963-71

Nakamura, H., & Ayer-Le Lievre, C.S. (1982). Mesoectodermal capabilities of the trunk neural crest of birds. *J Embryol Exp Morph.* 70: 1-18

Nakamura, K., Yano, H., Schaefer, E., & Sabe, H. (2001). Different modes and qualities of tyrosine phosphorylation of Fak and Pyk2 during epithelial-mesenchymal transdifferentiation and cell migration:analysis of specific phosphorylation events using site-directed antibodies. *Oncogene.* 20: 2626-35

Nakanishi, M. (1995). Gene introduction into animal tissues. *Crit Rev Ther Drug Carrier Syst.* 12: 263-310

Neumann, E., Schaeffer-Ridder, M., Wang, Y., & Hofschneider, P.H. (1982). Gene transfer into mouse lyoma cells by electroporation in high electric fields. *EMBO J.* 1: 841-5

Newgreen, D.F., & Minichiello, J. (1995). Control of epithelio-mesenchymal transformation: events in the onset of neural crest cell migration are separable and inducible by protein kinase inhibitors. *Dev Biol.* 170: 91-101

Nicolau, D., & Cudd, A. (1989). Liposomes as carriers of DNA. *Crit Rev Ther Drug Carrier Syst.* 6: 239

Nieto, A.M., Sargent, M.G., Wilkinson, D.G., & Cooke, J. (1994). Control of cell

behavior during vertebrate development by Slug, a zinc finger gene. *Science*. 264: 835-9

Nobes, C.D., & Hall, A. (1995). Rho, Rac, and Cdc42 GTPases regulate the assembly of multimolecular focal complexes associated with actin stress fibers, lamellipodia, and filopodia. *Cell*. 81: 53-62

Nobes, C.D., & Hall, A. (1999). Rho GTPases control polarity, protrusion, and adhesion during cell movement. *J Cell Biol*. 144: 1235-44

Noden, D.M. (1975). An analysis of the migratory behavior of avian cephalic neural crest cells. *Dev Biol*. 42: 106-30

Noden, D.M. (1986). Patterning avian craniofacial muscles. *Dev Biol*. 116: 347-56

Novak, A., Hsu, S.C., Leung-Hagesteijn, C.Y., Radeva, G., Papkoff, J., Montesano, R., Roskelley, C., & Dedhar, S. (1998). Cell adhesion and the integrin-linked kinase regulate the LEF-1 and beta-catenin signaling pathways. *Proc Natl Acad Sci USA*. 95: 4374-9

Ohki, S., Thacore, H., & Flanagan, T.D. (2004). Effects of temperature on viral glycoprotein mobility and a possible role of internal "viroskeleton" proteins in Sendai virus fusion. *J Membr Biol*. 199: 73-83

Ojakian, G.K., Nelson, W.J., & Beck, K.A. (1997). Mechanisms for de novo biogenesis of an apical membrane compartment in groups of simple epithelial cells surrounded by extracellular matrix. *J Cell Sci*. 110: 2781-94

Okada, Y. (1969). Factors in fusion of cells by HVJ. *Curr Top Microbiol Immunol*. 48: 102-8

Olofsson, B. (1999). Rho guanine dissociation inhibitors: pivotal molecules in cellular signalling. *Cell Signal*. 11: 545-54

Oloumi, A., McPhee, T., & Dedhar, S. (2004). Regulation of E-cadherin expression and beta-catenin/Tcf transcriptional activity by the integrin-linked kinase. *Biochim Biophys Acta*. 1691: 1-15

Palmiter, R.D., & Brinster, R.L. (1986). Germ-line transformation of mice. *Annu Rev Genet*. 20: 465-99

Perez-Alcala, S., Nieto, M.A., & Barbas, J.A. (2004). LSox5 regulates RhoB expression in the neural tube and promotes generation of the neural crest. *Development*. 131: 4455-65

Perry, M.M., Morrice, D., Hettle, S., & Sang, H. (1991). Expression of exogenous DNA during the early development of the chick embryo. *Roux's Arch Dev Biol*. 200: 312-9

Petitte, J.N., Liu, G., & Yang, Z. (2004). Avian pluripotent stem cells. *Mech Dev*. 121: 1159-68

Petropoulos, C.J., & Hughes, S.H. (1991). Replication-competent retrovirus vectors for the transfer and expression of gene cassetes in avian embryos. *J Virol*. 65: 3728-37

Pietri, T., Thiery, J.P., & Dufour, S. (2003). Differential expression of beta3 integrin gene in chick and mouse cranial neural crest cells. *Dev Dyn*. 227: 309-13

Platt, J.B. (1893). Ectodermic origin of the cartilage of the head. *Anat Anz*. 8: 506-9

Polakis, P. (2000). Wnt signaling and cancer. *Genes Dev*. 14: 1837-51

Potempa, S., & Ridley, A.J. (1998). Activation of both MAPK and phosphotidylinositide 3-kinase by Ras is required for HGF/SF-induced adherens junction disassembly. *Mol Biol Cell*. 9: 2185-95

Qian, J., Yang, J., Dragovic, A.F., Abu-Isa, E., Lawrence, T.S., & Zhang, M. (2005). Ionizing radiation-induced adenovirus infection is mediated by Dynamin 2. *Cancer Res*. 65: 5493-7

Quilliam, L.A., Kato, K., Rabun, K.M., Hisaka, M.M., Huff, S.Y., Campbell-Burk, S., & Der, C.J. (1994). Identification of residues critical for Ras(17N) growth-inhibitory phenotype and for Ras interaction with guanine nucleotide exchange factors. *Mol Cell Biol*. 14: 1113-21

Ramani, K., Hassan, Q., Venkaiah, B., Hasnain, S.E., & Sarkar, D.P. (1998). Site-specific gene delivery in vivo through engineered Sendai viral envelopes. *Proc Natl Acad Sci USA*. 95: 11886-90

Ray, J., Wolfe, J.H., Aguirre, G.D., & Haskins, M.E. (1998). Retroviral cDNA

transfer to the RPE: stable expression and modification of metabolism. *Invest Ophthalmol Vis Sci*. 39: 1658-66

Revel, J.P., & Brown, S.S. (1975). Cell junctions in development with particular reference to the neural tube. *Cold Spring Harb Symp Quant Biol*. 40: 433-55

Richards, R.J. (1992). The Meaning of Evolution. *Chicago:* University of Chicago Press.

Riddle, R.D., Johnson, R.L., Laufer, E., & Tabin, C. (1993). Sonic hedgehog mediates the polarizing activity of the ZPA. *Cell*. 75: 1401-16

Roe, T., Renolds, T.C., Yu, G., & Brown, P.O. (1993). Integration of murine leukemia virus DNA depends on mitosis. *EMBO J*. 12: 2099

Roura, S., Miravet, S., Piedra, J., de Herreros, A.G., & Duñach, M. (1999). Regulation of E-cadherin/catenin association by tyrosine phosphorylation. *J Biol Chem*. 274: 36734-40

Rovasio, R.A., Delouvee, A., Yamada, K.M., Timpl, R., & Thiery, J.P. (1983). Neural crest cell migration: requirements for exogenous fibronectin and high cell density. *J Cell Biol*. 96: 462-73

Ruoslahti, E., & Reed, J.C. (1994). Anchorage dependence, integrins, and apoptosis. *Cell*. 77: 477-8

Sakamoto, K., Nakamura, H., Takagi, M., Takeda, S., & Katsube, K. (1998). Ectopic expression of lunatic Fringe leads to downregulation of Serrate-1 in the developing chick neural tube; analysis using in ovo electroporation. *FEBS Lett*. 426: 337-41

Samuelson, S.S., Luther, P.W., Pumplin, D.W., & Bloch, R.J. (1993). Structures linking microfilament bundles to the membrane at focal contacts. *J Cell Sci*. 122: 485-96

Sanes, J.R., Rubenstein, J.L.R., & Nicolas, J.F. (1986). Use of recombinant retrovirus to study post-implantation cell lineage in mouse embryos. *EMBO J*. 5: 3133-42

Sang, H. (2004). Prospects for transgenesis in the chick. *Mech Dev*. 121: 1179-86

Sasai, Y., & De Robertis, E.M. (1997). Ectodermal patterning in vertebrate embryos. *Dev Biol*. 182: 5-20

Savagner, P., Boyer, B., Valles, A.M., Jouanneau, J., & Thiery, J.P. (1994). Modulations of the epithelial phenotype during embryogenesis and cancer progression. *Cancer Treat Res*. 71: 229-49

Savagner, P., Yamada, K.M., & Thiery, J.P. (1997). The zinc-finger protein slug causes desmosome dissociation, an initial and necessary step for growth factor-induced epithelial-mesenchymal transition. *J Cell Biol*. 137: 1403-19

Schiedner, G., Morral, N., Parks, R.J., Wu, Y., Koopmans, S.C., Langston, C., & Graham, F.L. (1998). Genomic DNA transfer with a high-capacity adenovirus vector results in improved in vivo gene expression and decreased toxicity. *Nat Genet*. 18: 180-3

Schlaepfer, D.D., & Hunter, T. (1996). Evidence for in vivo phosphorylation of the Grb2 SH2-domain binding site on focal adhesion kinase by Src-family protein-tyrosine kinases. *Mol Cell Biol*. 16: 5623-33

Sechrist, J., Serbedzija, G.N., Scherson, T., Fraser, S.E., & Bronner-Fraser, M. (1993). Segmental migration of the hindbrain neural crest does not arise from its segmental generation. *Development*. 118: 691-703

Sela-Donenfield, D., & Kalcheim, C. (1999). Regulation of the onset of neural crest migration by coordinated activity of BMP4 and Noggin in the dorsal neural tube. *Development*. 126: 4749-62

Selleck, M.A. (1996). Culture and microsurgical manipulation of the early avian embryo. *Methods Cell Biol*. 51: 1-21

Selleck, M.A.J., & Bronner-Fraser, M. (1996). The genesis of avian neural crest cells: a classic embryonic induction. *Proc Natl Acad Sci USA*. 93: 9352-7

Selleck, M.A.J., & Bronner-Fraser, M. (2000). Avian neural crest cell fate decisions: a diffusible signal mediates induction of neural crest by the ectoderm. *Int J Devl Neuroscience*. 18: 621-7

Shapiro, L., Fannon, A.M., Kwong, P.D., Thompson, A., Lehmann, M.S.,

Grübel, G., Legrand, J-F., & Hendrickson, W.A. (1995). Structural basis of cell-cell adhesion by cadherins. *Nature*. 374: 327-37

Shimaoka, M., Takagi, J., & Springer, T.A. (2002). Conformational regulation of integrin structure and function. *Annu Rev Biophys Biomol Struct*. 31: 485-516

Shook, D., & Keller, R. (2003). Mechanisms, mechanics and function of epithelial-mesenchymal transitions in early development. *Mech Dev*. 120: 1351-83

Shore, E.M., & Nelson, W.J. (1991). Biosynthesis of the cell adhesion molecule uvomorulin (E-cadherin) in Madin-Darby canine kidney epithelial cells. *J Biol Chem*. 266: 19672-80

Simons, K., & Fuller, S.D. (1985). Cell surface polarity in epithelia. *Annu Rev Cell Biol*. 1: 243-88

Skehel, J.J., & Wiley, D.C. (2000). Receptor binding and membrane fusion in virus entry: the influenza hemagglutinin. *Annu Rev Biochem*. 69: 531-69

Small, J.V., Stradal, T., Vignal, E., & Rottner, K. (2002). The lamellipodium: where motility begins. *Trends Cell Biol*. 12: 112-20

Smilenov, L.B., Mikhailov, A., Marcantonio, E.E., & Gundersen, G.G. (1999). Focal adhesion motility revealed in stationary fibroblasts. *Science*. 286: 1172-4

Smith, J. (1997). Brachyury and the T-box genes. *Curr Opin Genet Dev*. 7: 474-80

Stacey, D.W., Feig, L.A., & Gibbs, J.B. (1991). Dominant inhibitory Ras mutants selectively inhibit the activity of either cellular or oncogenic Ras. *Mol Cell Biol*. 11: 4053-64

Stanley, J.R., Tanaka, T.T., Mueller, S.M., Klaus-Kovtun, V., & Roop, D. (1988). Isolation of cDNA for bullous pemphigoid antigen by use of patients autoantibodies. *J Clin Invest*. 82: 1864-70

Steinberg, M.S., & Takeichi, M. (1994). Experimental specification of cell sorting, tissue spreading, and specific spatial patterning by quantitative differences in cadherin expression. *Proc Natl Acad Sci USA*. 91: 206-9

Stephens, L.E., Sutherland, A.E., Klimanskaya, I.V., Andrieux, A., Meneses, J., Pedersen, R.A., & Damsky, C.H. (1995). Deletion of beta 1 integrins in mice

results in inner cell mass failure and peri-implantation lethality. *Genes Dev.* 9: 1883-95

Stern, C.D. (1984). Hyaluronidases in early development. *Cell Biol Int Rep.* 8: 703-17

Stern, C.D., & MacKenzie, D.O. (1983). Sodium transport and the control of epiblast polarity in the early chick embryo. *J Embryol Exp Morphol.* 77: 73-98

Sternberg, B., Sorgi, F.L., & Huang, L. (1994). New structures in complex formation between DNA and cationic liposomes as visualized by freeze-fracture electron microscopy. *FEBS Letters.* 356: 361

Sternlicht, M.D., Lochter, A., Sympson, C.J., Huey, B., Rougier, J.P., Gray, J.W., Pinkel, D., Bissell, M.J., & Werb, Z. (1999). The stromal proteinase MMP3/stromelysin-1 promotes mammary carcinogenesis. *Cell.* 98: 137-46

Strachan, L.R., & Condic, M.L. (2003). Neural crest motility and integrin regulation are distinct in cranial and trunk populations. *Dev Biol.* 259: 288-302

Strachan, L.R., & Condic, M.L. (2004). Cranial neural crest recycle surface integrins in a substratum-dependent manner to promote rapid motility. *J Cell Biol.* 167: 545-54

Strauss, W.M., & Jaenisch, R. (1992). Molecular complementation of a collagen mutation in mammalian cells using yeast artificial chromosomes. *EMBO J.* 11: 417-22

Swaney, W.P., Sorgi, F.L., Bahnson, A.B., & Barranger, J.A. (1997). The effect of cationic liposome pretreatment and centrifugation on retrovirus-mediated gene transfer. *Gene Ther.* 4: 1379-86

Szelei, J., & Duda, F. (1989). Entrapment of high-molecular-mass DNA molecules in liposomes. *Biochem J.* 259: 549

Takagi, J., & Springer, T.A. (2002). Integrin activation and structural rearrangement. *Immuno Rev.* 186: 141-63

Taketo, M., & Shaffer, D.J. (1989). Deletions in a recombinant retrovirus genome associated with its expression in embryonal carcinoma cells. *J Virology.* 63: 4431

Takino, T., Tamura, M., Miyamori, H., Araki, M., Matsumoto, K., Sato, H., & Yamada, K.M. (2003). Tyrosine phosphorylation of the CrkII adaptor protein modulates cell migration. *J Cell Sci.* 116: 3145-55

Tamma, G., Klussmann, E., Maric, K., Aktories, K., Svelto, M., Rosenthal, W., & Valenti, G. (2001). Rho inhibits cAMP-induced translocation of aquaporin-2 into the apical membrane of renal cells. *Am J Physiol Renal Physiol.* 281: 1092–101

Teissie, J., & Ramos, C. (1998). Correlation between electric field pulse induced long-lived permeabilization and fusogenicity in cell membranes. *Biophys J.* 74: 1889-98

Testaz, S., Delannet, M., & Duband, J-L. (1999). Adhesion and migration of avian neural crest cells on fibronectin require the cooperating activities of multiple integrins of the beta1 and beta3 families. *J Cell Sci.* 112: 4715-28

Thomas, J.O. (2001). HMG1 and 2:architectural DNA-binding proteins. *Biochem Soc Trans.* 29: 395-401

Troiano, G.C., Tung, L., Sharma, V., & Stebe, K.J. (1998). The reduction in electroporation voltages by the addition of a surfactant to planar lipid bilayers. *Biophys J.* 75: 880-8

Tsalik, E.L. (2005). DNA-based immunotherapy to treat atopic disease. *Ann Allergy Asthma Immunol.* 95: 403-10

Tsukamoto, T., & Nigam, S.K. (1999). Cell-cell disassociation upon epithelial cell scattering requires a step mediated by the proteasome. *J Biol Chem.* 274: 24579-84

Tucker, G.C., Aoyama, H., Lipinski, M., Tursz, T., & Thiery, J.P. (1984). Identical reactivity of monoclonal antibodies HNK-1 and NC-1: conservation in vertebrates on cells derived from the neural primordium and on some leukocytes. *Cell Differ.* 14: 223-30

Tucker, R.P. (2004). Antisense knockdown of the beta 1 integrin subunit in the chicken embryo results in abnormal neural crest cell development. *Int J Biochem*

Cell Biol. 36: 1135-9

Ulmer, J.B., Donnelly, J.J., Parker, S.E., Rhodes, G.H., Felgner, P.L., Dwarki, V.J., Gromkowski, S.H., Deck, R.R., & Liu, M.A. (1993). Heterologous protection against influenza by injection of DNA encoding a viral protein. *Science*. 259: 1745-9

Unger, E.C., McCreery, T.P., & Sweitzer, R.H. (1997). Ultrasound enhances gene expression of liposomal transfection. *Invest Radiol*. 32(12): 723-7

Vallés, A.M., Boyer, B., Badet, J., Tucker, G.C., Barritault, D., & Thiery, J.P. (1990). Acidic fibroblast growth factor is a modulator of epithelial plasticity in a rat bladder carcinoma cell line. *Proc Natl Acad Sci USA*. 87: 1124-8

Vallin, J., Thuret, R., Giacomello, E., Faraldo, M.M., Thiery, J.P., & Broders, F. (2001). Cloning and characterization of three Xenopus slug promoters reveal direct regulation by LEF/beta-catenin signaling. *J Biol Chem*. 276: 30350-8

Valster, A., Tran, N.L., Nakada, M., Berens, M.E., Chan, A.Y., & Symons, M. (2005). Cell migration and invasion assays. *Methods*. 37: 208-15

Van Aelst, L., & D'Souza-Schorey, C. (1997). Rho GTPases and signaling networks. *Genes Dev*. 11: 2295-322

von Baer, K.E. (1828). Ueber Entwichlungsgeschichte der Tiere. *Königsberg:* Bornträger.

Vuori, K. (1998). Integrin signaling: tyrosine phosphorylation events in focal adhesions. *J Membrane Biol*. 165: 191-9

Wagner, E., Zenke, M., Cotten, M., Beug, H., & Birnstiel, M.L. (1984). Transferrin-polycation conjugates as carriers for DNA uptake into cells. *Proc Natl Acad Sci USA*. 81: 3476

Wang, C.Y., & Huang, L. (1989). Highly efficient DNA delivery mediated by pH-sensitive immunoliposomes. *Biochemistry*. 28: 9508

Wang, L., Yang, L., Luo, Y., & Zheng, Y. (2003). A novel strategy for specifically down-regulating individual Rho GTPase activity in tumor cells. *J Biol Chem*. 278: 44617-25

Ward, M., Scott, R.J., Davey, M.R., Clothier, R.H., Cocking, E.C., & Balls, M. (1986). Transfer of antibiotic resistant genes between yeast and mammalian cells under conditions favoring cell fusion. *Somat Cell Mol Genet*. 12: 101-9

Watanabe, M., Shirayoshi, Y., Koshimizu, U., Hashimoto, S., Yonehara, S., Eguchi, Y., Tsujimoto, Y., & Nakatsuji, N. (1997). Gene transfection of mouse primordial germ cells in vitro and analysis of their survival and growth. *Expr Cell Res*. 230: 76-83

Wennerberg, K., & Der, C.J. (2004). Rho-family GTPases: it's not only Rac and Rho (and I like it). *J Cell Sci.* 117: 1301-12

Weston, J.A. (1963). A radiographic analysis of the migration and localization of trunk neural crest cells in the chick. *Dev Biol*. 6: 279-310

Weston, J.A. (1991). Sequential segregation and fate of developmentally restricted intermediate cell populations in the neural crest lineage. *Dev Biol*. 25: 133-53

Whitcomb, J.M., & Hughes, S.H. (1992). Retroviral reverse transcriptase and integration: Progress and problems. *Annu Rev Cell Biol*. 8: 255-306

Wiche, G., Krepler, R., Artlieb, U., Pytela, R., & Aberer, W. (1984). Identification of plectin in different human cell types and immunolocalization at epithelial basal cell surface membranes. *Exp Cell Res*. 155: 43-9

Wilson, V., & Beddington, R. (1997). Expression of T protein in the primitive streak is necessary and sufficient for posterior mesoderm movement and somite differentiation. *Dev Biol*. 192: 45-58

Wilson, V., Manson, L., Skarnes, W.C., & Beddington, R.S. (1995). The T gene is necessary for normal mesodermal morphogenetic cell movements during gastrulation. *Development*. 121: 877-86

Wolff, J.A., Malone, R.W., Williams, P., Chong, W., Acsadi, G., Jani, A., & Felgner, P.L. (1990). Direct gene transfer into mouse muscle in vivo. *Science*. 247: 1465-8

Wolff, J.A., Ludtke, J.J., Acsadi, G., Williams, P., & Jani, A. (1992). Long-term persistence of plasmid DNA and foreign expression in mouse muscle. *Hum Mol*

Genet. 1: 363-9

Wrobel, I., & Collins, D. (1995). Fusion of cationic liposomes with mammalian cells occurs after endocytosis. *Biochim Biophys Acta*. 1235: 296

Wu, J., Saint-Jeannet, J-P., & Klein, P.S. (2003). Wnt-frizzled signaling in neural crest formation. *Trends Neurosci*. 26: 40-5

Yan, C.N., Li, F., Patterson, C., & Runge, M.S. (1998). High-voltage and high-salt buffer facilitates electroporation of human aortic smooth-muscle cells. *Biotechniques*. 24: 590-2

Yang, K., Faustinella, F., Xue, J.J., Whitson, J., Kampfl, A., Mu, X.S., Zhao, X., & Taglialatela, G. (1994). Optimizing liposome-mediated gene transfer in primary rat septo-hippocampal cell cultures. *Neurosci Lett*. 182: 287-90

Yang, N.S., Burkholder, J., Roberts, B., Martinell, B., & McCabe, D. (1993). In vivo and in vitro gene transfer to mammalian somatic cells by microparticle bombardment. *Proc Natl Acad Sci USA*. 90: 4455

Yokoyama, K., Kamata, N., Fujimoto, R., Tsutsumi, S., Tomonari, M., Taki, M., Hosokawa, H., & Nagayama, M. (2003). Increased invasion and matrix metalloproteinase-2 expression by Snail-induced mesenchymal transition in squamous cell carcinomas. *Int J Oncol*. 24: 891-8

Yonemitsu, Y., Kaneda, Y., Muraishi, A., Yoshizumi, T., Sugimachi, K., & Sueishi, K. (1997). HVJ (Sendai virus)-cationic liposomes: a novel and potentially effective liposome-mediated technique for gene transfer. *Gene Ther*. 4: 631-8

Yonemitsu, Y., Alton, E.W., Komori, K., Yoshizumi, T., Sugimachi, K., & Kaneda, Y. (1998). HVJ (Sendai virus) liposome-mediated gene transfer: current status and future perspectives (review). *Int J Oncol*. 12: 1277-85

Zarich, N., Oliva, J.L., Martinez, N., Jorge, R., Ballester, A., Gutierrez-Eisman, S., Garcia-Vargas, S., & Rojas, J.M. (2006). Grb2 is a negative modulator of the intrinsic Ras-GEF activity of hSos1. *Mol Biol Cell*. 17: 3591-7

Zelenin, A.V., Titomirov, A.V., & Kolesnikov, V.A. (1989). Genetic transformation

of mouse cultured cells with the help of high-velocity mechanical DNA injection. *FEBS Lett*. 244: 65

Zeng, M., Cerniglia, G.J., Eck, S.L., & Stevens, C.W. (1997). High-efficiency stable gene transfer of adenovirus into mammalian cells using ionizing radiation. *Hum Gene Ther*. 8: 1025-32

Zerbib, D., Almaric, F., & Teissie, J. (1985). Electric field mediated transformation: isolation and characterization of a TK+ subclone. *Biochem Biophys Res Comm*. 129: 611-8

Zhai, J., Lin, H., Nie, Z., Wu, J., Canete-Soler, R., Schlaepfer, W.W., & Schlaepfer, D.D. (2003). Direct interaction of focal adhesion kinase with p190RhoGEF. *J Biol Chem*. 278: 24865–73

Zhou, X., Klibanov, A., & Huang, L. (1992). Improving encapsulation of DNA in pH-sensitive liposomes for transfection. *J Lip Res*. 2: 125

Zimmermann, U. (1986). Electrical breakdown, electropermeabilization, and elctrofusion. *Rev Physiol Biochem Pharmacol*. 105: 176-256

Zimmermann, U., & Vienken, J. (1982). Electric field-induced cell-to-cell fusion. *J Membrane Biol*. 67: 165-82

Zimmermann, U., Scheurich, P., Pilwat, G., & Benz, R. (1981). Cells with manipulated functions: new perspectives for cell biology, medicine, and technology. *Angew Chem Int Ed Engl*. 20: 325-44

APPENDIX I:
DETAILED GUIDE TO ELECTRODE CONSTRUCTION

MATERIALS

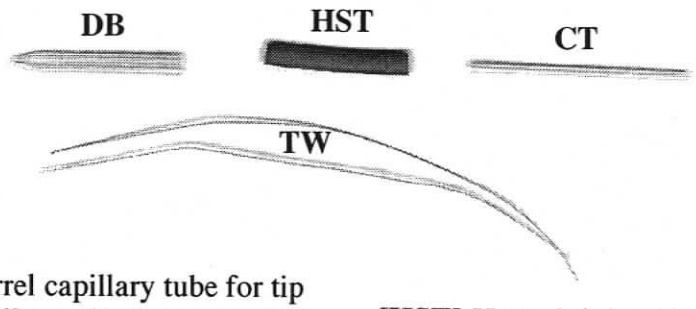

[DB] Double-barrel capillary tube for tip
- 1.2 mm x 0.68 mm, 4 inch, borosilicate glass
- eg. catalog #635000, A-M Systems
  < http://www.a-msystems.com >

[CT] Capillary tube for mounting shaft
- eg. catalog #626000, A-M Systems

[HST] Heat-shrink tubing
- any with an inside diameter snug to DB

[TW] Teflon-coated tungsten wire
- or any stiff, insulated wire, eg. catalog #796000, A-M Systems

TIP PREPARATION

1. Use a pipet puller to **draw** double-barrel capillary glass into a sharp point.

2. **Break back** the glass point to create openings of the desired diameter.
   - a diamond pen works well to etch a break line (this is the best way to create electrodes with larger tips)

3. **Check** the tips under microscope.
   - if you are creating a blunt surface suction electrode, discard the ones that are overly jagged or too much off angle. This is less important if you are creating an electrode for piercing, since it will be ground
   - if your breaks are square and straight enough, blunt electrodes do not need to be ground. Small irregularities will be removed in the forging step
   - if you decide to sharpen the electrode on a grinding wheel, you will need to rinse out the dust with distilled water.

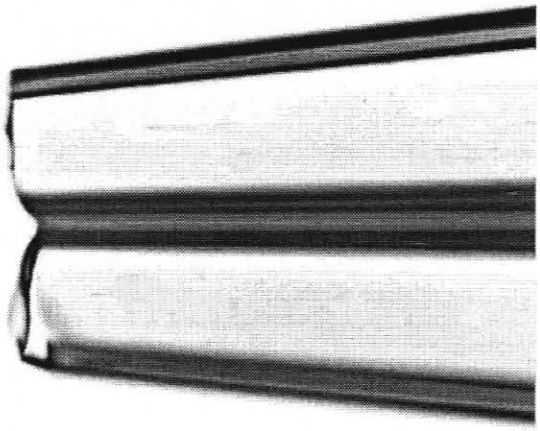

A pulled tip that is broken back. The breaks are straight enough to proceed directly to the forging step.

4. Blunt suction electrodes must be **smoothed** to avoid damaging the tissue. This can be done using an electric **forge** or by brief **flaming.**
   - the electrode should be held in a micromanipulator under a dissecting microscope. Once the glass becomes shiny and starts to melt inward, it needs to be withdrawn immediately to prevent the opening in the tip frombecoming overly closed. Sharpened electrode tips are not forged.

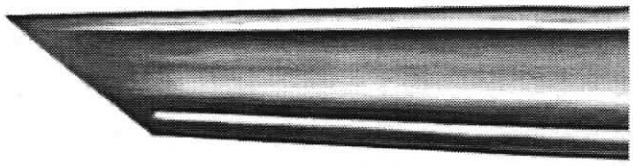

Tip sharpened by grinding, sideview

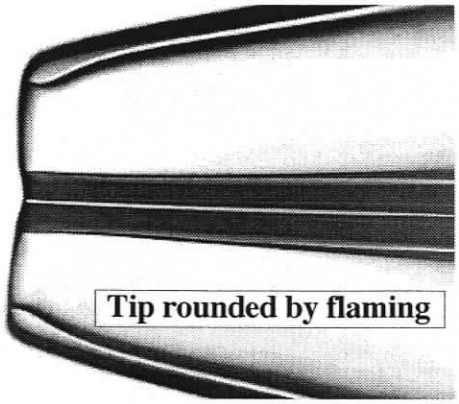

Tip rounded by flaming

ELECTRODE ASSEMBLY

❺ **Check** the tips under a microscope again. Ensure ground tips are sharp and free of dust. Ensure blunt tips are smooth and flat enough to form **good suction**, while still maintaining an acceptable diameter.

- at this point you can introduce a bend in the electrode (depending on the orientation of the application). Heat the middle of the tip and allow the glass to bend by gravity.
- you will probably want to shorten the shaft of the tip at this point; shorter electrodes are more controllable and use less wire. Use a diamond pen and briefly flame the broken ends by hand so they do not nick the Teflon-coated wire used in the next step.

❻ Prepare two equal segments of Teflon-coated **tungsten wire** of the appropriate length. Use a razor blade to **strip back** about 5 mm of Teflon from **all ends**.

❼ **Inset** one **wire** TW down each barrel of the glass electrode toward the **tip** DB.

Tip DB with wire inserted into each barrel. The Teflon has been striped back 5 mm, but is still visible on the right (▼).

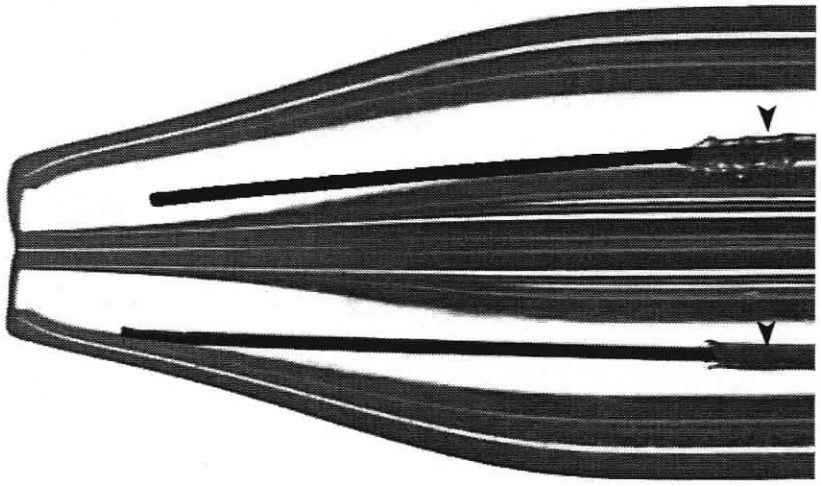

❽ Cut an appropriate length of **heat-shrink tubing** HST and thread the free ends of the wires through it. Push the tubing firmly down until it overlaps the shaft of the glass tip DB by about 5 mm.

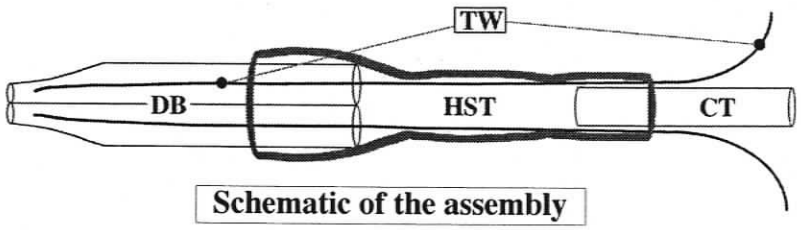

Schematic of the assembly

9. Use a soldiering iron to **shrink** the HST tubing tightly onto the **shaft** of the **tip** DB.
   - hold it near the heat, do not actually touch the iron.

10. Cut and flame the ends of a single-barrel glass **capillary tube** of appropriate length
    - place CT approximately 5 mm into the free end of the heat-shrink tubing HST.

11. **Shrink** the HST tubing around CT only **partly**: so that it is snug, but so that you can still move the wires.

12. Checking with a microscope, **adjust** the wires TW so their ends are even and near the tip of DB. Once you are satisfied with the wire positioning, carefully **shrink** the HST tubing the rest of the way around CT.

13. Finally, **seal** the ends of heat-shrink tubing to the glass using **hot melt glue** or epoxy. The seal needs to be air tight for effective control of suction. Let cool/cure, then begin localized electroporating.

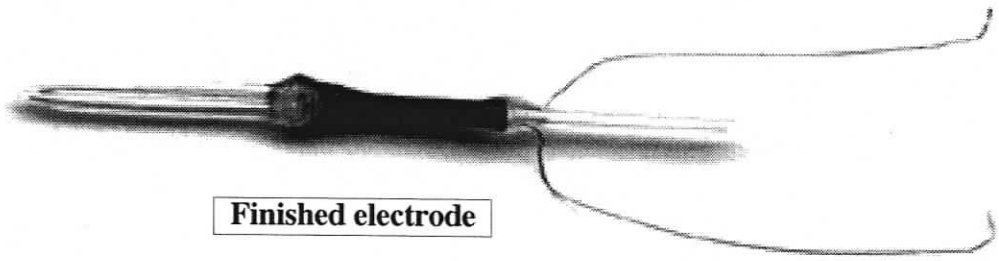

Finished electrode

GENERAL ADVICE & ELECTRODE CARE

- The most important part of electrode construction is creating a smooth tip that makes a good seal with the target tissue. Forging/flaming the tip is probably the step that requires the most practice and patience. If a forge is unavailable, a horizontal butane torch is the best substitute.

- Adjusting the position of the wires in relation to the end of the tip (~1 mm) is the second most important step. This is critical for reproducing the electroporation parameters between different electrodes.

- When optimizing electroporation parameters, begin first by titrating the voltage. The highest transfection efficiency is just below the threshold where tissue damage occurs. The number of pulses, pulse spacing, and pulse length can then be optimized; but, these

variables are less important.

- Obtaining good suction is the most important consideration for reliable and efficient electroporation. This can be checked by slightly drawing back the micromanipulator to make sure the tissue is attached. Be careful not to over apply suction, which can lead to tissue damage.

- When applying suction it is possible to displace the plasmid by drawing surrounding fluid into the electrode tip. If the plasmid is not in contact with the target tissue, transfection will not occur. This can be prevented by ejecting a small pool of plasmid just before the application of suction.

- Electrode life can be prolonged by rinsing the tip with distilled water immediately following each electroporation. Always draw water **into** the electrode—never expel large volumes out through the tip (which can lead to clogging). The rinse water can be removed by passing air through the electrode. It is useful to dedicate large wet and dry syringes for this purpose (separate from the screw-drive syringe used during electroporation).